
2 Ionic Surfactants and Ion-Specific Effects

Adsorption, Micellization, and Thin Liquid Films

Radomir I. Slavchov, Stoyan I. Karakashev, and Ivan B. Ivanov

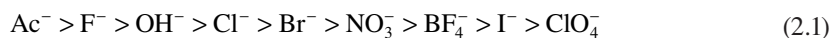
CONTENTS

2.1	Introduction	54
2.2	Adsorption of Ionic Surfactants from Dilute Solutions	56
2.2.1	Adsorption in the Absence of Ion-Specific Effects	56
2.2.1.1	Henry's Adsorption Constant of Nonionic Surfactants: Adsorption Energy and Thickness	56
2.2.1.2	Poisson–Boltzmann Equation and Electroneutrality: Gouy Equation	59
2.2.1.3	Thermodynamics of the Diffuse Double Layer: Adsorption and Surface Tension	61
2.2.1.4	Davies' Adsorption Isotherm	62
2.2.2	Adsorption Behavior at W G versus W O Interface: LE Layer and Spreading Pressure	63
2.2.3	Counterion-Specific Effects on the Adsorption of Ionic Surfactants from Dilute Solutions	68
2.2.3.1	Gouy Equation with Specific Interactions	68
2.2.3.2	Specific Interaction between an Ion and the Interface	70
2.2.4	Comparison with the Experiments	73
2.2.4.1	Experimental Verification of the Theory of Adsorption Constant K	73
2.2.4.2	Adsorption in the Presence of a Mixture of Counterions	80
2.3	EOS and Adsorption Isotherm of Dense Monolayers	82
2.3.1	Nonlocalized Adsorption of Nonionic Surfactants	82
2.3.1.1	The Area per Molecule α	84
2.3.1.2	The Interaction Parameter β	86
2.3.1.3	New EOS and Adsorption Isotherm for Nonionic Surfactants	88
2.3.2	Dense Adsorption Layers of Ionic Surfactants: Ion-Specific Effects	91
2.3.2.1	Equations of State and Adsorption Isotherms of Ionic Surfactants	91
2.3.2.2	Experimental Results and Analysis	94
2.3.2.3	Electrostatic and Ion-Specific Effects on the Adsorption Parameters K , α , and β	99
2.4	Hofmeister Effect on cmc of Ionic Surfactants and Disjoining Pressure in Foam Films	100
2.4.1	Effect of Counterion on the cmc of Ionic Surfactants	100
2.4.2	Ion-Specific Effect on the Disjoining Pressure of Foam Films Stabilized with Ionic Surfactants	106

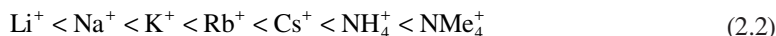
2.5 Summary and Conclusions	108
2.6 Prospects	110
List of Symbols and Abbreviations	111
Acknowledgments	112
References	112

2.1 INTRODUCTION

In 1887, F. Hofmeister published an article [1] in which the precipitation efficiency of different salts on proteins was investigated. Hofmeister found that the critical electrolyte concentration for protein precipitation exhibited regularity and ordered the ions by their efficiency; nowadays, this ordering is called the *Hofmeister series*. For a series of salts with the same cation and different anions, the precipitation efficiency increases (i.e., the precipitation concentration decreases) in the following sequence [2] (“Ac⁻” is acetate ion; F⁻ was added by us):



Similarly, for salts sharing the same anion, the Hofmeister series for the cations reads [2]:



(“Me” stands for methyl group). These ion sequences in series (Equations 2.1 and 2.2) were found to be approximately independent of the protein, although the *direction* of the effect depends [3,4], among other factors, on the sign of the protein’s net charge (in Hofmeister experiments, proteins were negatively charged). Since the work of Hofmeister, a large number of experimental studies have demonstrated similar regularities in various phenomena. The interested reader can find a collection of articles on the Hofmeister effect and related phenomena in two special issues of *Current Opinion in Colloid and Interface Science* in 2004 [5] and in perhaps the only book dedicated to this topic, *Specific Ion Effects* [2].

Earlier attempts for interpretation of the Hofmeister series and its effect on the interaction between proteins, macromolecules, or colloidal particles were qualitative and invoked mainly the ion size, the ion interaction with water, and the “hydration force” (see e.g., [5]). Ninham and coworkers were probably the first to advocate the role of the van der Waals forces for the interaction between ions in solution, for the adsorption of electrolytes, for the interaction between proteins or colloidal particles, etc. In a series of articles [2,6–15], Ninham and coworkers applied and tested Ninham’s idea for explaining the adsorption of simple electrolytes. The initial results were encouraging [7], but the subsequent efforts to obtain good quantitative results [8–10] met with difficulties. Tavares et al. [16] studied theoretically the Hofmeister effect on the interaction of charged proteins. They calculated the purely electrostatic and the van der Waals contributions and found that the van der Waals interaction gives rise to a strong attractive force. No comparison with experimental data was carried out.

In this chapter, we will concentrate on the Hofmeister effect on the properties of ionic surfactant solutions and related phenomena. Warszynski and coworkers [17–19] accounted explicitly for the role of the ion-specific effects in the ionic surfactants’ adsorption and determined their adsorption constants K_s . In ref. [17], they investigated the effects of Li⁺, Na⁺, NH₄⁺, K⁺, and Cs⁺ on the surface tension of anionic surfactant solutions, whereas ref. [18] was devoted to the anions. Aratono and coworkers [20–23] carried out numerous meticulous experimental studies, coupled with thermodynamic analysis, of the adsorption of a number of surfactants with various counterions at water|gas (W|G) and water|oil (W|O) interfaces. A large number of studies were dedicated to the ion-specific effects on the critical micelle concentration (cmc) of surfactants, see for example, refs. [24,25].

It is also worth mentioning two theories which did not address the Hofmeister effect, but played an important role in the theory of adsorption of ionic surfactants. The first one is the theory of Davies [26,27], who derived the equation of state (EOS) of dilute monolayers of ionic surfactants. The role of Davies' model in the theory of the adsorption of ionic surfactants is as significant as the ideal solution model is in the theory of solutions. The second theory belongs to Borwankar and Wasan [28], who proposed a simple approach for the derivation of the adsorption isotherm of ionic surfactants. We use both theories below.

Following Ninham's ideas, Ivanov et al. [29] proposed and tested experimentally a relatively simple theoretical model of the effect of the type of electrolyte on the adsorption constant of ionic surfactants. In the core of the theory is a quantity, u_{i0} , called *ion-specific adsorption energy*—it is equal to the van der Waals adsorption energy of an ion at the interface. It encompasses, in a single simple expression, all the major factors controlling ion-specific adsorption: the ion polarizability and ionization potential, the radius of the hydrated ion and the possible deformation of the hydration shell upon ion adsorption at the interface. The ion-specific adsorption energy u_{i0} turned out to be independent of the type of the surfactant, which allows using the calculated value for a given ion for the interpretation of adsorption data for different surfactants but with this same counterion. In ref. [30], the theory was successfully applied to other phenomena involving ionic surfactants: micellization, disjoining pressure of thin liquid films, and emulsion stability.

Our goal in this article is (i) to present concisely the results from refs. [29,30], related to some phenomena involving ionic surfactants and the Hofmeister effect, and to supplement them with more examples and new developments; (ii) to present a new EOS and a new adsorption isotherm for ionic surfactants, and to check them against surface/interfacial tension data; (iii) to discuss briefly the theories and experimental data of other authors, when they are related to the subject studied; and (iv) to outline some possible future developments (including extensions or refinements of the models presented) and several other phenomena to which the theory and the procedures presented here could be applied.

Practically all theories of adsorption of ionic surfactants (including the present one) are based on one or more theories of the nonionic ones. In several recent studies [31–34], it was shown that the most popular EOS of nonionic surfactants suffered from important shortcomings. Methods for overcoming these problems were suggested there and are discussed shortly in the present article.

The article is organized as follows: Section 2.2 is devoted to the adsorption of ionic surfactants from dilute surfactant solutions. The adsorption model used here is an extension of Henry's isotherm to ionic surfactants. That is why, in Section 2.2.1.1, we present briefly the theory developed in refs. [31,33] for the adsorption constants K_a , the adsorption thickness δ_a , and adsorption energy E_a . Sections 2.2.1.2 and 2.2.1.3 are devoted to the electrostatic and thermodynamic foundations of the theory of adsorption of ionic surfactants. In Section 2.2.1.4, the Davies adsorption isotherm for ionic surfactants [26,27], along with his expression for the surface potential, are derived and discussed. In Section 2.2.3, the difference in the adsorption behavior of ionic surfactants at W|G versus W|O interface is analyzed and the role of the spreading pressure and the liquid-expanded (LE) adsorbed layer is explained. The entire Section 2.2.3 is devoted to the counterion-specific effects on ionic surfactants adsorption, developed in ref. [29], more precisely—to the derivation of an equation for the central quantity of the theory—the *ion-specific adsorption energy* u_{i0} , and the development of a procedure for its theoretical calculation. The experimental verification of the theoretical results from Section 2.2 is given in Section 2.2.4. Davies model and the theory of the adsorption constant are analyzed by using numerous data for adsorption of ionic surfactants at W|G and W|O interfaces. The theory of the Hofmeister effect on the adsorption of ionic surfactants is compared with data for numerous individual counterions and their mixtures (Section 2.2.4.2). The main goal of Section 2.3 is the formulation and experimental verification of a new model of dense monolayers of ionic surfactants. Because it is an extension of the respective model for nonionic surfactants [31–33], in Sections 2.3.1.1 and 2.3.1.2, we present a rather detailed analysis and some new considerations about three basic quantities of the theory: the actual area of the molecule α , and the interaction constants B_{attr} and β . Section 2.3.1.3 presents the new

surface EOS and adsorption isotherm of nonionic surfactants, derived previously in refs. [32,33]. They are generalized in Section 2.3.2.1 for nonlocalized adsorption of ionic surfactants with ion-specific effects. The verification of the theory with data for adsorption of ionic surfactants at W|G and W|O interfaces led to satisfactory results (Section 2.3.2.2) and allowed the formulation of several new electrostatic and ion-specific effects on the adsorption parameters (Section 2.3.2.3).

The generality of the theory of the counterion-specific effects to ionic surfactants is demonstrated in Section 2.4 by the analysis of other phenomena involving ionic surfactants that are different from adsorption [30], namely, the cmc and disjoining pressure in thin liquid films. A theory (based on the model of Shinoda et al. [25]) of the Hofmeister effect on the cmc is presented. The cmc of ionic surfactants in the presence of a mixture of counterions is also considered. Section 2.5 summarizes the main results obtained and discussed in this article and outlines the possibility for refinement and extension of the theory of the phenomena considered as well as for its application to other phenomena.

In the cases analyzed in the present article, remarkable agreement between theory and experiment was found and the results were in agreement with the Hofmeister series (2.1 and 2.2). Despite the diversity of the phenomena studied, all interpretations were based on a single parameter: the ion-specific adsorption energy u_{i0} . For a given counterion, a single value of u_{i0} was used to explain various phenomena; this value was calculated from the same equation without using adjustable parameters. The success of the theory in explaining or predicting quantitatively the ion-specific effects on several different phenomena involving ionic surfactants makes us believe that, at least for ionic surfactants, it is close to a “firmly based theory,” which was missing according to Kunz et al. [15].

2.2 ADSORPTION OF IONIC SURFACTANTS FROM DILUTE SOLUTIONS

2.2.1 ADSORPTION IN THE ABSENCE OF ION-SPECIFIC EFFECTS

2.2.1.1 Henry's Adsorption Constant of Nonionic Surfactants: Adsorption Energy and Thickness

Before adsorption from dilute solutions of ionic surfactants, we will briefly discuss the basic theory of nonionic surfactants. The chemical potentials of a nonionic surfactant in an ideal solution of concentration C_s and in an ideal adsorbed monolayer of adsorption Γ_s are, respectively,

$$\mu^B = \mu_0^B + k_B T \ln C_s \quad (2.3)$$

$$\mu^S = \mu_0^S + k_B T \ln \Gamma_s \quad (2.4)$$

Here, superscripts “B” and “S” denote bulk and surface phase, and μ_0^S and μ_0^B are the corresponding standard chemical potentials. At equilibrium, the chemical potentials μ^B and μ^S must be equal. This leads to Henry's adsorption isotherm:

$$\Gamma_s = K_s C_s \quad (2.5)$$

where the adsorption constant K_s is defined by the relation

$$k_B T \ln K_s \equiv \mu_0^B - \mu_0^S \quad (2.6)$$

As it is obvious from the derivation, Henry's adsorption isotherm is valid only for adsorption layers consisting of noninteracting nonionic surfactant molecules, which is possible for dilute adsorption layers only.

The first step in our analysis will be the consideration of the dependence of K_s on the structure of the surfactant molecule and of the interface. The explicit expression for the adsorption constant K_s in terms of molecular parameters is usually written as

$$K_s = \delta_a \exp(E_a/k_B T) \quad (2.7)$$

where δ_a is referred to as the “thickness of the adsorbed layer,” and E_a is the adsorption energy. Davies and Rideal (Equation 4.2 in ref. [26]), proposed to use the length of the surfactant molecule for the thickness δ_a , an assumption adopted later by others (e.g., [35–37]). Davies and Rideal represented the adsorption energy E_a as

$$E_a = E_0 + u_{\text{CH}_2} n_C \quad (2.8)$$

Here, n_C is the number of carbon atoms in the hydrophobic chain and u_{CH_2} is the (positive) free energy of transfer of a $-\text{CH}_2-$ group from the solution to the adsorption layer. E_0 is the n_C -independent part of E_a , which was ascribed in ref. [26] solely to the adsorption energy E_{head} of the hydrophilic head (cf. Equation 4.3 in ref. [26]). In fact, the assumptions of Davies and Rideal for both δ_a and E_a are not entirely correct. More rigorous treatment based on classic statistical thermodynamics was given in ref. [31], which will be presented in the section below. The results will be compared with experimental data for ionic surfactants in Section 2.2.4.1.

The essential contributions to the interaction potential of a surfactant molecule with the surface are the following (Figure 2.1):

1. When the cap of the hydrophobic chain touches the surface, a portion of the water–hydrophobic phase interface of area α_\perp disappears. The contribution of this process to $u(z)$ is modeled as a contact potential at $z = n_C l_{\text{CH}_2}$ (l_{CH_2} is length per $-\text{CH}_2-$ group):

$$u_{(i)}(z) = \begin{cases} \sigma_0 \alpha_\perp, & z < n_C l_{\text{CH}_2} \\ 0, & z > n_C l_{\text{CH}_2} \end{cases} \quad (2.9)$$

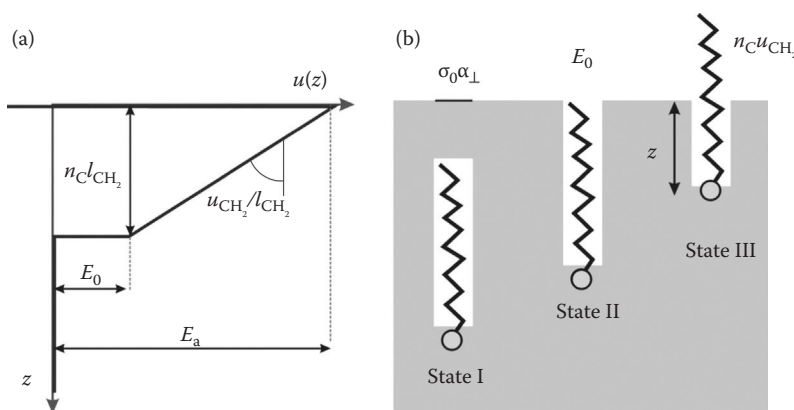


FIGURE 2.1 (a) Interaction potential $u(z)$ between a surfactant molecule and the interface as a function of the distance z between the ionic head and the surface (Equation 2.12). (b) According to the model we used, at distances $z > n_C l_{\text{CH}_2}$ (state I), there is no significant interaction. At $z = n_C l_{\text{CH}_2}$ (state II), energy is gained due to the disappearance of pure water surface of area α_\perp , and the transfer energy of the cap of the $-\text{CH}_3$ group (Equation 2.14). At shorter distances (state III), there is a linear dependence of u on z related to the energy of transfer $n_C u_{\text{CH}_2}$ of the hydrocarbon chain from water to the gas phase (Equation 2.11).

where σ_0 is the surface tension of the pure water–hydrophobic phase interface. For W|G interface at 25°C, $\sigma_0 = 72$ mN/m, and for a typical W|O, $\sigma_0 \approx 50$ mN/m. The cross-sectional area of the hydrocarbon tail is $\alpha_{\perp} = \pi R_{\text{CH}_2}^2 \approx 21 \text{ \AA}^2$ (following from the value $R_{\text{CH}_2} = 2.6 \text{ \AA}$ of the cross-sectional radius of the chain [38]). Thus, the energy $\sigma_0 \alpha_{\perp}$ is of the order of 10^{-20} J or approximately $2.5 \times k_B T$.

- Let the free energy of transfer of a single $-\text{CH}_2-$ group from the bulk solution to the adsorption layer be u_{CH_2} . For the energy u_{Me} of transfer of the $-\text{CH}_3$ group, we assume proportionality to the contact area of this group with water [39]. One can approximate the shape of $-\text{CH}_3$ as a cylinder with a cap. The lateral area of the cylinder is assumed equal to that of a $-\text{CH}_2-$ group, α_{\parallel} , and the cap area is assumed equal to the cross-sectional area α_{\perp} of the hydrocarbon tail. The values of the two areas are $\alpha_{\perp} = \pi R_{\text{CH}_2}^2 \approx 21 \text{ \AA}^2$ and $\alpha_{\parallel} = 2\pi R_{\text{CH}_2} l_{\text{CH}_2} \approx 21 \text{ \AA}^2$ (the values $R_{\text{CH}_2} = 2.6 \text{ \AA}$ and $l_{\text{CH}_2} = 1.26 \text{ \AA}$ were used [38]). Consequently, the two areas are equal and the energy corresponding to each of these areas is $u_{\text{CH}_2} \alpha_{\parallel}$. The energy pertaining to the cap can be represented as a contact potential with the same z -dependence as $u_{(i)}$ in Equation 2.9:

$$u_{(ii)}(z) = \begin{cases} u_{\text{CH}_2}, & z < n_C l_{\text{CH}_2} \\ 0, & z > n_C l_{\text{CH}_2} \end{cases} \quad (2.10)$$

The second part of u_{Me} (pertaining to the lateral area of $-\text{CH}_3$) is not included in Equation 2.10; it will be included in the next term, the potential $u_{(iii)}$. The contributions (1) and (2) were derived by Ivanov et al. [31] and independently by Kumpulainen et al. [40].

- Assuming for simplicity that the carbon chain remains normal to the interface, one can model the hydrophobic energy due to $-\text{CH}_2-$ adsorption (plus the lateral energy of the $-\text{CH}_3$ group) as a linear function of the distance z between the surfactant head and the interface:

$$u_{(iii)}(z) = u_{\text{CH}_2} z / l_{\text{CH}_2}, \quad n_C l_{\text{CH}_2} > z > 0 \quad (2.11)$$

- Although the hydrophilic head remains immersed in the hydrophilic phase, it also interacts with the interface. This interaction probably involves both short-range and long-range (such as van der Waals and electrostatic) forces. Because these forces are not yet fully understood, we will account for their contribution to the adsorption energy E_a by an empirical constant E_{head} .
- One finally assumes that the surfactant cannot desorb into the hydrophobic phase, that is, $u(z) = \infty$ at $z < 0$.

Combining contributions (1) through (5), one obtains an approximate expression for the interaction potential of a surfactant molecule with the interface (see [Figure 2.1](#)):

$$u(z) = \begin{cases} \infty, & 0 > z; \\ -E_a + u_{\text{CH}_2} z / l_{\text{CH}_2}, & n_C l_{\text{CH}_2} > z > 0; \\ 0 & z > n_C l_{\text{CH}_2}, \end{cases} \quad (2.12)$$

where the adsorption energy E_a is given by

$$E_a = E_{\text{head}} + \alpha_{\perp} \sigma_0 + u_{\text{CH}_2} (n_C + 1) \quad (2.13)$$

In Equation 2.12, the free energy of surfactant in the bulk solution is used as a reference state. Comparison of Equations 2.13 and 2.8 leads to an explicit expression for the empirical constant E_0 of Davies and Rideal [26]:

$$E_0 = E_{\text{head}} + u_{\text{CH}_2} + \alpha_{\perp} \sigma_0 \quad (2.14)$$

It encompasses not only E_{head} , as assumed by Davies and Rideal, but also all the other contributions to E_a , unrelated to the adsorption of the $-\text{CH}_2-$ chain.

Our next goal is to derive a new expression for the “thickness of the adsorbed layer” δ_a , and the relation of δ_a and the adsorption energy E_a to the adsorption constant K_s . This can be done by statistical calculation of the adsorption Γ_s . Using Boltzmann distribution, the potential $u(z)$ (Equation 2.12) and the Gibbs’ definition of adsorption as an excess [41], for an ideal monolayer, one can write:

$$\Gamma_s = C_s \int_0^{n_C l_{\text{CH}_2}} (e^{-u(z)/k_B T} - 1) dz = \frac{k_B T l_{\text{CH}_2}}{u_{\text{CH}_2}} e^{E_a/k_B T} \left(1 - e^{-n_C u_{\text{CH}_2}/k_B T} - \frac{n_C u_{\text{CH}_2}}{k_B T} e^{-E_a/k_B T} \right) C_s \quad (2.15)$$

This is, in fact, a detailed expression of Henry’s adsorption isotherm, $\Gamma_s = K_s C_s$. Because the exponents in the brackets are negligible, it yields Equation 2.7 for K_s . The comparison with Equation 2.7 shows that the adsorption layer thickness is

$$\delta_a = k_B T l_{\text{CH}_2} / u_{\text{CH}_2} \quad (2.16)$$

Using Tanford’s values for u_{CH_2} and l_{CH_2} , at 300 K, one obtains $\delta_a = 0.9$ and 1.2 \AA for W|O and W|G interfaces, correspondingly. This is in contrast with the assumption that δ_a is of the order of the thickness of the adsorption layer [26,37]: indeed, for chain length $n_C = 12$, the ratio of the two thicknesses, $n_C l_{\text{CH}_2}$ and δ_a , as defined by Equation 2.16, is approximately 12.

2.2.1.2 Poisson–Boltzmann Equation and Electroneutrality: Gouy Equation

Consider an electrolyte solution positioned in the semi-space $z > 0$, as illustrated in Figure 2.2. Let each surfactant ion possess charge e_s (only monovalent surfactants will be considered, so that $e_s = \pm e_0$, where e_0 is the elementary charge). Consequently, the surface where the surfactants’ heads are situated ($z = 0$, see Figure 2.2) has a surface charge density $e_s \Gamma_s$, due to the surfactant’s adsorption in the adsorbed layer Γ_s . This surface charge and the ions in the diffuse layer create electrostatic potential $\phi(z)$ in the electrolyte solution, which is determined, at first approximation, by the Poisson–Boltzmann equation

$$\epsilon \frac{d^2 \phi}{dz^2} = - \sum_i e_i C_i \exp(-e_i \phi / k_B T) \quad (2.17)$$

Here, ϵ is the absolute dielectric constant, e_i and C_i are the i th component charge, in units (C), and bulk molecular number concentration, in units (m^{-3}), k_B is Boltzmann constant, and T is absolute temperature. In this equation, the variables ϕ and $d\phi/dz \equiv -E$ (electric field) can be separated, by using the identity $2d^2\phi/dz^2 = d(E^2)/d\phi$. This leads to

$$d(E^2) = - \frac{2}{\epsilon} \sum_i e_i C_i \exp(-e_i \phi / k_B T) d\phi \quad (2.18)$$

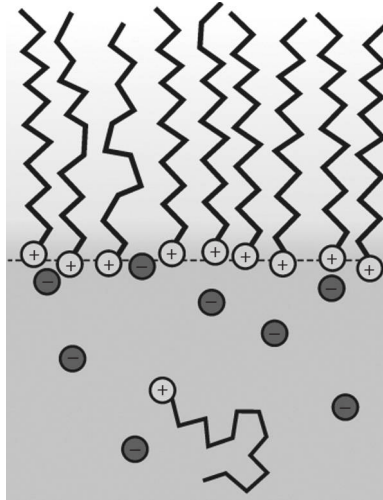


FIGURE 2.2 Structure of the adsorption layer. The adsorption of surfactant creates surface charge density at the interface. The surface charge is neutralized by the diffuse double layer.

The first integral of the Poisson–Boltzmann equation is obtained by integrating Equation 2.18 in limits $z = \infty$ to z , using as a first boundary condition, $E = 0$ and $\phi = 0$ at $z = \infty$:

$$E(z)^2 = \frac{2k_B T}{\epsilon} \sum_i C_i (e^{-e_i \phi(z)/k_B T} - 1) \quad (2.19)$$

The second boundary condition (at $z = 0$) is the Gauss condition for electroneutrality:

$$\epsilon E \Big|_{z=0} = e_s \Gamma_s \quad (2.20)$$

We will denote the surface potential $\phi(0)$ by ϕ^s . Setting $z = 0$ and $\phi = \phi^s$ into Equation 2.19, and eliminating $E(z = 0)$ from the electroneutrality condition (Equation 2.20), the Gouy equation is obtained [42]:

$$\frac{\kappa_0^2}{4} \Gamma_s^2 = \sum_i C_i (e^{-e_i \phi^s/k_B T} - 1) \quad (2.21)$$

Here, the quantity

$$\kappa_0^2 \equiv 2e_0^2/\epsilon k_B T \quad (2.22)$$

is the concentration-independent part of the Debye parameter: $\kappa^2 \equiv \kappa_0^2 C_t$ and $\kappa_0^2 \equiv 2 \times r_B$, where $r_B \equiv e_0^2/\epsilon k_B T$ is the so-called Bjerrum length. In the case of 1:1 electrolyte, the Gouy equation (Equation 2.21) simplifies to

$$\frac{\kappa_0}{4} \Gamma_s = \sqrt{C_t} \sinh(\Phi^s/2) \quad (2.23)$$

Here, C_t is the total electrolyte concentration in units (m^{-3}) and

$$\Phi^S \equiv e_0 |\phi^S| / k_B T \quad (2.24)$$

is the absolute value of the dimensionless surface potential. At high surface potentials ($\Phi^S \gg 1$), a good approximation of the Gouy equation (Equation 2.23) is

$$\Gamma_s = \frac{2}{\kappa_0} \sqrt{C_t} \exp(\Phi^S/2) \quad (2.25)$$

In the case of 1:1 electrolyte, Equation 2.19 can be integrated analytically. First, we take the root of Equation 2.19:

$$\frac{de_0\phi(z)/k_B T}{dz} = -\kappa_0 \sqrt{C_t} \left(e^{e_0\phi(z)/2k_B T} - e^{-e_0\phi(z)/2k_B T} \right) \quad (2.26)$$

Direct integration of Equation 2.26 gives an explicit relation between z and ϕ :

$$\kappa_0 \sqrt{C_t} z/2 = \operatorname{arctanh}\left(e^{e_0\phi/2k_B T}\right) - \operatorname{arctanh}\left(e^{e_0\phi^S/2k_B T}\right) \quad (2.27)$$

2.2.1.3 Thermodynamics of the Diffuse Double Layer: Adsorption and Surface Tension

The ion distribution in the electric double layer depends on the local potential $\phi(z)$. The ion adsorption Γ_j^{DL} of any ion j in the diffuse layer can be calculated by using Gibbs' definition of adsorption as an excess [41]:

$$\Gamma_j^{\text{DL}} \equiv C_j \int_0^\infty \left(e^{-e_j\phi(z)/k_B T} - 1 \right) dz \quad (2.28)$$

where the superscript "DL" indicates adsorption of the counterions, coions, and surfactant ions in the double layer only. In principle, the *total* surfactant adsorption is a sum of Γ_s^{DL} and the surface concentration Γ_s (which is the adsorption in the adsorption layer, driven by hydrophobic forces). The surfactant ions in the diffuse layer are repelled by the interface because they have the same charge. Usually, the surface potential Φ^S is high, so that the surfactant concentration in the diffuse layer is close to zero. This leads to a relatively small negative adsorption of the order of $\Gamma_s^{\text{DL}} \sim -C_s/\kappa$. Because $|\Gamma_s^{\text{DL}}| \ll \Gamma_s$, the adsorption of surfactant in the diffuse layer can be neglected. The same refers to the coions. Hence, under these conditions, only the adsorption of the counterions in the diffuse layer is of importance.

To calculate the integrals defined by Equation 2.28, it is convenient to change the integration variable to ϕ , by using the relation $dz = d\phi/(d\phi/dz)$,

$$\Gamma_j^{\text{DL}} \equiv C_j \int_{\phi^S}^0 \frac{\exp(-e_j\phi/k_B T) - 1}{d\phi/dz} d\phi \quad (2.29)$$

By inserting here the expression (2.26) for $d\phi/dz$, one can obtain explicit formulae for the adsorptions Γ_j^{DL} . For 1:1 electrolyte at high surface potential Φ^S , the result for the adsorption of the counterion i reads

$$\Gamma_i^{\text{DL}} = \frac{2C_i}{\kappa_0 \sqrt{C_t}} (e^{\Phi^{\text{S}/2}} - 1) \xrightarrow{\Phi^{\text{S}} \rightarrow \infty} \frac{2C_i}{\kappa_0 \sqrt{C_t}} \exp(\Phi^{\text{S}}/2) \quad (2.30)$$

To calculate the surface tension, the Gibbs isotherm is used [41]. If only one counterion of concentration C_i is present in the system, and the bulk solution is assumed ideal, one has

$$d\sigma = -k_{\text{B}}T\Gamma_s d \ln C_s - k_{\text{B}}T\Gamma_i^{\text{DL}} d \ln C_i \quad (2.31)$$

Because at high surface potential, the charge of the adsorbed layer is compensated only by the counterion in the diffuse layer, one has $\Gamma_i^{\text{DL}} = \Gamma_s$. Then, the Gibbs isotherm (2.31) simplifies to

$$d\sigma = -2k_{\text{B}}T\Gamma_s d \ln C \quad (2.32)$$

where C is the mean ionic activity of the surfactant [43–45], defined with

$$C = C_s^{1/2} C_i^{1/2} \quad (2.33)$$

If the solution is not ideal, the mean ionic activity C in Equation 2.32 will include the mean activity coefficient γ :

$$C = \gamma C_s^{1/2} C_i^{1/2} \quad (2.34)$$

2.2.1.4 Davies' Adsorption Isotherm

We now consider an ideal solution of ionic surfactant of concentration C_s in equilibrium with an "ideal" charged adsorbed monolayer with surface potential ϕ^{S} . The chemical potentials in the two states are

$$\mu^{\text{B}} = \mu_0^{\text{B}} + k_{\text{B}}T \ln C_s; \quad \mu^{\text{S}} = \mu_0^{\text{S}} + k_{\text{B}}T \ln \Gamma_s + e_s \phi^{\text{S}} \quad (2.35)$$

The difference from the corresponding expressions for nonionic surfactants (Equations 2.3 and 2.4), is the presence of the additional electrostatic energy term $e_s \phi^{\text{S}}$ in μ^{S} .

The condition for equilibrium between the surfactant molecules in the bulk solution and at the surface reads:

$$\mu_0^{\text{B}} + k_{\text{B}}T \ln C_s = \mu_0^{\text{S}} + k_{\text{B}}T \ln \Gamma_s + e_s \phi^{\text{S}} \quad (2.36)$$

Introducing here the dimensionless potential Φ^{S} (Equation 2.24), one obtains

$$\Gamma_s = K_s C_s \exp(-\Phi^{\text{S}}) \quad (2.37)$$

Equation 2.37 was first derived by Davies [26,27] (see also ref. [28]). The adsorption constant K_s in this equation is defined by Equation 2.6, but in this case, $\mu_0^{\text{B}} - \mu_0^{\text{S}}$ may contain electrostatic contributions.

The elimination of Γ_s from Equations 2.25 and 2.37 leads to an equation for the dependence of the surface potential Φ^{S} on the composition of the bulk solution [27]:

$$3\Phi^{\text{S}} = \ln \frac{\kappa_0^2 K_s^2}{4} + \ln \frac{C_s^2}{C_t} = 6 \ln \frac{\kappa_0 K_0}{2} + \ln \frac{C_s^2}{C_t} \quad (2.38)$$

Equation 2.38 shows that the surface potential Φ^S increases with C_s and K_s (due to the increased adsorption) and decreases with the total electrolyte concentration C_t (due to the additional screening effect of the electrolyte on the surface charge).

Inserting back the surface potential (2.38) into the isotherm (2.37), one obtains a generalization of Henry's isotherm for the adsorption of ionic surfactants:

$$\Gamma_s = K_0 C^{2/3} \quad (2.39)$$

where C is given by Equation 2.33, and K_0 is the adsorption constant of the ionic surfactant. It is related to Henry's constant K_s :

$$K_0 = (4K_s/\kappa_0^2)^{1/3} \quad (2.40)$$

The fact that according to Equation 2.39, Γ_s depends only on the mean ionic activity C is an explicit formulation of what is known as *salting-out effect* on ionic surfactant adsorption [44,45]. Equation 2.39 was first derived and confirmed by experimental data for $C_nH_{2n+1}SO_4^+$ at the W|O interface by Davies [27]. We will refer to this as Davies' isotherm. By using the procedure of Borwankar and Wasan [28], Ivanov et al. [29] derived Equation 2.39 and obtained the explicit expression (2.40) for K_0 (see also Section 2.3.2.1). According to Equation 2.40, K_0 should not depend on the electrolyte concentration, at least for moderate concentrations.

Substituting Equation 2.39 in the Gibbs isotherm (2.32) and integrating, one obtains the surface pressure isotherm:

$$\pi^S \equiv \sigma_0 - \sigma = 3k_B T K_0 C^{2/3} \quad (2.41)$$

which is also due to Davies [27]. Comparison with Equation 2.39 shows that $\pi^S = 3k_B T \Gamma_s$. Because the surface pressure of an ideal layer of a nonionic surfactant is $k_B T \Gamma_s$, it follows that the contribution to π^S of the double layer at high surface potential is [26]

$$\pi_{el}^S = 2k_B T \Gamma_s \quad (2.42)$$

For the sake of simplicity, until now, the ever-present counterion-specific effects were disregarded. It will be shown in Section 2.2.3 that these effects modify the adsorption constant, leading, instead of K_0 in Equations 2.39 and 2.41, to a new constant, $K = K_0 \exp(-u_{i0}/2k_B T)$, where u_{i0} is the counterion-specific adsorption energy (cf. Equation 2.56 below).

2.2.2 ADSORPTION BEHAVIOR AT W|G VERSUS W|O INTERFACE: LE LAYER AND SPREADING PRESSURE

Below, we analyze the experimental data for π^S versus the $2/3$ -power of the mean ionic activity $C^{2/3}$ at W|O and W|G interfaces for low and medium surfactant concentrations—data for sodium dodecyl sulfate, $C_{12}H_{25}SO_4Na$, at W|O and W|G interfaces in the presence of various concentrations of NaCl are shown in Figure 2.3. At W|G interface, the data exhibit two well-defined regions. At very low surface pressures (less than ca. 2–3 mN/m), a close-to-linear dependence without intercept is observed. At intermediate concentrations (up to cmc) and pressures, there is a second linear region, but with negative intercept. Denoting this intercept by π_0 , one can write for this region instead of Equation 2.41:

$$\pi^S = \pi_0 + 3k_B T K^{LE} C^{2/3} \quad (2.43)$$

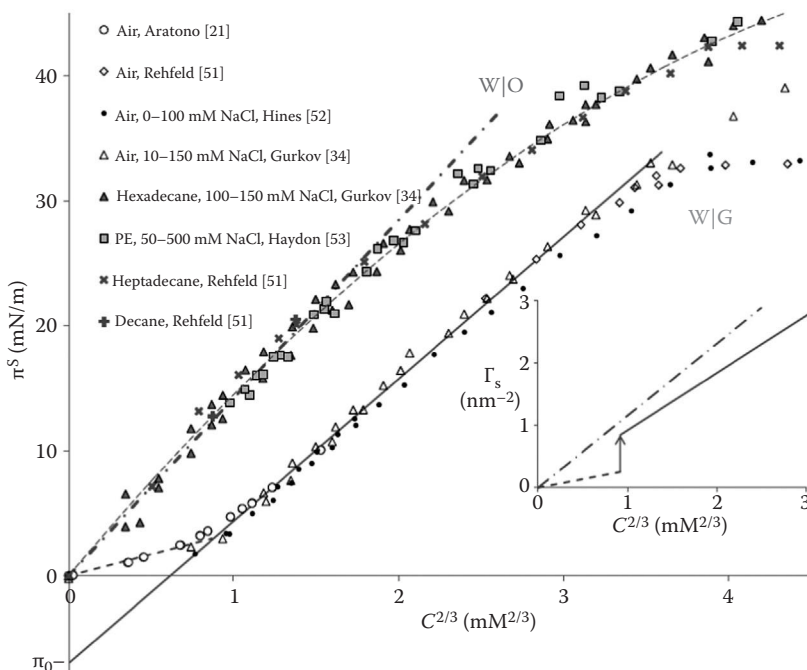


FIGURE 2.3 (See color insert.) Interfacial pressure π^S versus the $2/3$ -power of the mean activity $C^{2/3}$ for $C_{12}H_{25}SO_4Na$ solutions at different NaCl concentrations. (Data for the W|G surface from M. Aratono et al., *J. Colloid Interface Sci.* 98, 33–38, 1984; T.D. Gurkov et al., *Colloids Surf. A* 261, 29–38, 2005; S.J. Rehfeld, *J. Phys. Chem.* 71, 738–745, 1967; J.D. Hines, *J. Colloid Interface Sci.* 180, 488–492, 1996. With permission.) For the W|O interface, the oil is heptadecane, decane [51], hexadecane [34], and petroleum ether [53]. Solid line, data fit for the W|G in the range $C^{2/3} = 1.2$ to $3 \text{ mM}^{2/3}$ (the LE region), according to Equation 2.43. The short, dashed line stands for W|G data in the range $C^{2/3} = 0$ to $1 \text{ mM}^{2/3}$ (gaseous monolayer region). Dash-dot line, data fit of the W|O interface in the range $C^{2/3} = 0$ to $1.8 \text{ mM}^{2/3}$ (Equation 2.41). Long dashed line, quadratic fit of W|O data in the range $C^{2/3} = 0$ to $\text{cmc}^{2/3}$ (Equation 2.47). The adsorption parameters determined from these fits are listed in Table 2.1. Inset, the corresponding adsorption isotherms, $\Gamma_s(C^{2/3})$, calculated from Equation 2.39 with the adsorption parameters determined by the fits. The jump of Γ_s at $C = 0.81 \text{ mM}$ corresponds to a phase transition from a gaseous monolayer to LE state.

By analogy with Langmuir's treatment of noncharged monolayers [46], this behavior can be explained by assuming that the monolayer is in an LE state. In this state, the adsorbed hydrophobic tails form a very thin, but more or less dense, oil film spread onto the water phase. In contrast, in the first region, at lower concentrations, the surfactant molecules are in a gaseous state in which they are isolated from each other. The intersection point between the two lines probably corresponds to phase transition between the gaseous and the LE states (see Figure 2.3). Such a phase transition was also discussed by Aratono et al. [21], and observed with soluble nonionic surfactants by Kumpulainen et al. [40].

Langmuir's idea for the origin of π_0 (e.g., [47]) can be quantified as follows. Let σ_0^{WO} be the interfacial tension of the pure W|O interface, and let σ_0^{OG} be the oil–gas surface tension. The oil-like thin film formed by the adsorbed hydrophobic tails can be considered as a single “interface” (membrane) of interfacial tension $\sigma_0^{\text{M}} = \sigma_0^{\text{WO}} + \sigma_0^{\text{OG}}$, which for this system is the counterpart of the interfacial tension of the pure interface σ_0 . The hydrophilic heads of the surfactant are “adsorbed” at the W|O interface of the thin film. If their adsorption is ideal, one can use Equation 2.41 with σ_0 replaced with σ_0^{M} to calculate σ :

$$\sigma = \sigma_0^{\text{OG}} + \sigma_0^{\text{WO}} - 3k_{\text{B}}TK^{\text{LE}}C^{2/3} \quad (2.44)$$

However, by definition, the surface pressure π^S at the W|G interface is defined with respect to the pure W|G surface of tension σ_0^{WG} , that is, $\pi^S = \sigma_0^{WG} - \sigma$. Inserting Equation 2.44 into this definition, and comparing the result to Equation 2.43, one obtains

$$\pi_0 = \sigma_0^{WG} - \sigma_0^{WO} - \sigma_0^{OG} \quad (2.45)$$

According to these simple considerations, the intercept π_0 coincides with the spreading coefficient of a hydrocarbon on water [46]. Therefore, π_0 is referred to as *spreading pressure*. Langmuir's explanation of π_0 is confirmed by the data in Figure 2.3. Indeed, the spreading coefficient of dodecane on water is -6.4 mN/m (the values $\sigma_0^{WO} = 53.7$, $\sigma_0^{OG} = 25.3$, and $\sigma_0^{WG} = 72.6$ mN/m at 22°C were used [48]), versus $\pi_0 = -7$ mN/m determined from the data in Figure 2.3. However, this picture is oversimplified, and as will be shown in Section 2.2.4 below, π_0 , in fact, depends on the counterion,* and probably on the surfactant ionic head. The reason for these dependences is not yet clear.

The situation is different with the adsorption at the W|O interface. In this case, there is no oil-gas interface. Then, in Equation 2.45, one must replace σ_0^{WG} with σ_0^{WO} , and σ_0^{OG} with σ_0^{OO} (the latter is of course zero). Thus, one finds $\pi_0 = 0$, in accordance with the data in Figure 2.3: indeed, the surface pressure at the W|O interface follows rather well the simple dependence of Davies (Equation 2.41), with no intercept, up to $C^{2/3} \approx 2$ mM $^{2/3}$ ($C \approx 3$ mM).

The following observations deserve additional attention:

1. In accordance with the salting-out effect and Equation 2.32, the surface tension σ depends on the mean activity C only, as defined by Equation 2.34. Indeed, regardless of the electrolyte concentration, all data fall on two master curves π^S versus $C^{2/3}$ (one for W|G and one for water-alkane interface). This is so only if activities rather than concentrations are used—this also follows from Equation 2.32. The activity coefficients γ in Figure 2.3 were calculated by the formula [43,49]

$$\lg \gamma = -\frac{A\sqrt{C_t}}{1+B\sqrt{C_t}} + bC_t \quad (2.46)$$

If the total electrolyte concentration $C_t = C_{el} + C_s$ is in units (M), the Debye constant is $A = 0.5108$ M $^{-1/2}$ (at 298.15 K); for the empirical constants B and b , we used the mean values $B = 1.25$ M $^{-1/2}$ and $b = 0.0083$ M $^{-1}$ for all salts.

2. The dependence of π^S on $C^{2/3}$ is linear up to surface pressures of approximately 25 mN/m for W|O and 30 mN/m for W|G interfaces (the values of the slopes and the adsorption parameters are listed in Table 2.1). The respective values of $C^{2/3}$ are approximately 1.8 and 3.2 mM $^{2/3}$. The difference between the two systems is due to the larger second virial coefficient (larger repulsive interactions) at the W|O interface, which leads to earlier deviation from ideality. This is evident from the values of the respective second virial coefficients (for details, see Section 2.3.2.2 below).
3. At the W|G interface, the line drawn for the gaseous adsorbed layer is only tentative, as the validity of the Davies isotherm in this region is questionable due to the low potential and the possible effects of the charge discreteness. Phase transition from gaseous to LE state occurs at the W|G at $C = 0.81$ mM, corresponding to π^S of approximately 3.0 mN/m (Aratono et al. [21] found 0.83 mM and 3.9 mN/m, respectively). This corresponds to a transition from $\Gamma_s = 0.24$ nm $^{-2}$ to $\Gamma_s = 0.78$ nm $^{-2}$, that is, from a less dense gaseous structure to a more dense liquid-like monolayer (see the Γ_s vs. $C^{2/3}$ plot in Figure 2.3).

* cf. Figure 2.12.

TABLE 2.1
Values of the Adsorption Parameters

	Linear Fit with Equation 2.43			Quadratic Fit (Equation 2.47)	
	$d\pi^S/dC^{2/3}$ (mN/mM ^{2/3} m)	π_0 (mN/m)	K	π_0 (mN/m)	K
W G, LE	11.4	-7.0	129	-9.1	156
W O	13.5	0	161	0	178

Note: Determined from the data in Figure 2.3, according to Equation 2.47 for W|O interface and Equation 2.43 for W|G ($T = 25^\circ\text{C}$).

4. A number of different procedures were tested to determine K , including linear regression on a few initial points (straight lines in Figure 2.3) and square polynomial fit (long dashed curve in Figure 2.3) with the equation

$$\pi^S = \pi_0 + 3k_BTKC^{2/3} + bC^{4/3} \quad (2.47)$$

which is, in fact, Equation 2.134 derived in Section 2.3 below. Although the linear regression model looks satisfactory, we prefer the result from the polynomial fit because it generally yields K values closer to the ones obtained by using more realistic models, such as those discussed in Section 2.3.

5. From the $\pi^S(C^{2/3})$ data and Equation 2.47, we found for the LE region $K^{\text{LE}} = 156$ (Table 2.1). The latter is very close to the value for adsorption at W|O interface, $K^{\text{WO}} = 178$, which suggests that both processes are similar.

Davies also accounted for the cohesive (i.e., negative spreading) pressure of soluble ionic surfactants at the W|G interface [27]. However, neither Langmuir [46] nor Davies [27] used the simple isotherm (Equation 2.44). Instead, Langmuir used a correction for steric repulsion between the

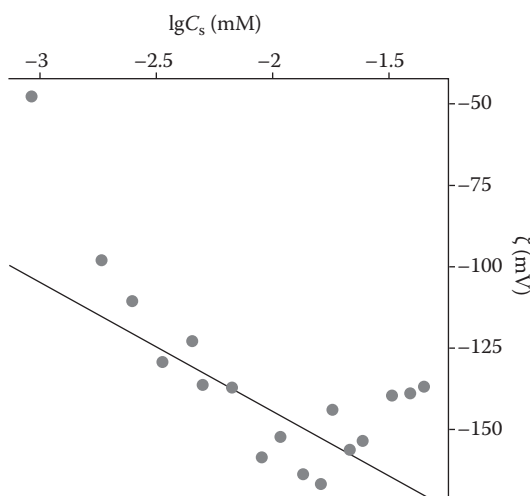


FIGURE 2.4 Dependence of the ζ potential (mV) at the water–hexadecane interface on $\lg C_s$ (mM) for $C_{12}H_{25}SO_4Na^+$ in the presence of 10 mM of NaCl [34]. Solid line, theoretical dependence (Equation 2.38) of the surface potential Φ^S (assumed equal to the ζ potential) on C_s , with no adjustable parameters ($K = 178$; see Table 2.1).

TABLE 2.2
Specific Adsorption Energies of the Ions Considered ($T = 298$ K)

Cation	R_b (Å)	n_w Equation 2.67	R_h (Å) Equation 2.68	N_w Equation 2.70	L_{ww} Equation 2.69 (m ⁶) × 10 ⁸⁰	$\alpha_{p,i}$ (Å ³)	I_i (J) × 10 ¹⁸	L_{wi} Equation 2.69 (m ⁶) × 10 ⁸⁰	$u_{i0}/k_B T$ Type I, Equation 2.65	$u_{i0}/k_B T$ Type II, Equation 2.66
Li ⁺	0.69 ¹	5.22	2.41	0.13	41.5	0.03 ¹	12.1 ²	11.5		-0.09
Na ⁺	1.02 ¹	3.53	2.18	0.40	134	0.15 ³	7.58 ²	53.1		-0.33
NH ₄ ⁺	1.53 ⁴	2.35	2.14	1.36	453	1.64 ¹	2.13 ²	378	-0.61	
K ⁺	1.41 ¹	2.55	2.12	1.07	354	0.79 ³	5.07 ²	253	-0.90	
Rb ⁺	1.65 ⁵	2.18	2.17	1.71	568	1.4 ¹	4.41 ²	431	-0.98	
NMe ₄ ⁺	2.80 ¹	1.29	2.94	8.36	2770	9.08 ¹	2.43 ²	2220	-1.05	
Anion	R_b (Å)	n_w	R_h (Å)	N_w	L_{ww} (m ⁶) × 10 ⁸⁰	$\alpha_{p,i}$ (Å ³)	I_i (J) × 10 ¹⁸	L_{wi} Equation 2.69 (m ⁶) × 10 ⁸⁰	$u_{i0}/k_B T$, Type I	$u_{i0}/k_B T$, Type II
Ac ⁻	1.65 ¹	2.18	2.17	1.71	568	5.50 ¹	0.544 ¹	545		-0.185
OH ⁻	1.33 ¹	2.71	2.11	0.90	297	2.04 ¹	0.345 ¹	134		-0.736
F ⁻	1.33 ¹	2.71	2.11	0.90	297	1.04 ²	0.545 ¹	99.1		-0.891
Cl ⁻	1.64 ¹	2.20	2.17	1.68	557	3.59 ²	0.580 ¹	359	-1.43	
Br ⁻	1.95 ¹	1.85	2.31	2.82	937	5.07 ²	0.540 ¹	480	-2.32	
NO ₃ ⁻	2.00 ¹	1.80	2.33	3.05	1010	3.93 ¹	0.631 ¹	420	-2.83	
N ₃ ⁻	1.95 ¹	1.85	2.31	2.82	937	4.45 ¹	0.444 ¹	360	-2.93	
ClO ₄ ⁻	2.40 ¹	1.50	2.61	5.26	1750	5.25 ²	0.758 ¹	642	-3.28	
BF ₄ ⁻	2.30 ¹	1.57	2.53	4.63	1540	2.80 ¹	0.902 ¹	388	-3.84	

Source: (1) From Marcus, Y. *Ion Properties*. Marcel Dekker, New York, 1997. (2) From Nikolskij, B.P. *Handbook of Chemistry*. Khimija, Leningrad, 1963 [in Russian]. (3) From Tavares, F.W. et al., *J. Phys. Chem. B* 108, 9228–9235, 2004. (4) Dietrich, B. et al., *J. Phys. Chem.* 91, 6600–6606, 1987. (5) Lide, D.R. (Ed.). *CRC Handbook of Chemistry and Physics* (83rd ed.). CRC Press, Boca Raton, FL, 2002.

Note: R_b , bare ion radius; n_w , hydration number (Equation 2.67); R_h , hydrated ion radius (Equation 2.68); N_w , number of water molecules in the ensemble, replaced by the ion upon adsorption (Equation 2.70); L_{ww} , London constant of this ensemble (Equation 2.69); $\alpha_{p,i}$, polarizability of the ion; I_i , second ionization potential of the cations and negative electron affinity of the anions; u_{i0} , ion-specific adsorption energy, Equation 2.66 for ions of type I (no deformation of the hydration shell) and Equation 2.65 for ions of type II (with deformation of the hydration shell). The ions in the table are ordered by increasing absolute values of u_{i0} . The sequence of both cations and anions is the same as in Hofmeister series (Equations 2.1 and 2.2), but for the cations this order corresponds to increasing efficiency as opposite to the series (Equation 2.2).

heads, whereas Davies introduced an empirical dependence of π_0 on Γ_s . We prefer to discuss the attractive and repulsive interactions between the adsorbed molecules separately in Section 2.3.

In Figure 2.4, the Davies model was tested further by comparison of the theoretical surface potential ϕ^S (Equation 2.38), with ζ potential measurements at the water–hexadecane interface [34]. All parameters in Equation 2.38 are known. In fact, the experimental data also involves ion-specific effects. Hence, the calculation of ϕ^S was performed with Equations 2.56 and 2.58 in Section 2.2.3 below, which accounts for the effect of the counterion on K and on ϕ^S ; the value $u_{i0} = -0.34 k_B T$ was used for Na^+ (Table 2.2). It turned out that the contribution of the ion-specific effect to ϕ^S is small. Taking into account the experimental difficulties (see also ref. [50]), the theoretical predictions seem adequate.

Another test of the model behind in Equations 2.41 and 2.43—the adequacy of the results for K (Equation 2.40)—will be given in Section 2.2.4.

2.2.3 COUNTERION-SPECIFIC EFFECTS ON THE ADSORPTION OF IONIC SURFACTANTS FROM DILUTE SOLUTIONS

2.2.3.1 Gouy Equation with Specific Interactions

We turn now to the theoretical treatment of the influence of the van der Waals interactions (which we consider as the most important specific interaction) of the counterions with the interface on the adsorption of a monovalent ionic surfactant. Toward this goal, an extended Poisson–Boltzmann equation involving both electrostatic and van der Waals potentials, is solved approximately. The ensuing generalized form of the Gouy equation, along with some thermodynamic considerations, will be used in the remaining parts of this section to account for the ion-specific effects on the adsorption and related phenomena with ionic surfactants.

Near the adsorbed layer of an ionic surfactant, the van der Waals forces between the counterion and the bulk phases lead to an increase of the local concentration of counterions in the diffuse double layer. The repulsive interactions disallow the counterion to approach the interface at a distance that is less than its radius R (bare or hydrated). Both interactions, repulsive and attractive, were modeled in a simple manner in ref. [29] by the following expression for the energy $u_i(z)$ of specific interaction between the ion and the interface:

$$u_i(z) = \frac{R_i^3}{(R_i + z)^3} u_{i0} \quad (2.48)$$

Here, R_i is the ionic radius (of the bare or of the hydrated ion, as will be discussed in Section 2.2.3.2) and u_{i0} is the van der Waals energy of an ion in the plane $z = 0$ situated at distance R_i from the interface (Figure 2.5). If one assumes that the van der Waals energy (Equation 2.48) and the electrostatic energy $e_i \phi^S$ are additive, the Boltzmann distribution will involve the sum of the two: $e_i \phi^S + u_i(z)$. The Poisson–Boltzmann equation (Equation 2.17) will then read:

$$\varepsilon \frac{d^2 \phi}{dz^2} = - \sum_i e_i C_i e^{-(e_i \phi + u_i(z))/k_B T} \quad (2.49)$$

This equation can be integrated by analogy with the derivation of Gouy equation (Equation 2.21), by using $2d^2 \phi/dz^2 = d(E^2)/d\phi$ and the Gauss condition (Equation 2.20). The result is

$$e_0^2 \Gamma_s^2 = -2\varepsilon \sum_i e_i C_i e^{-u_{i0}/k_B T} \int_0^{\phi^S} e^{-e_i \phi/k_B T} e^{-(u_i(z) - u_{i0})/k_B T} d\phi \quad (2.50)$$

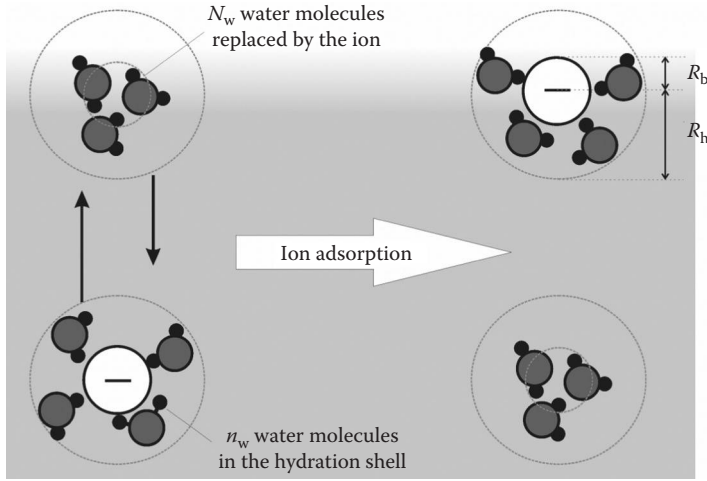


FIGURE 2.5 (See color insert.) Scheme of the process of adsorption of type I ions. Left, the ion is in the bulk. Right, the ion is at the interface. The n_w hydrating water molecules might be pushed away by the interface, so that the shortest distance of approach of the ion to the interface is the bare ion radius R_b . Upon adsorption, the ion exchanges position with an ensemble of N_w water molecules. For type II ions, the shortest distance of approach of the ion to the interface is the hydrated ion radius R_h .

At high surface potentials, only the counterions need to be taken into account in the sum in the right-hand side of this equation. This approximation is of crucial importance for the success of our theory because it simplifies all subsequent calculations. It can be also used in the case of ionized proteins and polymers (when $|\phi^S/k_B T| \gg 1$), but not for the adsorption of simple electrolytes. In the latter case, both cations and anions (whose properties are similar) have comparable participation in the diffuse layer whose local potential depends, in fact, on the small differences in their local concentrations [54]. With this approximation, the integrals on the right-hand side of Equation 2.50 can be evaluated by using an iterative procedure [29]. As zeroth iteration, one can use in the integrand the results for the case of the absent ion-specific effect obtained in Section 2.2.1.4, that is, one must set in Equation 2.50 $\phi^S = \phi_0^S$, where ϕ_0^S is given by Equation 2.38, and $z = z_0(\phi)$, given by Equation 2.27. Integration by parts then leads to

$$\int_0^{\phi_0^S} e^{-e_i \phi / k_B T} e^{-(u_i(z_0) - u_{i0}) / k_B T} d\phi = -\frac{k_B T}{e_i} e^{\phi_0^S} (1 - F_u) \quad (2.51)$$

where F_u stands for the expression

$$F_u = e^{-\phi_0^S} \left[e^{u_{i0} / k_B T} + \int_0^{\phi_0^S} e^{-e_i \phi / k_B T} \frac{de^{-(u_i(z_0) - u_{i0}) / k_B T}}{d\phi} d\phi \right] \quad (2.52)$$

At high surface potentials, the value of F_u was found to be much smaller than unity [29], so that it can be neglected in Equation 2.51. Using this approximation, one substitutes Equation 2.51 into Equation 2.50 to obtain a generalization of the Gouy equation (Equation 2.21), accounting for the ion-specific effect:

$$\Gamma_s^2 = \frac{4}{\kappa_0^2} \sum_i C_i e^{-u_{i0} / k_B T} e^{\phi_0^S} \quad (2.53)$$

(the Debye parameter κ_0 is given by Equation 2.22). If only one counterion is present in the system, Equation 2.53 simplifies to

$$\Gamma_s^2 = \frac{4}{\kappa_0^2} C_t e^{-u_{i0}/k_B T} e^{\Phi_0^S} \quad (2.54)$$

Substituting here the expression for the zeroth approximation of the surface potential Φ_0^S (Equation 2.38), one obtains an extension of the Davies isotherm $\Gamma_{s0} = K_0 C^{2/3}$ (Equation 2.39), accounting for ion-specific interactions:

$$\Gamma_s = K_0 e^{-u_{i0}/2k_B T} C^{2/3} \equiv K C^{2/3} \quad (2.55)$$

Here, C is the mean activity (Equation 2.33). Based on Equation 2.55 and the expression in Equation 2.40 for the nonspecific adsorption constant K_0 , one finds the expression for the ion-specific adsorption constant K :

$$K = K_0 e^{-u_{i0}/2k_B T} = \left(4K_s/\kappa_0^2\right)^{1/3} e^{-u_{i0}/2k_B T} \quad (2.56)$$

This procedure also allows for the determination of the first iteration of the surface potential Φ^S . To do so, the EOS (Equation 2.37) is used, with Γ_s given by Equation 2.55. After solving the result with respect to Φ^S , one obtains

$$\Phi^S = \frac{1}{3} \ln \frac{\kappa_0^2 K_s^2}{4} - \frac{1}{3} \ln \frac{C_s^2}{C_t} + \frac{u_{i0}}{2k_B T} \quad (2.57)$$

The comparison of Equations 2.55 and 2.57 with the respective zeroth (nonspecific) approximations for the surface potential Φ_0^S (Equation 2.38), and the adsorption Γ_{s0} (Equation 2.39), leads to

$$\Gamma_s = \Gamma_{s0} \exp(-u_{i0}/2k_B T), \quad \Phi^S = \Phi_0^S + u_{i0}/2k_B T \quad (2.58)$$

Note that the procedure is applied to the EOS (Equation 2.37) of an “ideal” monolayer. For other systems in which the surfactant molecules interact directly with each other (e.g., with van der Waals or steric forces), it is possible that other system parameters are affected (examples will be given in Sections 2.3 and 2.4).

In Equation 2.53, it is assumed that the surface charge density is due to the surfactant ions only (i.e., it is $e_s \Gamma_s$). In reality, the counterions can also penetrate into the adsorbed layer and in the empty spaces between the surfactant heads, but because of the relatively low values of the specific adsorption energies u_{i0} (cf. Table 2.2), they do not remain firmly bound (unlike the surfactant ions) to the interface. Hence, most common ions must be treated as part of the diffuse layer. This was proven directly by Shimamoto et al. [22], who studied experimentally, using total reflection X-ray absorption, the fine structure of ion distribution in the adsorbed and diffuse layers.

2.2.3.2 Specific Interaction between an Ion and the Interface

The adsorption potential of the counterion u_{i0} is related to a number of parameters, among them: the molecular or ion static polarizabilities, $\alpha_{p,w}$ and $\alpha_{p,i}$, and the ionization potentials I_w and I_i of the water molecule and the counterion, as well as the radii of the hydrated and bare ion (R_h and R_b , respectively). These parameters are not always available and even when they are, they are not very reliable. As shown in ref. [29], the adsorption energy u_{i0} depends strongly on the choice of the

parameters and can vary by orders of magnitude. When several values of a given parameter were available in the literature, all were tested and the one providing the best coincidence with the experimental data was retained.

In ref. [29], the calculation of the energy u_{i0} was performed, using the London expression for the intermolecular potential u_{ij} between molecules of types i and j at a distance r_{ij} [39]:

$$u_{ij} = -L_{ij}/r_{ij}^6 \quad (2.59)$$

where the London constant L_{ij} is related to the static polarizabilities $\alpha_{p,i}$ and $\alpha_{p,j}$ and the ionization potentials I_i and I_j of the interacting species:

$$L_{ij} = \frac{3\alpha_{p,i}\alpha_{p,j}}{2} \frac{I_i I_j}{I_i + I_j} \quad (2.60)$$

Upon adsorption, the counterion displaces an ensemble of N_w water molecules (Figure 2.5). In the initial state (before adsorption), the ion is in the bulk and has energy u_i^B and the N_w water molecules are at the interface, with total energy u_w^S (subscript indices “i” and “w” stand for “ion” and “water,” respectively, whereas superscript indices “S” and “B” stand for “surface” and “bulk,” respectively; see Figure 2.5). In the final state (adsorbed ion), the ion and the water molecules have exchanged positions and their energies became u_i^S and u_w^B , respectively. Thus, the ion adsorption energy u_{i0} , which is equal to the change in the energy upon adsorption, is

$$u_{i0} = (u_i^S - u_i^B) - (u_w^S - u_w^B) \quad (2.61)$$

The hydration shell of the large ions is loose because they have lower hydration numbers n_w and a larger area of bare ions. That is why it is assumed that when they are adsorbed, the hydration shell is deformed by the interface, as shown in Figure 2.5. Hence, they can approach the interface up to a distance equal to the radius R_b of the bare ion. We will refer to them as “type I ions.” They correspond to the chaotropes of Collins [55]. Smaller ions (“type II”) have denser adsorption shells, which cannot be rearranged upon adsorption, so that they will most probably remain immersed in water, along with their hydration layer. Therefore, they can approach the interface only to distances equal to R_h . Type II ions correspond to the cosmotropes of Collins [55].

We will first calculate the energy u_i^S of the type I ions. Toward this aim, the London potential (Equation 2.59) is integrated over the volume of the water phase excluding the hydration shell, with r_{ij} being the distance between the volume element $d^3r = r dr d\phi dz$ and the ion positioned at $r = 0, z = 0$ (that is, the integration is over $z > -R_b$ and $r^2 + z^2 < R_h^2$). The integration is performed in cylindrical coordinates:

$$u_i^S = - \int_{-R_b}^{R_h} \int_{\sqrt{R_h^2 - z^2}}^{\infty} \frac{L_{iw}\rho_w 2\pi r dr dz}{(r^2 + z^2)^3} - \int_{R_h}^{\infty} \int_0^{\infty} \frac{L_{iw}\rho_w 2\pi r dr dz}{(r^2 + z^2)^3} = - \frac{2\pi}{3} \frac{L_{iw}\rho_w}{R_h^3} \left(1 + \frac{3}{4} \frac{R_b}{R_h} \right) \quad (2.62)$$

here ρ_w is the molecular number concentration of water. Similarly, the bulk energy of the ion is (integration in spherical coordinates)

$$u_i^B = - \int_{R_h}^{\infty} \frac{L_{iw}}{r_{iw}^6} \rho_w 4\pi r_{iw}^2 dr_{iw} = - \frac{4\pi}{3} \frac{L_{iw}\rho_w}{R_h^3} \quad (2.63)$$

The respective energies of the ensemble of water molecules (assuming a sphere of radius R_h , or a part of it) are

$$u_w^S = -\frac{2\pi}{3} \frac{L_{ww}\rho_w}{R_h^3} \left(1 + \frac{3}{4} \frac{R_b}{R_h}\right); \quad u_w^B = -\frac{4\pi}{3} \frac{L_{ww}\rho_w}{R_h^3} \quad (2.64)$$

Substituting Equations 2.62 through 2.64 into the expression (Equation 2.61) for u_{i0} , one obtains an explicit relation for the adsorption energy with the ionic properties of type I ions:

$$u_{i0} = \left(1 - \frac{3}{4} \frac{R_b}{R_h}\right) \frac{2\pi}{3} \frac{\rho_w}{R_h^3} (L_{iw} - L_{ww}) \quad (2.65)$$

To calculate u_{i0} for type II ions, one must set $R_h = R_b$ in Equation 2.65, which simplifies the expression to

$$u_{i0} = \frac{\pi}{6} \frac{\rho_w}{R_h^3} (L_{iw} - L_{ww}) \quad (2.66)$$

The values of the hydration number n_w and the radius R_h of the hydrated ion depend strongly on the method used for their determination and can vary widely (see, e.g., p. 143 in ref. [56]). It seems that more reasonable results can be obtained by model calculations, rather than experimentally. For monovalent ions, Marcus [57] found that the hydration number n_w can be represented by the empirical relation

$$n_w = A_v/R_i \quad (2.67)$$

where $A_v = 3.6 \text{ \AA}$ for all ions. He further assumed that the hydrating n_w water molecules, considered as spheres with radius $R_w = 1.38 \text{ \AA}$ and volume $v_w = 11 \text{ \AA}^3$, are smeared around the ion, forming a layer of thickness $R_h - R_b$ and volume:

$$n_w v_w = \frac{4\pi}{3} (R_h^3 - R_b^3) \quad (2.68)$$

The last relation is used to calculate R_h . The values of n_w and R_h calculated in this way [29,57,58] are shown in Table 2.2. Robinson and Stokes (Equation 9.27 in ref. [43]) used a similar approach, but with a water molecular volume of $v_w = 30 \text{ \AA}^3$, which follows from the density of water. They also used different values of the hydration number n_w , which were calculated from the ion diffusivity (see Table 11.10 in ref. [43]). Ivanov et al. [29] calculated the radius R_h using both sets of parameters; for the ions of interest, the results for R_h did not differ much from each other. Both sets of R_h , those calculated by the method of Marcus and by the method of Robinson and Stokes, differ however much from the often-quoted values (e.g., in ref. [39]) of $R_h = 3.8, 3.6,$ and 3.3 \AA for $\text{Li}^+, \text{Na}^+,$ and K^+ , respectively, and $3.5, 3.3,$ and 3.3 \AA for $\text{F}^-, \text{Cl}^-,$ and Br^- , respectively.

The London constants L_{iw} for the ion–water molecule interaction, and L_{ww} for the interaction of N_w water molecules with a single water molecule are calculated directly from Equation 2.60:

$$L_{iw} = \frac{3\alpha_{p,i}\alpha_{p,w}}{2}, \quad L_{ww} = \frac{3}{4} N_w \alpha_{p,w}^2 J_w \quad (2.69)$$

For the calculation of L_{ww} , the ensemble of N_w water molecules is regarded as a sphere with polarizability $N_w \alpha_{p,w}$ [29]. The number N_w was assumed to be equal to the ratio between the volume of the bare ion and the volume of one water molecule [13]:

$$N_w = R_b^3 / R_w^3 \quad (2.70)$$

where R_w is the radius of the water molecule. For the value of R_w , two possibilities were tested in ref. [29]: (i) the average volume per molecule (30 \AA^3), based on the water density, yields $R_w = 1.93 \text{ \AA}$; and (ii) the actual volume of a water molecule, 11 \AA^3 , corresponds to $R_w = 1.38 \text{ \AA}$. Better agreement with the experimental data was obtained with the second option, $R_w = 1.38 \text{ \AA}$. The value of the static polarizability of water used was $\alpha_{p,w} = 1.48 \text{ \AA}^3$ and that of the ionization potential was $I_w = 2.02 \times 10^{-18} \text{ J}$ [59].

The values of the ionization potentials of the ions I_i are also questionable. In ref. [29], the ionization potential in vacuum was used for halogen ions. For the alkaline ions, it was corrected for the hydration effect, although the correction was small. Later, we found some new data about the system parameters, which showed that the hydration correction was even smaller and hereafter it was disregarded. For the cations, we used the second ionization potential because the first one corresponds to the ionization of the respective atom, not ion. Because the anions have already accepted one extra electron, their ionization potential must be equal to the negative value of the electron affinity.

2.2.4 COMPARISON WITH THE EXPERIMENTS

In the theoretical parts of this section (Subsections 2.2.1 through 2.2.3), we showed that a complete theory of the adsorption constant K and the adsorption isotherm of dilute monolayers requires detailed, more rigorous treatment of several important effects (most of which are new): (i) contribution $\sigma_0 \alpha_\perp$ to the adsorption energy E_a (cf. Equation 2.13) due to the penetration of the adsorbing surfactant tail through the clean interface; (ii) correct theory and new expression (Equation 2.16) for the adsorption “thickness” δ_a ; (iii) purely electrostatic (nonspecific) contribution to the adsorption constant K_0 (Equation 2.40); (iv) effect and nature of the spreading pressure π_0 in LE monolayers; and (v) ion-specific effect on the adsorption constant K (Equation 2.56); (vi) origin and calculation of the ion-specific adsorption energy u_{i0} (Equations 2.61, 2.65, and 2.66). It turned out that these effects must be properly accounted for to give adequate treatment and interpretation of the experimental data. Although our ultimate goal is to check our theory of the Hofmeister effect, cf. (v) and (vi), we were forced by the logic of the study to analyze first effects (i–iv) and to relegate the analysis of the ion-specific effect to the end of this subsection.

2.2.4.1 Experimental Verification of the Theory of Adsorption Constant K

Our expression for the adsorption energy E_a differs from Equation 4.3 of Davies and Rideal [26] with the presence of the new terms $\sigma_0 \alpha_\perp$ and the additional u_{CH_2} . As shown in Section 2.2.1.1 and in Figure 2.1, this term stems from the disappearance of area α_\perp of interfacial tension σ_0 when the surfactant molecule is adsorbed at the interface. To demonstrate the significance of this energy, we will analyze the data by Rehfeld [51] and Gillap et al. [62] for the adsorption of $C_{12}H_{25}SO_4Na$ at various W|O interfaces, where the oil phase is varied—this is a simple way to change the interfacial tension σ_0 of the *clean* surface without excessively affecting the other parameters of Equation 2.13, and allows direct observation of the expected effect of σ_0 on K .

Substituting the expression (Equation 2.7) for K_s into the definition (Equation 2.56) of K , and using the result (Equation 2.13) for the adsorption energy E_a , one obtains

$$\ln K + \frac{u_{i0}}{2k_B T} \equiv \ln K_0 = \text{const} + \frac{u_{CH_2}}{3k_B T} n_C + \frac{\alpha_\perp}{3k_B T} \sigma_0 \quad (2.71)$$

where

$$\text{const} = \frac{E_{\text{head}}}{3k_B T} + \frac{u_{\text{CH}_2}}{3k_B T} + \frac{1}{3} \ln \frac{4\delta_a}{\kappa_0^2} \quad (2.72)$$

In Equation 2.71, we preferred to correct the experimental adsorption constant K with the term $u_{i0}/2k_B T$, standing for the ion-specific adsorption energy of Na^+ ion ($u_{i0} = -0.34 \times k_B T$; cf. Table 2.2), to obtain the counterion-independent constant K_0 (Equation 2.40).

The effect of the nature of the hydrophobic phase is twofold. First (and more important), the change of the oil will affect σ_0 in the last term in Equation 2.71. The interfacial tension σ_0 of the pure W|O interfaces in Rehfeld's experiments ranges from 31.3 mN/m for water–1-hexene to 53.2 mN/m for water–heptadecane. According to Equation 2.71, this corresponds to a difference of approximately 0.4 in the value of $\ln K_0$. The second effect of the hydrophobic phase is on the transfer energy u_{CH_2} , which also depends, to a certain extent, on the nature of the oil. According to Tanford [38], the energy u_{CH_2} for transfer of a $-\text{CH}_2-$ group from water to hydrocarbons does not differ significantly for alkanes and alkenes. Aveyard and Briscoe [63] found only a weak dependence of u_{CH_2} on the length of the alkanes. We could not find data for the aromatic and cyclic hydrocarbons used by Rehfeld, but the relatively good coincidence between theoretical dependence and experimental values depicted in Figures 2.6 and 2.7 suggests that this second effect is smaller. Therefore, for all systems considered, only the term $\sigma_0 \alpha_{\perp}$ in Equation 2.71 will vary significantly with the nature of the oil.

Three typical surface pressure isotherms $\pi^S(C^{2/3})$ for oils of different interfacial tensions σ_0 , based on the data of Rehfeld [51], are shown in Figure 2.6. From these data, the values of K were determined according to Equation 2.47 and corrected with $u_{i0}/2k_B T$ according to Equation 2.71 to obtain the counterion-independent quantity $\ln K_0$. The obtained $\ln K_0$ values for several different oils with the same surfactant $\text{C}_{12}\text{H}_{25}\text{SO}_4\text{Na}$ are plotted in Figure 2.7 in coordinates $\ln K_0$ versus σ_0 .

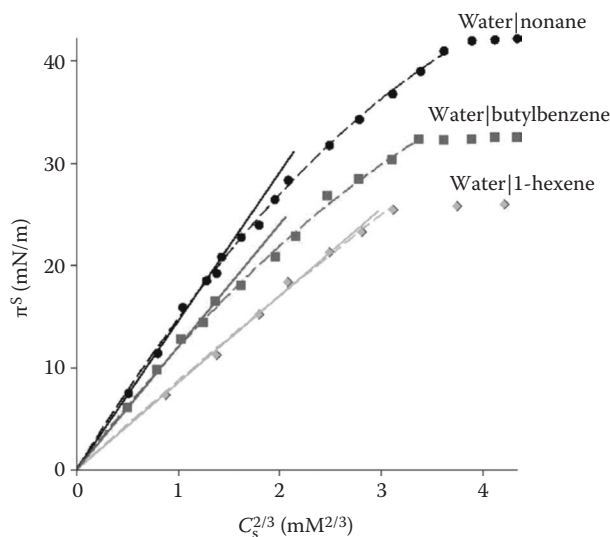


FIGURE 2.6 Surface pressure π^S versus $2/3$ -power of surfactant concentration $C_s^{2/3}$ for adsorption of $\text{C}_{12}\text{H}_{25}\text{SO}_4\text{Na}$ at the W|O interface for three typical oils with different interfacial tensions ($\sigma_0 = 50.9, 40.1,$ and 31.3 mN/m for water–nonane, water–butylbenzene, and water–1-hexene, respectively). (Experimental data from S.J. Rehfeld, *J. Phys. Chem.* 71, 738–745, 1967. With permission.) $T = 25^\circ\text{C}$. Solid lines, the linear dependence (Equation 2.39); dashed lines, fit with quadratic polynomial (Equation 2.47), up to cmc. From the polynomial dependences, the adsorption constants K , used in Figure 2.7, are determined.

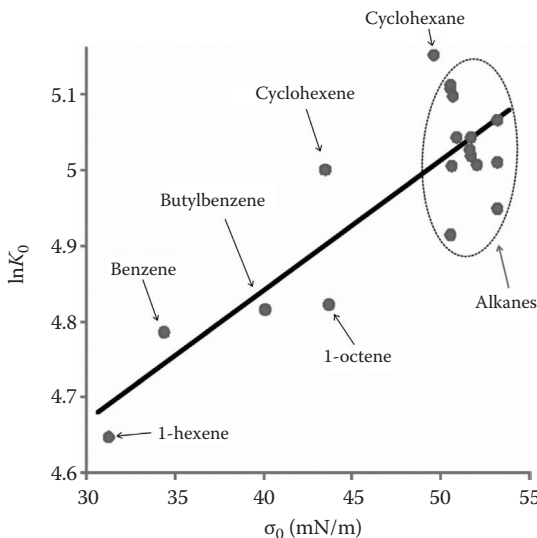


FIGURE 2.7 Dependence of $\ln K_0$ of $C_{12}H_{25}SO_4Na$ on the interfacial tensions σ_0 of the pure W|O interfaces. All points are determined from plots similar to those in Figure 2.6. The values of K were calculated from quadratic fit of π^s versus $C_s^{2/3}$ (Equation 2.47), and were corrected for the counterion effect according to Equation 2.71 to yield K_0 . Solid line, theoretical dependence (Equation 2.71), with the theoretical slope $\alpha_{\perp}/3k_B T = 0.0172$ m/mN (Equation 2.71), corresponding to $\alpha_{\perp} = 21.2 \text{ \AA}^2$ [38]. The intercept is 4.16 ± 0.08 .

The line is plotted according to Equation 2.71 with the theoretical slope $\alpha_{\perp}/3k_B T = 0.0172$ m/mN, corresponding to the value $\alpha_{\perp} = 21.2 \text{ \AA}^2$ given by Tanford [38] for the hydrocarbon chain cross-sectional area. The theoretical intercept, calculated using Equations 2.71 and 2.72 with values from the parameters given in Section 2.2.1.1, is 4.8. Its experimental value, according to Figure 2.7, is 4.16 ± 0.08 , which is reasonably close to the theoretical prediction. These data confirm our theory of the adsorption energy and thickness (Equations 2.13 and 2.16).

We now turn to the dependence of the adsorption constant K on the number of carbon atoms n_C in the hydrophobic tail of homologous surfactants. It is obvious from Figure 2.8 that the addition of $-\text{CH}_2-$ groups leads to a strong increase of the surface pressure π^s , which is related, according to Equation 2.71, to the energy u_{CH_2} of transfer of a $-\text{CH}_2-$ group from water to the hydrophobic phase. Both Tanford [38] and Davies and Rideal (Table 4I in ref. [26]) cite different values of u_{CH_2} for W|O and W|G interfaces. For the water–alkane interface, Tanford gives $u_{\text{CH}_2}^{\text{WO}} = 5.75 \times 10^{-21}$ J versus Davies and Rideal’s $u_{\text{CH}_2}^{\text{WO}} = 5.98 \times 10^{-21}$ J. For the W|G surface, Tanford gives $u_{\text{CH}_2}^{\text{WG}} = 4.35 \times 10^{-21}$ J. Davies and Rideal found that $u_{\text{CH}_2}^{\text{WG}}$ depends on the coverage: for dilute monolayers, $u_{\text{CH}_2}^{\text{WG}} = 4.17 \times 10^{-21}$ J, whereas for denser monolayers (90 \AA^2 per molecule) $u_{\text{CH}_2}^{\text{WG}} = 4.85 \times 10^{-21}$ J.

We will analyze the effect of the chain length n_C of a homologous series of surfactants on the value of K_0 at different W|O interfaces (Figure 2.8a). Because the interfacial tensions σ_0 of the oils used in the experiment (especially of the nonsaturated ones) differ significantly, we transformed Equation 2.71 in such a way that this effect was eliminated. This was achieved by subtracting the term $\alpha_{\perp}\sigma_0/3k_B T$ and adding instead a term $\alpha_{\perp}\sigma_0^{\text{alkane}}/3k_B T$ referring to a typical alkane, for example, decane with $\sigma_0^{\text{alkane}} = 52$ mN/m. As a result, a new adsorption constant, K_0^{alkane} , independent of σ_0 was introduced:

$$\ln K_0^{\text{alkane}} \equiv \ln K_0 + \frac{\alpha_{\perp}}{3k_B T} (\sigma_0^{\text{alkane}} - \sigma_0) = \text{const} + \frac{\alpha_{\perp}}{3k_B T} \sigma_0^{\text{alkane}} + \frac{u_{\text{CH}_2}}{3k_B T} n_C \quad (2.73)$$

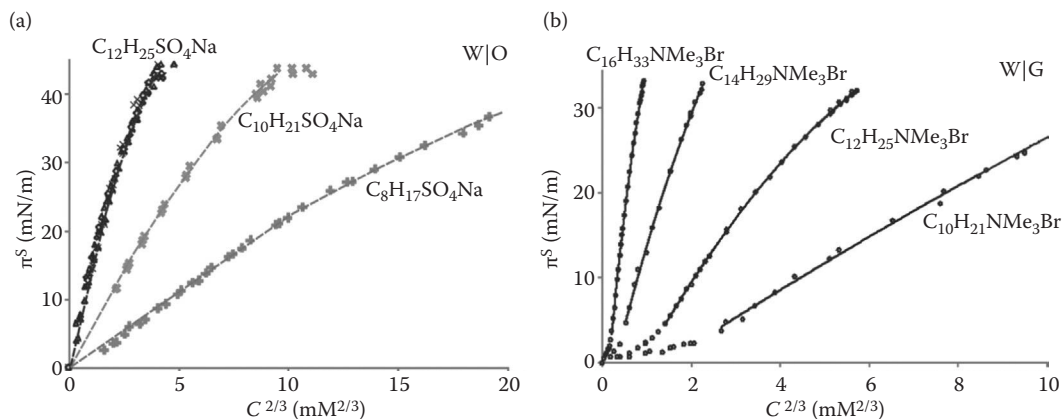


FIGURE 2.8 Dependence of the surface pressure π^S versus $2/3$ -power of the mean activity, $C^{2/3}$. (a) Alkylsulfates of different chain lengths at the W|O interface, with or without added NaCl. The data for $C_{12}H_{25}SO_4Na$, with various amounts of NaCl, are the same as in Figure 2.3; the data for $C_8H_{17}SO_4Na$ and $C_{10}H_{21}SO_4Na$ at the water–decane interface with the addition of 50 to 500 mM of NaCl [64]. The data were processed as in Figure 2.6: dashed lines are quadratic fits with Equation 2.47. (b) Alkyltrimethylammonium bromides of different chain lengths at the W|G interface. Data for $C_{10}H_{21}NMe_3Br$ with 0 to 10 mM NaBr [18]. (Data for $C_{12}H_{25}NMe_3Br$, $C_{14}H_{29}NMe_3Br$, and $C_{16}H_{33}NMe_3Br$ from Aratono, M. personal communication, 2010. With permission.) Solid lines correspond to quadratic fits (Equation 2.47). From the fits, the values of the adsorption constants K were obtained; the results are used in Figure 2.9.

K_0^{alkane} is the expected adsorption constant of a surfactant with n_C carbon atoms at the water–alkane interface. The data for adsorption of sodium alkylsulfates and alkyltrimethylammonium bromides at the W|O interface, plotted in Figure 2.9, confirms Equation 2.73. The value $u_{CH_2}^{WO} = 5.75 \times 10^{-21}$ J, quoted by Tanford, was used to draw the lines.

We now turn to the adsorption of homologous series of surfactants at the W|G surface in the LE region (Figure 2.8b). We determined the adsorption constant K for each particular system by fitting the experimental data $\pi^S(C^{2/3})$ with Equation 2.47. Because σ_0 is the same for all surfactants, the analysis can be carried out by using Equation 2.71. The calculated dependence of $\ln K_0$ on n_C for the LE monolayers at W|G is again linear, as shown in Figure 2.9, that is, Equation 2.71 is valid. Surprisingly, within experimental error, the slope is the same as for the W|O interface, that is, u_{CH_2} is again 5.75×10^{-21} J, which is considerably larger than the values quoted by Davies and Rideal, 4.17 to 4.85×10^{-21} J [26]. The coincidence of the W|G and W|O values of u_{CH_2} is certainly because the transfer of a $-CH_2-$ group is from water to an LE adsorption layer (and not to a gas!), which is nearly equivalent to a transfer from water to oil. We found it difficult to estimate the corresponding energy of transfer from water to *gaseous* monolayers due to the insufficient and contradictory data for adsorption in this region.

In Figure 2.10, the surface pressure isotherms of four $C_{12}H_{25}NMe_3^+$ salts at the W|G surface are shown. Obviously, the counterion can drastically increase the surface activity of the surfactant ion, and the effect of the counterion follows the Hofmeister series (Equation 2.2). Similar curves were obtained (but not shown) for the other surfactants considered below—alkylsulfates and 1-dodecyl-4-dimethyl aminopyridinium ($C_{12}H_{25}PyrNMe_2^+$) halogenides.

Our aim now is to demonstrate how the results in Figure 2.10 can be explained quantitatively with the model developed in Section 2.3. Equation 2.56 can be presented in logarithmic form:

$$\ln K = \ln K_0 - \frac{1}{2} \frac{u_{i0}}{k_B T} \quad (2.74)$$

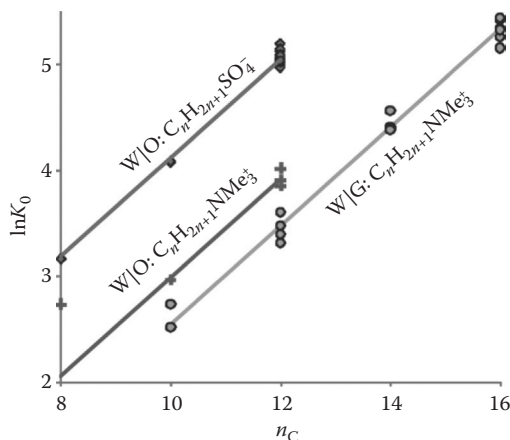


FIGURE 2.9 Dependence of the logarithm of the adsorption constant $\ln K_0$ on the number of carbon atoms n_C in the hydrocarbon chain. Circles, data for alkylsulfates at the W|O interface; the values of K_0 were calculated from $\pi^S(C_s^{2/3})$ dependences similar to those shown in Figure 2.8. The data for $C_{12}H_{25}SO_4Na$ are from the same sources as in Figure 2.7; data for $C_8H_{17}SO_4Na$ and $C_{10}H_{21}SO_4Na$ with 0 to 500 mM of NaCl, and the oil is either decane [64] or other alkanes [62]. Correction for σ_0 was made, and all data were reduced to $\sigma_0 = 52$ mN/m according to Equation 2.73. Crosses, adsorption of alkyltrimethylammonium salts at the W|O interface. Data for $C_8H_{17}NMe_3^+$ and $C_{10}H_{21}NMe_3^+$ with decane in the presence of 0 to 500 mM NaCl [64]; data for $C_{12}H_{25}NMe_3Br$ and Cl with hexane, hexadecane [65], and petroleum ether and 0 to 500 mM NaCl [53]. Diamonds, data for the adsorption of alkyltrimethylammonium bromides and chlorides at the W|G surface, with various amounts of salt [18,65,66]. Lines, the theoretical dependence (Equation 2.71) with the value $u_{CH_2} = 5.75 \times 10^{-21}$ J given by Tanford [38]. The intercepts were determined as fitting parameters: -0.55 for alkylsulfates at the W|O interface, -1.63 for alkyltrimethylammonium salts at the W|O interface, and -2.12 at the W|G interface.

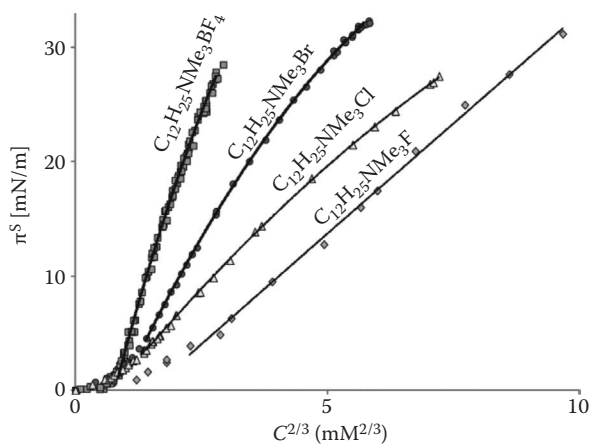


FIGURE 2.10 Surface pressure π^S versus $C^{2/3}$ ($2/3$ -power of the mean activity) for $C_{12}H_{25}NMe_3^+$ salts at the W|G surface. The surface pressure at a given concentration increases in accordance with Hofmeister series ($BF_4^- > Br^- > Cl^- > F^-$). Data for $C_{12}H_{25}NMe_3BF_4$ with the addition of 0 to 15 mM NaBF₄ [20]; $C_{12}H_{25}NMe_3Br^-$ and Cl^- are without additives [20,65]; the data for $C_{12}H_{25}NMe_3F$ are obtained with 100 mM NaF added to 0 to 15 mM $C_{12}H_{25}NMe_3Br$ solutions [68]. $T = 23^\circ C$ to $25^\circ C$. The lines are quadratic fits. The results were used for calculation of the respective adsorption constants K , used in Figure 2.11.

This suggests that the model can be checked by plotting $\ln K$ versus u_{i0} . We found scarce experimental data for surface tension of the same ionic surfactant with different counterions (with or without added salt). To expand the databases to the full set of counterions of interest, we used the relation (Equation 2.71) between K_0 and the number of carbon atoms n_C . We were able to recalculate, from the value of K of any surfactant from a homologous series, the adsorption constant K_{12} for a surfactant with $n_C = 12$:

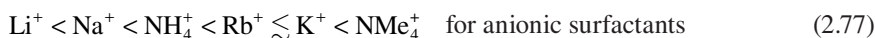
$$\ln K_{12} = \ln K - \frac{u_{\text{CH}_2}}{3k_B T} (n_C - 12) \quad (2.75)$$

where $u_{\text{CH}_2} = 5.75 \times 10^{-21}$ J as determined above. For a homologous series of surfactants with the same ionic head at the same interface and temperature, this standard constant K_{12} should depend on u_{i0} only (Equations 2.71 and 2.72).

The specific adsorption energies u_{i0} of the ions were taken from Table 2.2. The values of K were found by curve-fitting with the quadratic dependence (Equation 2.47). They were then used to calculate the nonspecific adsorption constant K_0 for each of the surfactant ions through Equation 2.74. In agreement with the theory, the obtained values of $\ln K_0$ are the same for a given surfactant ion with any considered counterion. In some cases, adsorption data for a mixture of two counterions only were available, for example, refs. [18,67,68]. Then, the value of K_0 , which is unique for the two counterions, was determined by using a procedure described in Section 2.2.4.2; after that, K was recalculated for the prevailing ion from Equation 2.56, $K = K_0 \exp(-u_{i0}/2k_B T)$.

The dependence of the adsorption constant on the adsorption energy u_{i0} of the counterion is illustrated in Figure 2.11, where $\ln K_{12}$ versus $-u_{i0}/k_B T$ is plotted for three different surfactant ions. The lines are drawn according to Equation 2.74 by using the theoretical slope 1/2 and the average values of $\ln K_0$ for each surfactant ion: 4.80 ± 0.13 for $\text{C}_{12}\text{H}_{25}\text{SO}_4^-$, 3.74 ± 0.02 for $\text{C}_{12}\text{H}_{25}\text{PyrNMe}_2^-$, and $\ln K_0 = 3.28 \pm 0.10$ for $\text{C}_{12}\text{H}_{25}\text{NMe}_3^+$. The theory describes the data adequately. Note that the values of the adsorption energy u_{i0} listed in Table 2.2 were obtained without using any free adjustable parameter.

Below, we arranged the counterions according to the experimental values of the adsorption constants K_{12} (Figure 2.11), that is, according to their “adsorption efficiency” for a given surfactant head group:



Because of the relation (Equation 2.74) between K and u_{i0} , the order will remain the same if one uses as criterion the absolute value of u_{i0} (see Table 2.2). The cation series (Equation 2.77) follows the Hofmeister series (Equation 2.2), with one exception—the NH_4^+ ion. In contrast, although the sequence (Equation 2.76) of the anions is the same as the Hofmeister series (Equation 2.1), the signs “<” and “>” are opposite, that is, the “adsorption efficiency” in Equation 2.76 increases whereas the “precipitation efficiency” in Equation 2.1 decreases from left to right. A possible reason for the coincidence of the two series of cations is that Hofmeister worked only with negatively charged proteins, similar to interfaces with adsorbed anionic surfactants, corresponding to Equation 2.77. The situation with the anions is the opposite—Hofmeister’s proteins were negatively charged, whereas the interface with adsorbed cationic surfactants is positive. This explanation is in agreement with the finding of Schwierz et al. [4], who argued that the relative order of anions may reverse depending on the charge of the

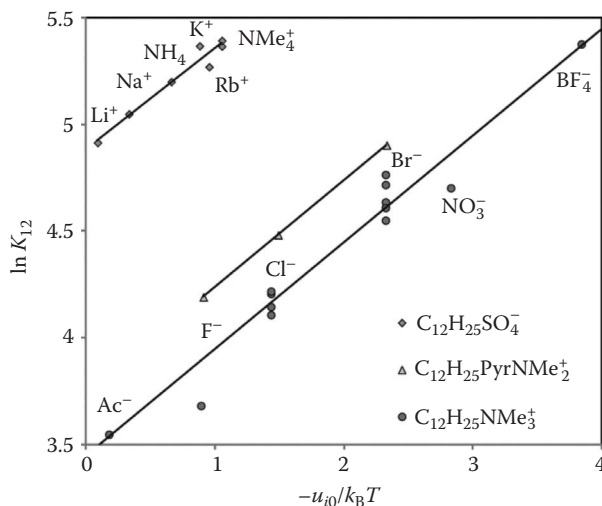


FIGURE 2.11 Dependence of the adsorption constant K_{12} on the ion adsorption energy $-u_{i0}/k_B T$ of surfactants with three different head groups at the W|G surface. The values of K_{12} were determined from $\pi^s(C^{2/3})$ data as those in Figure 2.10. For this plot, we used the calculated values of u_{i0} (Table 2.2), corresponding to the model presented in Sections 2.2.3.1 and 2.2.3.2. Lines, comparison with the theoretical dependence with fixed slope 1/2 (Equation 2.74). Sources: $C_{12}H_{25}SO_4^-$ with Li^+ alone [67,69] and Li^+ with added 1 mM NH_4^+ [67]; for Na^+ (Figure 2.3); NH_4^+ and NMe_4^+ stand for 5 to 10 mM NH_4^+ or NMe_4^+ with 1 to 3 mM Li^+ [67]; K^+ and Rb^+ are without added salt [69]; $T = 23^\circ C$ to $33^\circ C$. K values for $C_{12}H_{25}PyrNMe_2^+$ halogenides are calculated from Koelsch's data [70] (no added salt or 100 mM $NaF/NaCl/NaBr$ added to $C_{12}H_{25}PyrNMe_2Br$ at room temperature). $C_{12}H_{25}NMe_3^+$ is from Aratono (BF_4^- with the addition of 0–10 mM $NaBF_4$, $NaCl$, $NaBr$ [20,21,65] and Bergeron [66]). Data for $C_{10}H_{21}NMe_3^+$ (Br^- with 0–10 mM $NaCl$ [18,66]), $C_{14}H_{29}NMe_3^+$ (Cl^- and Br^- [65,66]), and $C_{16}H_{33}NMe_3^+$ (Cl^- and Br^- in the presence of 0–100 mM salt [18,65,66]; 10–100 mM Ac^- , NO_3^- or F^- in the presence of 0–0.5 mM Br^- [18]) are also used in this figure—the corresponding adsorption constants K of these surfactants were reduced to the standard constant K_{12} of $C_{12}H_{25}NMe_3^+$ through Equation 2.75. All measurements with $C_nH_{2n+1}NMe_3^+$ have been performed at $T = 20^\circ C$ to $25^\circ C$.

surface, with $I^- > Cl^- > F^-$ on positively charged surfaces but $F^- > Cl^- > I^-$ on negatively charged surfaces (see also ref. [3]).

The Hofmeister effect also influences the other parameters in the surface pressure isotherm (Equation 2.47). We found a strong correlation between the spreading pressure π_0 of the surfactant and its counterion. In Figure 2.12, the spreading pressure of $C_nH_{2n+1}NMe_3^+$ salts is plotted against u_{i0} . The dependence is close to linear; the spreading pressure increases in absolute value with $-u_{i0}$.

The good coincidence between the theoretical dependence Equation 2.74 with the theoretical values of u_{i0} (Table 2.2) and experiment, demonstrated above, suggests that the effect of the type of counterions on the adsorption constant K is due not only to steric reasons, related to ion size, as it is sometimes assumed [71–73], but is also due to van der Waals interactions.

There are at least three effects that we observed and partially explained but we believe that they still need additional in-depth analysis and clarification: (i) the factors determining the value of the nonspecific adsorption constant K_0 of the surfactant; (ii) the value and nature of the adsorption constant of a surfactant at W|G surface in *gaseous* monolayers; and (iii) the reason for the dependence of the spreading pressure π_0 on the ion-specific adsorption energy u_{i0} (Figure 2.12). We have some preliminary ideas and calculations but we lack, for the time being, enough reliable data to check and improve them. Hence, we postpone these issues for future studies.

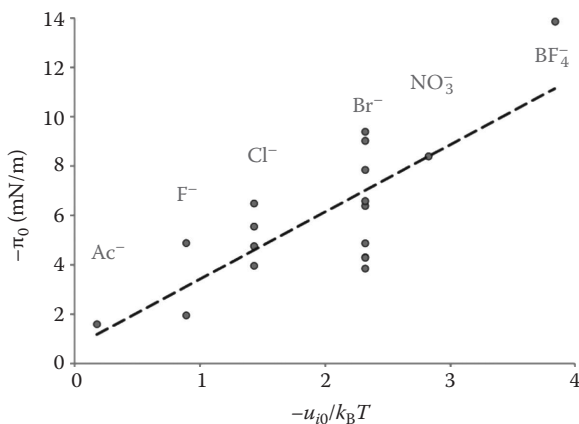


FIGURE 2.12 Hofmeister effect on Langmuir's spreading pressure π_0 of $C_nH_{2n+1}NMe_3^+$ salts at the W|G surface: dependence of $-\pi_0$ on $-u_{i0}/k_B T$. The spreading pressure is equivalent to the intercept of the quadratic fits of $\pi^S(C^{2/3})$ (Figure 2.10). π_0 shows strong correlation with the ion adsorption energy u_{i0} . Data sources as in Figure 2.11.

2.2.4.2 Adsorption in the Presence of a Mixture of Counterions

Often, ionic surfactants are used with a mixture of counterions, for example, refs. [18,20]. Well-studied experimentally are systems with two counterions, one of which came with the surfactant and the second one with the salt additive (e.g., $C_{12}H_{25}SO_4^-Na^+$ in the presence of KCl additive). To derive an analogue of the isotherm (Equation 2.55); for a mixture of two counterions, one must use the multi-ion form of the generalized Gouy equation (Equation 2.53) instead of its one-counterion version (Equation 2.54). By analogy with the derivation of Equations 2.55 through 2.57, the expression for the zeroth approximation for the potential Φ_0^S (Equation 2.38), is inserted into the Gouy equation (Equation 2.53) to give:

$$\Gamma_s^2 = \left(\frac{4K_s}{\kappa_0^2} \right)^{2/3} \sum_i C_i e^{-u_{i0}/k_B T} \frac{C_s^{2/3}}{C_t^{1/3}} \quad (2.78)$$

After taking the square root of this equation and making some rearrangements, a generalization of the adsorption isotherm (Equation 2.55) for ion mixtures is obtained:

$$\Gamma_s = K_0 \left(\sum_i x_i e^{-u_{i0}/k_B T} \right)^{1/2} C_t^{1/3} C_s^{1/3} \quad (2.79)$$

where K_0 is given by Equation 2.40, C_t is the total electrolyte concentration, and $x_i = C_i/C_t$ is the fraction of i th counterions from all counterions. For the most common case of two counterions, Equation 2.79 can be rewritten as

$$\Gamma_s = K_0 \left(x_1 e^{-u_{10}/k_B T} + x_2 e^{-u_{20}/k_B T} \right)^{1/2} C_t^{1/3} C_s^{1/3} \quad (2.80)$$

We proceed now to the calculation of the surface pressure π^S . If the adsorption of the coion is neglected, Gibbs isotherm reads:

$$d\pi^S = \Gamma_1 d\mu_1 + \Gamma_2 d\mu_2 + \Gamma_s d\mu_s \quad (2.81)$$

If the bulk surfactant solution is ideal, Equation 2.81 yields $C_s(\partial\pi^S/\partial C_s)_{C_1, C_2} = k_B T \Gamma_s$. This equation can be integrated, after substituting into it Γ_s from Equation 2.80. The result is:

$$\pi^S = 3k_B T K_0 \left(\frac{C_1}{C_t} e^{-u_{10}/k_B T} + \frac{C_2}{C_t} e^{-u_{20}/k_B T} \right)^{1/2} C_t^{1/3} C_s^{1/3} + \pi_0(C_1, C_2) \quad (2.82)$$

The integration constant π_0 is Langmuir's spreading pressure. In the case of the W|O interface, it is obvious that $\pi_0 = 0$ if the small effect of the salt itself on σ_0 [6,74] is neglected. If only one counterion is present in the system, then $C_1 = C_t$ and $C_2 = 0$, and the bracket in the above equation simplifies to $\exp(-u_{i0}/2k_B T)$, and Equation 2.82 becomes identical to the one-counterion surface tension isotherm (Equation 2.43). Equation 2.82 is compared in Figure 2.13 to experimental data from ref. [18] for solutions of $C_{16}H_{33}NMe_3X$ and NaX , where X stands for Cl^- and Br^- . For these two ions and the data in the figure, we assumed that the dependence of the spreading pressure π_0 on C_1 and C_2 was negligible.

For the W|O interface, where $\pi_0 = 0$, one can determine the adsorptions Γ_1 and Γ_2 of the two counterions from the surface pressure isotherm (Equation 2.82). From Gibbs isotherm (Equation 2.81), it follows that

$$\Gamma_1 = \frac{C_1}{k_B T} \left(\frac{\partial \pi^S}{\partial C_1} \right)_{C_2, C_s} \quad \text{and} \quad \Gamma_2 = \frac{C_2}{k_B T} \left(\frac{\partial \pi^S}{\partial C_2} \right)_{C_1, C_s} \quad (2.83)$$

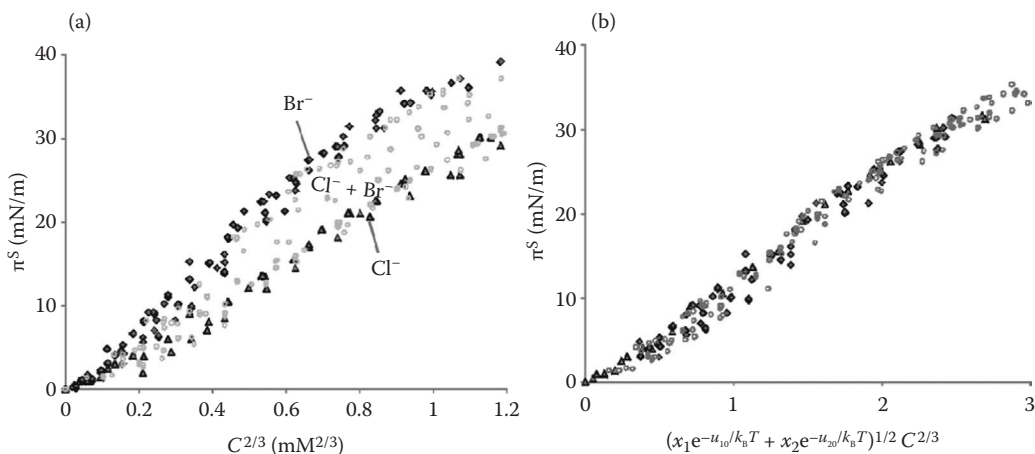


FIGURE 2.13 (See color insert.) (a) Surface pressure π^S versus $2/3$ -power of the mean activity $C^{2/3}$ for $C_{16}H_{33}NMe_3Cl$ with or without added $NaCl$ (diamonds); $C_{16}H_{33}NMe_3Br$ with or without $NaBr$ (triangles); $C_{16}H_{33}NMe_3^+$ in the presence of both ions Cl^- and Br^- (empty circles) at the W|G surface. The data for a single counterion, Cl^- or Br^- , falls on separate master curves according to the salting-out effect (Equation 2.32), with slopes $3k_B TK_{Br}$ and $3k_B TK_{Cl}$ correspondingly. In contrast, the data for the counterion mixtures are dispersed between these two curves. (b) Drawn in coordinates π^S versus $(e^{-u_{10}/k_B T} x_1 + e^{-u_{20}/k_B T} x_2)^{1/2} C_t^{1/3} C_s^{1/3}$, all data fall on a single master curve with slope $3k_B TK_0$, according to Equation 2.80. (Data from Para, G. et al., *Adv. Colloid Interface Sci.* 122, 39–55, 2006.)

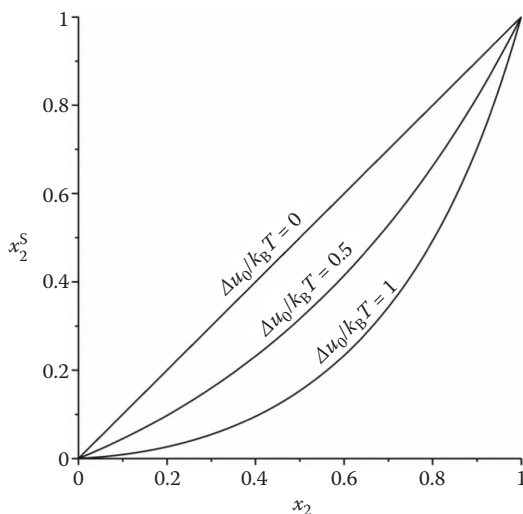


FIGURE 2.14 Interface composition $x_2^S = \Gamma_2/\Gamma_s$ as a function of the bulk composition $x_2 = C_2/C_t$ at different values of the difference $\Delta u_0 = (u_{20} - u_{10})/k_B T$. The surface is enriched with the ion having larger (in absolute value) ion adsorption energy u_{i0} .

Here, substituting π^S from Equation 2.82 with $\pi_0 = 0$, one can obtain the adsorptions of both counterions and thereby, together with Equation 2.80, the composition of the interface in terms of molar parts $x_i^S \equiv \Gamma_i/\Gamma_s$:

$$x_2^S = 1 - x_1^S = x_2 \frac{1 + \frac{1}{2} x_1 [1 - e^{(u_{20} - u_{10})/k_B T}]}{x_2 + x_1 e^{(u_{20} - u_{10})/k_B T}} \quad (2.84)$$

The dependence of the surface composition x_2^S on the bulk composition x_2 at three values of the difference $(u_{20} - u_{10})/k_B T$ is illustrated in Figure 2.14.

2.3 EOS AND ADSORPTION ISOTHERM OF DENSE MONOLAYERS

2.3.1 NONLOCALIZED ADSORPTION OF NONIONIC SURFACTANTS

Most theories of the EOS and adsorption isotherms of ionic surfactants are obtained by simply extending theories of nonionic surfactants to account for the electrostatic interaction. This is usually done by using the Gouy equation (Equation 2.21), for example, see refs. [28,36,75]. Our analysis revealed that most of the problems encountered in the theory of adsorption of ionic surfactants stem, in fact, from certain drawbacks of the respective theories of nonionic surfactants. These problems were dealt with in refs. [31–33]; for the readers' convenience, we will present in this section a brief account of some of the findings from these articles.

The two most widely used EOS for nonionic surfactants are those of Langmuir–Frumkin (usually called the Frumkin equation) and the two-dimensional (2-D) equation of van der Waals (also known as the Volmer–De Boer equation):

1. Frumkin EOS [76,77],

$$\frac{\pi^S}{k_B T} = -\frac{1}{\alpha_L} \ln(1 - \alpha_L \Gamma_s) - B_{\text{att}} \Gamma_s^2 \quad (2.85)$$

Here, α_L is the area parameter of Langmuir's model (we will show in Section 2.3.1.1 that α_L is different from the cross-sectional area of the molecule); B_{attr} is the attractive part of the second virial coefficient accounting for the long-ranged attractive interactions between the adsorbed molecules (see Section 2.3.1.2).

2. Van der Waals EOS [78,79],

$$\frac{\pi^S}{k_B T} = \frac{\Gamma_s}{1 - \alpha_V \Gamma_s} - B_{\text{attr}} \Gamma_s^2 \quad (2.86)$$

Here, α_V is the area parameter of Volmer's model, also different from the cross-sectional area of the molecule.

A third important EOS for hard discs (unfortunately, not much used in the literature) was derived by Helfand et al. [80]. If their result is modified with the same attractive term $-B_{\text{attr}} \Gamma_s^2$ as in Equations 2.85 and 2.86, the following equation is obtained:

3. Modified Helfand–Frisch–Lebowitz (HFL) EOS [31,33,80],

$$\frac{\pi^S}{k_B T} = \frac{\Gamma_s}{(1 - \alpha \Gamma_s)^2} - B_{\text{attr}} \Gamma_s^2 \quad (2.87)$$

The first terms on the right-hand sides of Equations 2.85 through 2.87 refer to hard core interactions only and were proposed by Langmuir [76], Volmer [78], and Helfand et al. [80], respectively. The attractive term $-B_{\text{attr}} \Gamma_s^2$ was introduced into the Langmuir isotherm by analogy with the three-dimensional van der Waals EOS by Frumkin [77], to make it applicable to surfactants with large hydrophobic tails. De Boer [79] did the same for Volmer EOS, and in refs. [31,33], it was done for the EOS of HFL. One must keep in mind that an additive term, proportional to Γ_s^2 , strictly speaking, can account only for the contribution of binary collisions, that is, it is correct only for low surface concentrations, whereas the hard core parts are valid (in the framework of the respective model) for any surface concentration.

Let us discuss the physical model behind these equations. The Langmuir EOS can be applied for adsorption on a 2-D lattice of adsorption centers if the following conditions hold [81]: (i) each center can be occupied only by one molecule, (ii) the molecules cannot exchange positions over the surface and jump from center to center, and (iii) the adsorbed molecules do not interact with each other neither by attractive nor by repulsive forces. The first two limitations must also apply to Frumkin EOS (Equation 2.85). Quite obviously, the combination of these conditions cannot be realized with a fluid adsorbed layer—despite this, the Langmuir and Frumkin EOSs have been widely applied to such systems. One possible reason is the fact that the integration of Langmuir EOS with Gibbs adsorption isotherm to eliminate Γ_s leads exactly to the empirical Szyszkowski equation [82], which describes well the dependence of the surface tension σ on the surfactant concentration C_s for low-molecular weight nonionic surfactants.

Tonks [83] has shown that the equation of Volmer is rigorous for delocalized adsorption of solid rods at a line. However, such a one-dimensional (1-D) model is hardly applicable to a 2-D fluid interface. A more realistic model for the adsorbed monolayer of nonionic surfactant would be a 2-D system of hard discs. Reiss et al. [84] developed a very astute procedure (which they called *scaled particle theory*) for treating systems of hard core particles. They solved exactly several problems, related to hard particles, but it turned out that the 2-D case (hard discs at interfaces) had in principle no exact analytical solution [85]. Nevertheless, Helfand et al. [80] succeeded in deriving an almost exact simple 2-D EOS for nonattracting hard discs (the original HFL equation is Equation 2.87 with

$B_{\text{attr}} = 0$). It is impossible to present in a concise manner their theory and we refer the interested reader to their original article [80]. Rusanov [86] obtained their result using a totally different approach.

The respective adsorption isotherms can be obtained by integrating the Gibbs equation for non-ionic surfactant ($d\pi^S = k_B T \Gamma_s d \ln C_s$): by substituting in it π^S from either Equations 2.85, 2.86, or 2.87, and integrating with respect to Γ_s , one finds the corresponding adsorption isotherms for nonionic surfactants*:

$$1. \text{ Langmuir-Frumkin: } K_s C_s = \frac{\Gamma_s}{1 - \alpha_L \Gamma_s} \exp(-2B_{\text{attr}} \Gamma_s) \quad (2.88)$$

$$2. \text{ van der Waals: } K_s C_s = \frac{\Gamma_s}{1 - \alpha_V \Gamma_s} \exp\left(\frac{\alpha_V \Gamma_s}{1 - \alpha_V \Gamma_s} - 2B_{\text{attr}} \Gamma_s\right) \quad (2.89)$$

$$3. \text{ Modified HFL: } K_s C_s = \frac{\Gamma_s}{1 - \alpha \Gamma_s} \exp\left[\frac{\alpha \Gamma_s (3 - 2\alpha \Gamma_s)}{(1 - \alpha \Gamma_s)^2} - 2B_{\text{attr}} \Gamma_s\right] \quad (2.90)$$

The isotherm, following from the original HFL EOS, can be obtained by setting $B_{\text{attr}} = 0$ in Equation 2.90. Equations 2.88 through 2.90 will be extended in Section 2.3.2 to ionic surfactants.

2.3.1.1 The Area per Molecule α

The reliability of the hard core parts of Equations 2.85 through 2.87 (with $B_{\text{attr}} = 0$) can be checked by comparing their virial expansions in terms of Γ_s with the exact virial EOS, obtained numerically [80], namely,

$$\pi^S/k_B T = \Gamma_s + 2\alpha\Gamma_s^2 + 3.128\alpha^2\Gamma_s^3 + 4.262\alpha^3\Gamma_s^4 + 4.95\alpha^4\Gamma_s^5 + \dots \quad (2.91)$$

This expansion can be compared with the virial expansion of the hard core part of the HFL EOS (Equation 2.87):

$$\pi^S/k_B T = \Gamma_s + 2\alpha\Gamma_s^2 + 3\alpha^2\Gamma_s^3 + 4\alpha^3\Gamma_s^4 + 5\alpha^4\Gamma_s^5 + \dots \quad (2.92)$$

Equation 2.92 nearly coincides with the exact expansion (Equation 2.91). This means that HFL EOS (Equation 2.87) with $B_{\text{attr}} = 0$, is a very good approximation for the nonlocalized adsorption of rigid discs both at low and high surface coverages. In contrast, the expansions of the hard core parts of Langmuir and Volmer EOS (Equations 2.85 and 2.86), are in obvious disagreement with Equation 2.91:

$$\text{Langmuir: } \pi^S/k_B T = \Gamma_s + \alpha_L \Gamma_s^2/2 + \alpha_L^2 \Gamma_s^3/3 + \alpha_L^3 \Gamma_s^4/4 + \alpha_L^4 \Gamma_s^5/5 + \dots, \quad (2.93)$$

$$\text{Volmer: } \pi^S/k_B T = \Gamma_s + \alpha_V \Gamma_s^2 + \alpha_V^2 \Gamma_s^3 + \alpha_V^3 \Gamma_s^4 + \alpha_V^4 \Gamma_s^5 + \dots \quad (2.94)$$

* Helfand et al. derived only the EOS with $B_{\text{attr}} = 0$ (Equation 2.87). The adsorption isotherms (Equation 2.90), based on this equation, and its modification for interacting surfactants (Equation 2.87), were also derived and extended to ionic surfactants in refs. [29,31–33]. However, because these isotherms are virtually straightforward consequences of Equation 2.87, we prefer to call all of them modified adsorption isotherms of HFL.

This could be expected because their physical bases are very different from nonlocalized adsorption at fluid interfaces. The above conclusions are visualized in Figure 2.15, where the curves correspond to the indicated EOS and the points refer to the exact numerical values. The plot of the HFL equation almost coincides with the numerical values, which confirms that it is nearly exact. The Langmuir and Volmer EOS are in substantial error compared with the exact numerical solution.

It is interesting to find out how the values of α_L and α_V are related to the actual area α used in the HFL model. To answer this question, Ivanov et al. [31] compared the ratio $\pi^S/k_B T \Gamma_s$, predicted by the three equations. Because the left-hand sides of the three EOS (Equations 2.85 through 2.87) are model-independent and equal, so must be the right ones. After dividing the three equations by Γ_s (for easier calculations) and setting the so-obtained right-hand side equal, one arrives at the following conditions for the identity of Langmuir and HFL EOS:

$$-\frac{1}{\alpha_L \Gamma_s} \ln(1 - \alpha_L \Gamma_s) = \frac{1}{(1 - \alpha \Gamma_s)^2} \quad (2.95)$$

Similarly, for Volmer and HFL EOS, one has:

$$\frac{1}{1 - \alpha_V \Gamma_s} = \frac{1}{(1 - \alpha \Gamma_s)^2} \quad (2.96)$$

Equation 2.96 can be easily solved for $\alpha_V(\Gamma_s)$:

$$\alpha_V/\alpha = 2 - \alpha \Gamma_s \quad (2.97)$$

In contrast, the relation between α_L and α can be found only by numerically solving Equation 2.95. The asymptotic behavior of the solution for α_L at $\Gamma_s \rightarrow 0$ is

$$\alpha_L/\alpha = 4 - \frac{14}{3} \alpha \Gamma_s + \dots \quad (2.98)$$

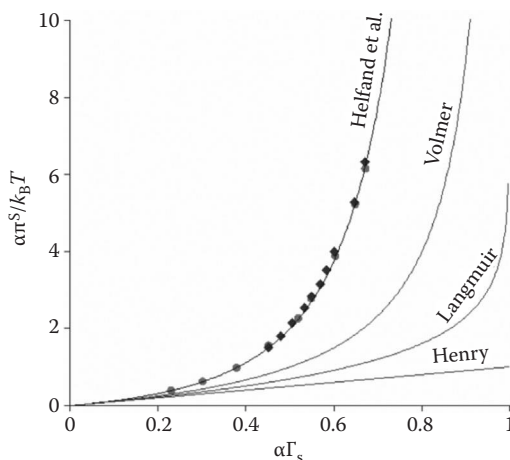


FIGURE 2.15 Dependence of the dimensionless surface pressure $\alpha \pi^S/k_B T$ on the surface coverage $\alpha \Gamma_s$: comparison of the hard core parts of HFL, Volmer, and Langmuir EOS (Equations 2.85 through 2.87; solid lines) with Henry's EOS ($\pi^S/k_B T = \Gamma_s$) and exact numerical calculations for delocalized adsorption of rigid discs at fluid interface (points). Circles, Monte Carlo calculations [80]; diamonds, dynamic calculations [80]. For all lines, α denotes the area per molecule (α , α_V , or α_L) corresponding to the plotted EOS.

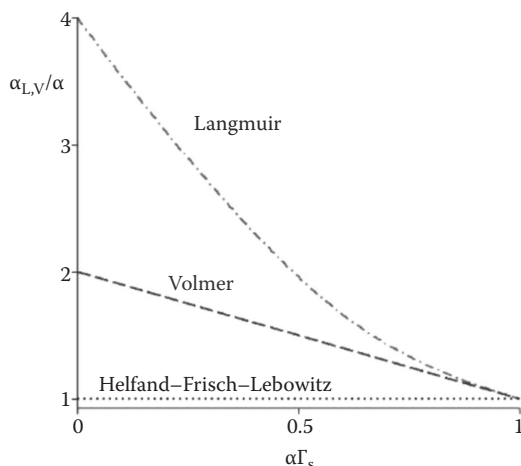


FIGURE 2.16 Dependence of the ratio of the area parameters α_L and α_V to the actual molecular area $\alpha = \pi d^2/4$ (d – molecular diameter) on the surface coverage $\alpha\Gamma_s$ for the EOS of Langmuir (dash-dot line) and Volmer (dashed line; cf. Equations 2.95 through 2.97). For comparison, we have plotted the dotted line, which presents the analogous ratio (which is unity) for the molecular area of the HFL model.

whereas at $\alpha\Gamma_s \rightarrow 1$ it is $\alpha_L/\alpha = 2 - \alpha\Gamma_s + \dots$. The obtained dependences of α_L and α_V on $\alpha\Gamma_s$ are shown in Figure 2.16. Rusanov [87] had ideas similar to ours about the dependence of the minimum area per molecule on the adsorption Γ_s . By using a different approach, he found the limiting values 4 and 1 at $\alpha\Gamma_s \rightarrow 0$ and $\alpha\Gamma_s \rightarrow 1$, respectively, for the Langmuir model. For the initial slope at $\Gamma_s \rightarrow 0$, however, he obtained -6.616 instead of our value $-14/3$ (see Equation 2.98).

The results from this section lead to the conclusion that the area per molecule, determined by using a model isotherm whose hard core part is different from the HFL equation, may not be a true physical constant, but may depend on the model used and the adsorption Γ_s .

2.3.1.2 The Interaction Parameter β

At low coverages, EOS can be expanded into virial series with respect to the powers of Γ_s :

$$\frac{\pi^s}{k_B T} = \Gamma_s + B_2 \Gamma_s^2 + B_3 \Gamma_s^3 + \dots \quad (2.99)$$

The second virial coefficient B_2 for hard particles of diameter d (cross-sectional area $\alpha = \pi d^2/4$) with attractive potential $u(r)$ between two particles at a distance r is (cf. e.g., ref. [81]):

$$B_2 = -\pi \int_0^\infty (e^{-u/k_B T} - 1) r dr = 2\alpha - \pi \int_d^\infty (e^{-u/k_B T} - 1) r dr \quad (2.100)$$

The second integral in this equation is, in fact, B_{attr} in Equations 2.85 through 2.87. Its value depends on the model used for $u(r)$, as will be demonstrated below with two examples.

In the first example, it is assumed that $u(r)$ is small and long-ranged. If $|u/k_B T| \ll 1$, then the exponent in Equation 2.100 can be expanded into series up to the linear term. If in addition $u(r)$ is represented by the London potential, $u = -L/r^6$ (L is London interaction constant), then B_{attr} is:

$$B_{\text{attr}} \equiv \pi \int_d^\infty (e^{-u/k_B T} - 1) r dr \approx -\frac{\pi}{k_B T} \int_d^\infty u(r) r dr = \frac{\pi L}{4k_B T d^4} \quad (2.101)$$

B_{attr} has dimension of area, so it seems natural to scale it with the area of the molecule α . The result is $B_{\text{attr}}/\alpha = u_c/k_B T$, where the contact potential $u_c = L/d^6$ is the absolute value of the attraction energy at contact between the molecules (u at $r = d$). We will call the parameter $\beta \equiv u_c/k_B T$ the *attraction constant*. Consequently, Equation 2.100 reads:

$$B_2 = 2\alpha - B_{\text{attr}} = 2\alpha - \alpha\beta \quad (2.102)$$

This result for B_2 can also be obtained by expanding the modified HFL equation (Equation 2.87) into a series in terms of $\alpha\Gamma_s$ and using $B_{\text{attr}} = \alpha\beta$.

The second example, which we will use in Section 2.3.1.3, is the short-ranged “sticky potential,” introduced by Baxter [88]:

$$u(r) = \begin{cases} \infty, & r > d; \\ -E, & d < r < d(1 + \lambda); \\ 0, & r > d(1 + \lambda). \end{cases} \quad (2.103)$$

It is represented in Figure 2.17 by a solid line: up to the minimum distance d between the molecules the potential energy u is $+\infty$; then, in the potential well between d and $d(1 + \lambda)$, where $\lambda < 1$, it remains constant and equal to $-E(\lambda)$; after that it becomes zero. When two particles are in the attractive potential well and $\lambda \rightarrow 0$, the particles “stick” (hence, the name of the potential). It is assumed that under these conditions, $E \rightarrow \infty$ but in such a way that the attractive potential well gives finite contribution to B_{attr} . Baxter proposed an attraction potential depending logarithmically on λ . We will use the following expression (slightly different from Baxter’s) for E :

$$E = k_B T \ln (u_c/k_B T \lambda) \quad (2.104)$$

In the limit $\lambda \rightarrow 0$, the energy $E \rightarrow \infty$. Here, u_c is still an undetermined coefficient. Substituting the expression (Equation 2.104) for E into Equation 2.101, and performing the integration (by keeping λ constant), one finds an expression that gives the evolution of B_{attr} with λ ; in the limit $\lambda \rightarrow 0$, it leads to the final expression for B_{attr} :

$$B_{\text{attr}} = 4\alpha \left(\frac{u_c}{k_B T} - \lambda \right) \left(1 + \frac{\lambda}{2} \right) \xrightarrow{\lambda \rightarrow 0} 4\alpha \frac{u_c}{k_B T} \quad (2.105)$$

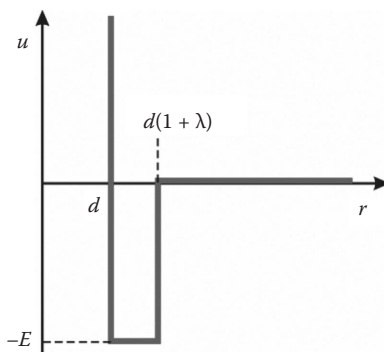


FIGURE 2.17 Scheme of the sticky potential (Equation 2.103; solid line).

Thus, for sticky potential, one has

$$B_{\text{attr}} = 4\alpha\beta; \quad B_2 = 2\alpha - 4\alpha\beta, \quad \text{where} \quad \beta = u_c/k_B T \quad (2.106)$$

The limiting transition $\lambda \rightarrow 0$ affects only the well width λd . The “moment of sticking” corresponds to $\lambda = 0$; hence, it is natural to assume that u_c is again the absolute value of the contact energy—for example, for discs attracting each other with the London potential, u_c is given again by $u_c = L/d^6$.

Unlike B_2 (and hence, B_{attr}), which depends on the model used for $u(r)$, the attractive constant $\beta = u_c/k_B T$ depends only on the nature of the interacting molecules and its value can be considered as a measure of the strength of this interaction—this allows easier comparison between different surfactants. The dependence of B_{attr} on the model used for $u(r)$ is reflected by the difference in the numerical coefficients in the expressions in Equations 2.102 and 2.106 for the cases of small, long-ranged potential and sticky potential, respectively.

2.3.1.3 New EOS and Adsorption Isotherm for Nonionic Surfactants

We checked the reliability of the basic EOS, discussed in the beginning of this section, by using experimental interfacial tension data for $\text{C}_{12}\text{H}_{25}\text{SO}_4\text{Na}$ [51], $\text{C}_{12}\text{H}_{25}\text{NMe}_3\text{Cl}$ [65,89], and $\text{C}_{12}\text{H}_{25}\text{NMe}_3\text{Br}$ [65] at the W|O interface. We considered the adsorption at the water–hexane interface because for W|O systems, β must be positive and small [39], and this fact can be used as a criterion for the correctness of a given isotherm. Ionic surfactants were selected because the nonionics are usually soluble in oil. We processed the data using three adsorption isotherms (Equations 2.88 through 2.90), based on the three basic EOS with attraction: Frumkin (Equations 2.85), van der Waals (Equations 2.86), and the modified HFL equations (Equations 2.87). The results for α and β , where $\beta = B_{\text{attr}}/\alpha$ as given by Equation 2.102, are summarized in Table 2.3 (the data processing is described in Section 2.3.2.2).

All three isotherms were fitted with high-precision (coefficient of determination R_d^2 higher than 0.999), but led to very different results for α and β . Thus, we reach a very important conclusion: the good fit of the data does not guarantee that the adsorption model is correct. The data for α confirm our conclusions in Section 2.3.1.1, namely, that the value of the area per molecule α strongly depends on the model used, and only the HFL model leads to realistic values, of the order of 20 to 25 \AA^2 . The most troubling result, however, is related to the values of β , which theoretically is expected to have positive value close to zero [39]. Instead, β was found negative for all isotherms. Because we had no doubt about the validity of the HFL model with $\beta = 0$, we concluded that the reason for the poor results was the way the attraction between the surfactant molecules was accounted for in Equations 2.85 through 2.87.

This gave us the impetus to derive in ref. [32] a new, hopefully more correct, EOS and adsorption isotherm whose hard core repulsion part is the same as in the original HFL model (see Equations

TABLE 2.3
Adsorption Parameters α and β , Obtained by Curve-Fitting of the Interfacial Tension Data for the Water–Hexane Interface by Using the Corresponding Models (Frumkin, van der Waals, and Modified HFL)

Model	$\text{C}_{12}\text{H}_{25}\text{SO}_4\text{Na}$ [51]		$\text{C}_{12}\text{H}_{25}\text{NMe}_3\text{Cl}$ [65,89]		$\text{C}_{12}\text{H}_{25}\text{NMe}_3\text{Br}$ [65]	
	α [\AA^2]	β	α [\AA^2]	β	α [\AA^2]	β
Frumkin: Equations 2.85 and 2.88	41.4	−1.7	48.1	−2.2	42.6	−1.7
van der Waals: Equations 2.86 and 2.89	30.0	−3.2	35.3	−4.3	31.5	−3.0
Modified HFL: Equations 2.87 and 2.90	20.6	−1.3	24.4	−2.0	21.9	−1.0

2.87 and 2.90 with $B_{\text{attr}} = 0$). The new isotherm was thoroughly checked with experimental data for several nonionic surfactants and performed quite well [33]. Here, we will present a brief account of this model, and in Section 2.3.2 below, it will be extended to ionic surfactants.

To find some clues for the derivation for the 2-D case, first the 1-D case of nonlocalized adsorption was solved. The 1-D system considered consists of N_s rods, each of length d , strung on a straight thread of total length ℓ (which is the 1-D counterpart of the surface area A), interacting with a sticky potential. The convenient thermodynamic potential for this problem is the Gibbs isothermic–isobaric potential for N_s molecules: $G = N_s \mu_s$ (Chapters 1 and 2 in ref. [81]). The partition function Δ_p for the system under consideration is:

$$\Delta_p = \int_0^{\infty} Z \exp(-\ell \pi^\ell / k_B T) d\ell, \quad G = -k_B T N_s \ln \Delta_p \quad (2.107)$$

where Z is the canonical partition function of the adsorbate, and π^ℓ is the line pressure (J/m). The integration over ℓ in Equation 2.107 corresponds to an increase of the system length ℓ from 0 to ∞ at constant temperature, pressure π^ℓ , and number of adsorbed molecules N_s . From the Gibbs–Duhem equation of this system, one can calculate the adsorption Γ_s :

$$N_s d\mu_s = \ell d\pi^\ell \rightarrow \frac{1}{\Gamma_s} = \frac{\ell}{N_s} = \frac{d\mu_s}{d\pi^\ell} = -k_B T \left(\frac{\partial \ln \Delta_p}{\partial \pi^\ell} \right)_{N_s} \quad (2.108)$$

The last equation leads to the EOS. This approach is rigorous but rather complicated because of the necessity to know the partition function Z .

Hemmer and Stell [90] simplified the required calculation significantly. They argued that if the intermolecular potential is short enough, it will act only between neighboring molecules. Hence, they replaced the partition function Z in Equation 2.107 with $\exp(-u/k_B T)$, where u is the short range intermolecular potential (Equation 2.103). Because ℓ is variable, it was replaced in Equation 2.107 by the distance r between the interacting molecules. Thus, Equation 2.107 was simplified to [90]:

$$\Delta_p = \int_0^{\infty} e^{-u(r)/k_B T} e^{-\pi^\ell r / k_B T} dr \quad (2.109)$$

This equation was used in ref. [32] to derive a new EOS by inserting the expression for $u(r)$ (Equation 2.103). One can easily solve the obtained integral to find:

$$\ln \Delta_p = \ln \frac{k_B T}{\pi^\ell} - \frac{\pi^\ell d}{k_B T} + \ln \left[e^{-\lambda \pi^\ell d / k_B T} \left(1 - \frac{\beta}{\lambda} \right) + \frac{\beta}{\lambda} \right] \quad (2.110)$$

where $\beta = u_\ell / k_B T$. From Equations 2.110 and 2.108, one has:

$$\frac{1}{\Gamma_s d} = \frac{k_B T}{\pi^\ell d} + 1 + \frac{\lambda e^{-\lambda \pi^\ell d / k_B T} \left(1 - \frac{\beta}{\lambda} \right)}{e^{-\lambda \pi^\ell d / k_B T} \left(1 - \frac{\beta}{\lambda} \right) + \frac{\beta}{\lambda}} \quad (2.111)$$

In the limit $\lambda \rightarrow 0$, Equation 2.111 yields:

$$\frac{1}{\Gamma_s d} = \frac{k_B T}{\pi^\ell d} + 1 - \frac{\beta}{1 + \beta \pi^\ell d / k_B T} \quad (2.112)$$

This is a quadratic equation with respect to π^ℓ ; solving it, one obtains the EOS $\pi^\ell(\Gamma_s)$:

$$\frac{\pi^\ell}{k_B T} = \frac{R_\beta^{\text{ID}} - 1}{2\beta d}, \quad \text{where} \quad R_\beta^{\text{ID}} = \sqrt{1 + 4\beta \frac{\Gamma_s d}{1 - \Gamma_s d}} \quad (2.113)$$

This result was obtained by Gurkov and Ivanov [32] and also by Tutschka and Cuesta [91]. The latter authors used a different method and Equation 2.113 for them was an intermediate result while solving a different problem.

By multiplying Equation 2.113 by $1 + R_\beta^{\text{ID}}$, one can transform it to

$$\frac{\pi^\ell}{k_B T} = \frac{\Gamma_s}{1 - \Gamma_s d} \times \frac{2}{1 + R_\beta^{\text{ID}}} \quad (2.114)$$

The first factor in the right-hand side is the hard core part of the new EOS, which is the same as the hard core part of Volmer EOS (Equation 2.86).

To derive the 2-D analogue of Equation 2.114, a heuristic approach was used in ref. [33]. It was based on a useful procedure for deriving an EOS, proposed by Hemmer and Stell [90], which accounts rigorously for the attraction between hard spheres up to terms of the order of B_{attr}^2 . This procedure was modified in ref. [33] for the case of a 2-D fluid composed of attracting hard core particles. The respective result for π^S is:

$$\pi^S = \pi_{\text{hc}}^S + \frac{B_{\text{attr}}}{B_{\text{hc}}} \left(\pi_{\text{hc}}^S - \Gamma_s \frac{\partial \pi_{\text{hc}}^S}{\partial \Gamma_s} \right) \quad (2.115)$$

where the subscript ‘‘hc’’ denotes ‘‘hard core.’’ If π_{hc}^S is given by HFL EOS (Equation 2.87) with $B_{\text{attr}} = 0$, then $B_{\text{hc}} = 2\alpha$ (Equation 2.106). For sticky potential, $B_{\text{attr}} = 4\alpha\beta$, so that Equation 2.115 yields:

$$\frac{\pi^S}{k_B T} = \frac{\Gamma_s}{(1 - \alpha\Gamma_s)^2} \left(1 - 4\beta \frac{\alpha\Gamma_s}{1 - \alpha\Gamma_s} \right) \quad (2.116)$$

On the other hand, Equation 2.114 can be expanded in power series in β :

$$\frac{\pi^\ell}{k_B T} \xrightarrow{\beta \rightarrow 0} \frac{\Gamma_s}{1 - \Gamma_s d} \left(1 - \beta \frac{\Gamma_s d}{1 - \Gamma_s d} + \dots \right) \quad (2.117)$$

A comparison of Equations 2.116 and 2.117 reveals that they have an analogous structure: the respective hard core terms, $\Gamma_s/(1 - \Gamma_s d)$ for the Volmer and $\Gamma_s/(1 - \alpha\Gamma_s)^2$ for HFL equations, are multiplied by the same function of β and Γ_s , with the only difference being the numerical coefficients 1 and 4, respectively. In the case of Equation 2.117, this function stems from the expansion of the factor containing R_β^{ID} , it is not difficult to realize that the two functions will become identical if the numerical coefficient in R_β^{ID} (Equation 2.113), is changed from 4 to 16. Hence, it was hypothesized that the analogue of the 1-D EOS (Equation 2.113) for 2-D adsorption must read:

$$\frac{\pi^S}{k_B T} = \frac{\Gamma_s}{(1 - \alpha\Gamma_s)^2} \times \frac{2}{1 + R_\beta}, \quad R_\beta = \sqrt{1 + 16\beta \frac{\alpha\Gamma_s}{1 - \alpha\Gamma_s}} \quad (2.118)$$

The corresponding adsorption isotherm was obtained by substituting π^S from Equation 2.118 into Gibbs isotherm ($d\pi^S = k_B T \Gamma_s d \ln C_s$) and integrating. The result was

$$K_s C_s = \frac{\Gamma_s}{(1 - \alpha\Gamma_s)} \left(\frac{2}{1 + R_\beta} \right)^{\frac{1+8\beta}{4\beta}} \times \exp \left[\frac{\alpha\Gamma_s(4 - 3\alpha\Gamma_s)}{(1 - \alpha\Gamma_s)^2} \times \frac{2}{1 + R_\beta} \right] \quad (2.119)$$

The new adsorption isotherm (Equation 2.119) was checked numerically in ref. [33] by direct calculation of the third virial coefficient—it turned out to be very close to the one obtained by the expansion in series up to Γ_s^3 of Equation 2.118. This gives hope that Equations 2.118 and 2.119 will work reasonably well at least for small β and moderate degrees of coverage $\alpha\Gamma_s$. Note that the expansions in β used above are much more general and precise than the virial expansions in Γ_s with the same number of terms. The new adsorption isotherm was confirmed in ref. [33] by extensive analysis of the adsorption data obtained with dimethyl alkylphosphine oxides in refs. [92] and [93], and with aliphatic acids in refs. [94] and [95].

2.3.2 DENSE ADSORPTION LAYERS OF IONIC SURFACTANTS: ION-SPECIFIC EFFECTS

2.3.2.1 Equations of State and Adsorption Isotherms of Ionic Surfactants

We will now modify the EOS of Equations 2.85 through 2.87 and 2.118, and the corresponding adsorption isotherms Equations 2.88 through 2.90 and 2.119, to make them applicable to ionic surfactants in the presence of ion-specific effects. A formal thermodynamic derivation similar to the one in Section 2.2.1.4 is possible, but we will instead use the two-stage adsorption procedure of Borwankar and Wasan [28], which better reveals the pitfalls of the derivation. These authors accounted for the electrostatic and nonelectrostatic contributions to the adsorption Γ_s , by assuming that (i) when the surfactant ion is in the bulk of the solution, it is under the action of the electrostatic potential $\phi(z)$ only, and its concentration C_s^S at the subsurface $z = 0$ is determined by Boltzmann distribution with the surface potential ϕ^S : $C_s^S = C_s \exp(-e_s \phi^S / k_B T)$; and (ii) After the ionic head has reached the surface $z = 0$, the hydrophobic tail is adsorbed. They also assumed that the adsorption constant K_s of process (ii) was the same as for a nonionic surfactant with the same tail.

We now apply their procedure to all adsorption isotherms for nonionic surfactants. According to assumption (i) above, the concentration of surfactant ions at $z = 0$ will be C_s^S . If applied to the equilibrium between the subsurface and the surface (with C_s^S instead of C_s), all isotherms can be written in the general form

$$K_s C_s^S \equiv K_s C_s \exp(-\Phi^S) = \Gamma_s \gamma^S(\alpha\Gamma_s, \beta) \quad (2.120)$$

Here, γ^S is the surface activity coefficient of the ionic surfactant, which depends on the adsorption model: γ^S can be easily deduced by setting the right-hand side of Equation 2.120 to be equal to the right-hand side of the adsorption isotherms, Equations 2.88 through 2.90 and 2.119. We will use Equation 2.120 to obtain the adsorption isotherm $\Gamma_{s0}(C)$ of ionic surfactants in the absence of ion-specific effects, which will be used as a zeroth approximation afterward. We will denote by subscript “0” the quantities pertaining to the case of absent ion-specific effects—these are Γ_{s0} , K_0 , and α_0 . Substituting in Equation 2.120 the factor $\exp(-\Phi^S)$ from the Gouy equation (Equation 2.25),

after elementary algebra (see also Equations 2.33, 2.40, and 2.56), one obtains the nonspecific adsorption isotherm of an ionic surfactant:

$$K_0 C^{2/3} = [\gamma^S(\alpha_0 \Gamma_{s0}, \beta)]^{1/3} \Gamma_{s0} \quad (2.121)$$

K_0 is defined by Equation 2.40 and C is mean activity (Equation 2.34). If one sets $\gamma^S = 1$, Equation 2.121 simplifies to Davies isotherm (Equation 2.39).

To obtain the first iteration of the adsorption isotherm of dense monolayers in the presence of ion-specific effects, we will use the first equation (Equation 2.58), which is a direct corollary of the generalized Gouy equation (Equation 2.54). We write it now as

$$\Gamma_{s0} = \Gamma_s \exp(u_{i0}/2k_B T) \quad (2.122)$$

Substituting Γ_{s0} from Equation 2.122 into the adsorption isotherm (Equation 2.121), one obtains

$$KC^{2/3} = [\gamma^S(\alpha \Gamma_s, \beta)]^{1/3} \Gamma_s \quad (2.123)$$

Here, K is the ion-specific constant given by Equation 2.56. We have defined the ion-specific molecular area α as

$$\alpha = \alpha_0 \exp(u_{i0}/2k_B T) \quad (2.124)$$

This equation is the quantitative formulation of the Hofmeister effect on the effective area per molecule α , which will be discussed in Section 2.3.2.3. It reveals that the higher the absolute value of the counterion adsorption energy u_{i0} is, the smaller the molecular area α . That α may depend on the nature of the counterion was inferred by Goddard and coworkers based on their data obtained with insoluble nonadecylbenzene sulfonate monolayers with different cations [96] or docosyltrimethylammonium monolayers with different anions [97].

By applying the result (Equation 2.123) to the adsorption isotherms (Equations 2.88 through 2.90) and using Equation 2.102, $B_{\text{attr}} = \alpha\beta$, one obtains the respective isotherms of ionic surfactants:

1. Langmuir–Frumkin:

$$KC^{2/3} = \frac{\Gamma_s}{(1 - \alpha_L \Gamma_s)^{1/3}} \exp(-2\beta \alpha_L \Gamma_s/3) \quad (2.125)$$

2. van der Waals:

$$KC^{2/3} = \frac{\Gamma_s}{(1 - \alpha_V \Gamma_s)^{1/3}} \exp\left[\frac{\alpha_V \Gamma_s}{3(1 - \alpha_V \Gamma_s)} - \frac{2}{3} \beta \alpha_V \Gamma_s\right] \quad (2.126)$$

3. modified HFL:

$$KC^{2/3} = \frac{\Gamma_s}{(1 - \alpha \Gamma_s)^{1/3}} \exp\left[\frac{\alpha \Gamma_s (3 - 2\alpha \Gamma_s)}{3(1 - \alpha \Gamma_s)^2} - \frac{2}{3} \beta \alpha \Gamma_s\right] \quad (2.127)$$

Setting in the last equation $\beta = 0$, one obtains:

4. HFL:

$$KC^{2/3} = \frac{\Gamma_s}{(1 - \alpha\Gamma_s)^{1/3}} \exp \left[\frac{\alpha\Gamma_s(3 - 2\alpha\Gamma_s)}{3(1 - \alpha\Gamma_s)^2} \right] \quad (2.128)$$

5. The new isotherm (Equation 2.119) leads to:

$$KC^{2/3} = \frac{\Gamma_s}{(1 - \alpha\Gamma_s)^{1/3}} \left(\frac{2}{1 + R_\beta} \right)^{\frac{1+8\beta}{12\beta}} \times \exp \left[\frac{\alpha\Gamma_s(4 - 3\alpha\Gamma_s)}{3(1 - \alpha\Gamma_s)^2} \times \frac{2}{1 + R_\beta} \right] \quad (2.129)$$

with R_β given by Equation 2.118.

Next, we proceed to the surface pressure π^S . For high surface potentials, Φ^S , this task is easy because the contribution of the electrical double layer to the surface pressure π^S is $2k_B T \Gamma_s$ (as we already showed in Section 2.1.3). For dense monolayers, this can be proven rigorously in the following way. As a starting point, we use the Gibbs isotherm (Equation 2.32). To obtain the convenient exponent $C^{2/3}$, we will rewrite it as

$$d\pi^S = 3k_B T \Gamma_s d \ln C^{2/3} \quad (2.130)$$

Substituting $C^{2/3}$ from Equation 2.123, one obtains

$$d\pi^S = k_B T \Gamma_s d \ln \gamma^S \Gamma_s + 2k_B T d \Gamma_s \quad (2.131)$$

The first term in this equation is the same for both ionic and nonionic surfactants. The second one refers to ionic surfactants only. Equation 2.131 can be written in integral form:

$$\pi^S = \pi_0^S(\Gamma_s) + 2k_B T \Gamma_s \quad (2.132)$$

where $\pi_0^S(\Gamma_s)$ is the expression for the EOS of a nonionic surfactant. Hence, it is enough to add a term $2k_B T \Gamma_s$ to the right-hand side of EOS (Equations 2.85 through 2.87 and 2.118) for nonionic surfactants to obtain the corresponding EOS for ionic surfactants. The EOS (Equation 2.132) determines the dependence of π^S on the adsorption Γ_s and, together with the adsorption isotherm (Equation 2.123), it parametrically defines the dependence of π^S on C_s .

By expanding in series of Γ_s any of the adsorption isotherms (Equations 2.125 through 2.129), and inverting the series, one obtains:

$$\Gamma_s = KC^{2/3} - \frac{2}{3} B_2 K^2 C^{4/3} + \dots, \quad (2.133)$$

in which $B_{\text{attr}} = 4\alpha\beta$ for Equation 2.129 and $B_{\text{attr}} = \alpha\beta$ for the other isotherms. The corresponding dependence of π^S on C follows directly from the integration of Gibbs isotherm (Equation 2.130):

$$\pi^S/k_B T = 3KC^{2/3} - B_2 K^2 C^{4/3} + \dots \quad (2.134)$$

This is the virial expansion of $\pi^S(C)$. We used this equation to determine K in Section 2.4.

2.3.2.2 Experimental Results and Analysis

We already showed that Frumkin, van der Waals, and the modified HFL models yield some unreliable results (cf. Table 2.3). That is why we will perform analysis of the experimental data for $\pi^s(C)$ only with two models, each comprising an EOS $\pi^s(\Gamma_s)$ and an adsorption isotherm $\Gamma_s(C)$ —these are the HFL model (Equations 2.87 and 2.128 with $B_{\text{attr}} = 0$) and the new model (Equations 2.118 and 2.129). In both EOS, $2k_B T \Gamma_s$ is added according to Equation 2.132.

Several factors complicate the determination of the parameters K , α , β and π_0 of the two models from experimental data. First of all, this is the number of fitting parameters (four for the new model for W|G; three for HFL model for W|O interface). This leads to a broad minimum of the merit function—the dispersion of $\pi(C^{2/3})$. The insufficient experimental information (small number of available data for different surfactants and interfaces) makes the problem even worse.

A second problem is that the experimental data $\pi^s(C)$ are usually known with rather high errors. The main reasons for these errors are [52,98]: (i) extremely pure water, salt, and surfactant and careful formulation of the experimental conditions are essential for reliable results; and (ii) careful calibration is needed for all types of tensiometric methods. The last factor usually affects the absolute value of the surface tension σ , but not the difference between its two subsequent values. Often, quite different experimental curves for the same system can be made to coincide by suitably shifting them in the vertical direction. An example with data for $C_{12}H_{25}SO_4Na$ at the water–hexane interface is shown in Figure 2.18. The data of Aratono [99] are 3.5 mN/m lower than the results of Rehfeld [51], and 5.5 mN/m higher than the results of Gillap et al. [62]. The original three sets of data differ in Figure 2.18a but coincide when suitably shifted in Figure 2.18b. This problem makes it difficult to determine exactly the spreading pressure π_0 , especially when the authors have not measured the interfacial tension of the pure interface (at zero surfactant concentration).

A third problem is the assessment of the reliability of the obtained parameters K , α , β , and π_0 . In the case of multiparametric nonlinear models (such as the HFL defined with Equations 2.128 and 2.87, and the new model defined with Equations 2.118 and 2.129), this assessment requires detailed and cumbersome numerical analysis of the merit function (similar to the one in ref. [33]).

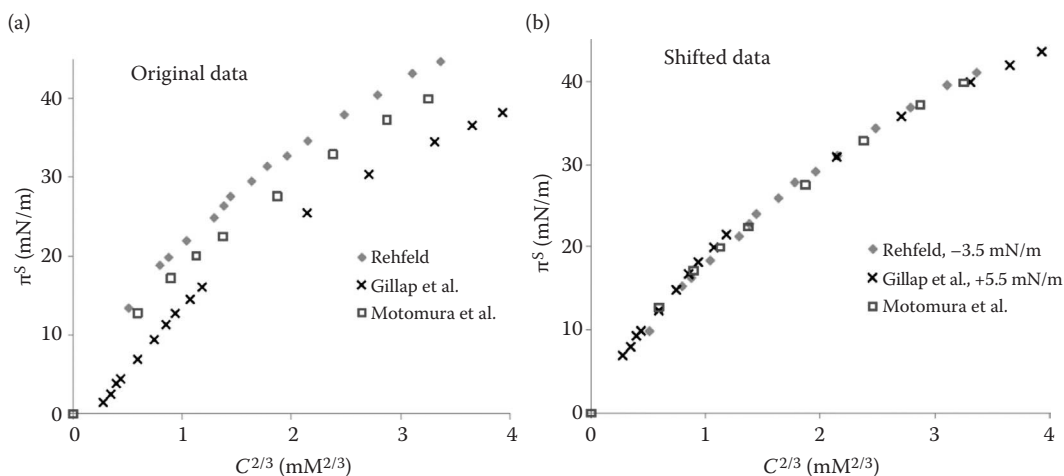


FIGURE 2.18 (See color insert.) Surface tension versus $C^{2/3}$ for $C_{12}H_{25}SO_4Na$ at water–hexane interface. (a) The three sets differ in absolute values, which we attribute to incorrect calibration of the tensiometers. (b) When suitably shifted, all data coincide. (Data from Rehfeld, S.J., *J. Phys. Chem.* 71, 738–745, 1967; Gillap, W.R. et al., *J. Colloid Interface Sci.* 26, 232–236, 1968; Motomura, K. et al., *J. Colloid Interface Sci.* 67, 247–254, 1978.)

These three problems will be tackled in a future publication in preparation, in which the verification of the adsorption theory will be performed on more systems. Instead of such a detailed approach, which cannot be presented concisely in this chapter, we will use a simpler procedure for illustrative purposes that yields, we believe, reasonable results.

This procedure involves the following steps:

1. Determination of Γ_s from the experimental dependence $\pi^S(C^{2/3})$ by numerical differentiation. To calculate Γ_s , we followed Rehfeld [51] who proposed to smooth the experimental data $\pi^S(C)$ with a quadratic regression model.

$$\pi^S = b_0 + b_1 \ln C^{2/3} + b_2 \ln^2 C^{2/3} \quad (2.135)$$

where the coefficients b_i are determined from the curve fitting. This dependence is further used to calculate the adsorption Γ_s according to Gibbs isotherm (Equation 2.130):

$$\Gamma_s = \frac{C^{2/3}}{3k_B T} \frac{d\pi^S}{dC^{2/3}} = \frac{1}{3k_B T} (b_1 + 2b_2 \ln C^{2/3}) \quad (2.136)$$

It turned out that the dependence (Equation 2.136) approximates these adsorption isotherms well in the moderate to high surfactant concentration region.* The approximation fails at $C \rightarrow 0$ because Equation 2.136 yields $\Gamma_s \rightarrow -\infty$, but this region is unimportant for the concentration ranges considered below.

2. The values of Γ_s found by procedure (1) plotted versus $C^{2/3}$ represent numerically the “experimental” adsorption isotherm $C^{2/3}(\Gamma_s)$. Similarly, the values of π^S from the experimental curves $\pi^S(C^{2/3})$ plotted versus the respective calculated values of Γ_s yield the “experimental” EOS. As an example, the “experimental” $\pi^S(\Gamma_s)$ points for $C_{12}H_{25}NMe_3Br$ at W|G and W|O interface are presented in Figure 2.19a. The processing of the so-obtained EOS and adsorption isotherm is easy for two reasons. First, the fitting procedure is performed with explicit theoretical functions $\pi_{th}(\Gamma_s; \alpha, \beta, \pi_0)$ and $\Gamma_{th}(\Gamma_s; K, \alpha, \beta)$. These are Equations 2.129 and 2.118, the latter with added $2k_B T \Gamma_s$. Second, the EOS and the adsorption isotherm both involve one less parameter—Equation 2.118 for $\pi^S(\Gamma_s)$ does not contain K , whereas Equation 2.129 for $C^{2/3}(\Gamma_s)$ does not contain π_0 . We chose to use only the $\pi^S(\Gamma_s)$ data, as they are less sensitive to the failure of Rehfeld’s procedure (Equation 2.136) at $C \rightarrow 0$. In summary, the parameters α , β , and π_0 are determined from the curve-fitting of $\pi^S(\Gamma_s)$, obtained with Rehfeld’s procedure (Equations 2.135 and 2.136), with the theoretical models Equations 2.129, 2.118, and 2.132. This procedure was applied with the new adsorption model at the W|G interface and with the HFL model at the water–hexane interface.
3. With α , β , and π_0 obtained from (2), there is only one undetermined parameter left: the adsorption constant K . To determine this, the theoretical adsorption isotherm and EOS (Equations 2.129 and 2.118), were solved numerically with fixed values of α , β , and π_0 as obtained from (2). This leads to the theoretical relation $\pi_{th}(C^{2/3}; K)$. It was compared with the original experimental data π^S versus $C^{2/3}$, to determine the value of K (the simplex method was used for minimization of the dispersion of π^S vs. $C^{2/3}$). This step is illustrated in Figure 2.19b, where the points are experimental data for $C_{12}H_{25}NMe_3Br$ at the W|G and W|O interfaces and the fitting curves are shown.

* The results, presented in Table 2.3 and discussed in Section 2.3.1.3, were obtained by calculating the values of Γ_s using the above procedure. These data for Γ_s were then used for the fits of the adsorption isotherms of Frumkin, van der Waals, and the modified HFL (Equations 2.125 through 2.128).

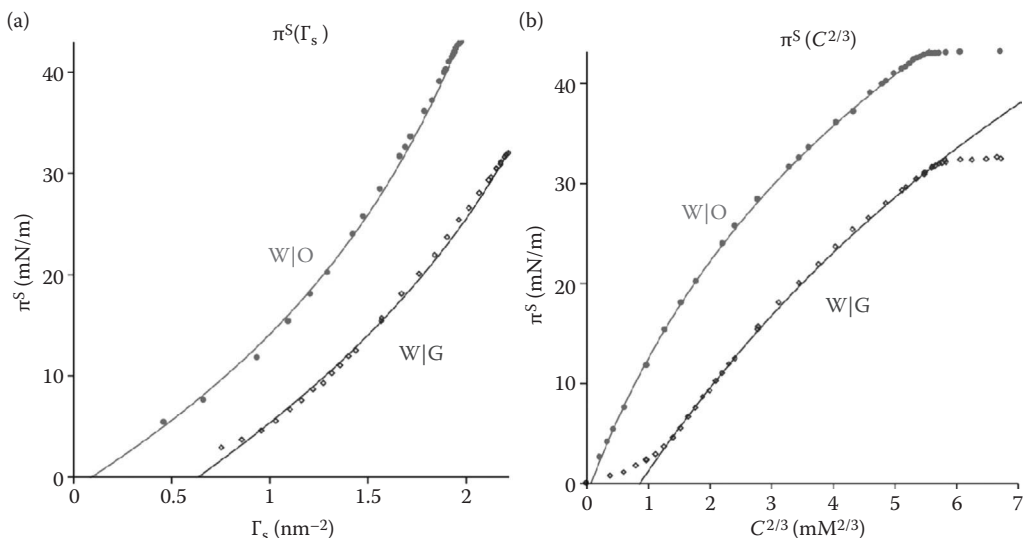


FIGURE 2.19 Illustration of the curve-fitting procedure used for determination of the adsorption parameters of $C_{12}H_{25}NMe_3Br$ at W|G and W|O interfaces [65]. (a) EOS, π^S versus Γ_s , “Experimental” values of Γ_s were obtained using Rehfeld’s procedure (Equation 2.136). The lines are fits based on HFL EOS (W|O interface; Equations 2.87 and 2.132), and the new EOS (W|G; Equation 2.118). The parameters α , β , and π_0 given in Table 2.3 were obtained from these fits. (b) π^S versus $C^{2/3}$. The points are experimental data [65]. The lines are fits with HFL (Equations 2.87 and 2.128), and the new model (Equations 2.118 and 2.129). The values of α , β , and π_0 are those determined from π^S versus Γ_s in (a), and the values of K in Table 2.3 are determined as fitting parameters.

The surfactants we chose to study using this procedure at the water–hexane and W|G interfaces were $C_{12}H_{25}SO_4Na$ [51,52], $C_{12}H_{25}NMe_3Cl$, and $C_{12}H_{25}NMe_3Br$ [65,21,89]. The reason for this choice was that such a combination of surfactants allowed us to study the main effects that we were expecting: the effects of the ionic head and the counterion on the adsorption parameters. For this reason, we chose the same hydrophobic tail (dodecyl), and the same oil (hexane, the only one for which we found adsorption data for the three surfactants). For the W|G surface, we used only the data for the LE state, that is, those after the kink in the W|G curves $\pi^S(C^{2/3})$ in Figure 2.19b.

The results obtained for the adsorption parameters (K , α , β , π_0) are shown in Table 2.4. The calculated values of the adsorption constant K and the excess pressure π_0 in the LE state can be compared with those obtained from Figures 2.3 and 2.10 after direct quadratic regression analysis of the experimental data $\pi^S(C^{2/3})$, see Equation 2.134, which does not involve any model for the intermolecular interaction. The differences for the K values are less than 4% and those for the π_0 values less than 15%. The standard errors for α vary between 2.5% and 5%, whereas those for β vary between 20% and 30%. The relative values of the errors are in qualitative agreement with the numerical analysis, performed in ref. [33], which revealed that the errors were smallest for α , increased for K , and were even larger for β .

However, we met problems with fitting the data for the water–hexane interface with the new model (Equations 2.118 and 2.129). We obtained reasonable data for α and β , but the errors in the obtained values of K were large. Similar problems appeared in ref. [33] with the alkyldimethylphosphine oxide compounds with short chain length at the W|G surface—because they exhibited very small values of β (~ 0.1), the fitting problems were then ascribed to the fact that the new adsorption isotherm (Equation 2.129) contains a power $(1 + 8\beta)/4\beta$, which diverges at $\beta \rightarrow 0$ and thus probably makes the fit uncertain for small β . Similar small values of β were then obtained

TABLE 2.4
Parameters of the Adsorption

Surfactant, Interface	Quadratic Regression (Equation 2.134)			HFL Model (Equations 2.128 and 2.87)			New Model (Equations 2.118 and 2.129)				Nonspecific Parameters (W G)		
	π_0 (mN/m)	K	B_2 (Å ²)	π_0 (mN/m)	K	α (Å ²)	π_0 (mN/m)	K	α (Å ²)	β	$u_{i0}/k_B T$	K_0	α_0 (Å ²)
C ₁₂ H ₂₅ SO ₄ Na, water–hexane [51]	5.9	196	21.3	3.45	266	22.9							
C ₁₂ H ₂₅ SO ₄ Na, W G [52]	−9.1	156	12.0				−10.5	155	20.3	0.58	−0.33	131	24.0
C ₁₂ H ₂₅ NMe ₃ Cl, water–hexane [21,65]	0	131	30.4	1.94	127	29.6							
C ₁₂ H ₂₅ NMe ₃ Cl, W G [89]	−4.0	63.3	20.4				−4.2	60.6	31.2	0.65	−1.43	29.6	63.8
C ₁₂ H ₂₅ NMe ₃ Br, water–hexane [65]	0.26	142	20.8	−1.14	187	23.5							
C ₁₂ H ₂₅ NMe ₃ Br, W G [65]	−9.0	117	19.2				−8.2	113	23.3	0.33	−2.32	35.4	74.3

Note: The parameters for the W|O interface were obtained by curve-fitting with the HFL model (Equations 2.128, 2.87, and 2.132), and those for W|G with the new model (Equations 2.118, 2.129, and 2.132).

for the water–hexane interface from the new isotherm (Equation 2.129) and we believe that the reason for the small values obtained for K is the same. We are currently working to resolve this problem. That is why we decided to confine ourselves to the water–hexane interface with data obtained from the HFL model only (Equations 2.128 and 2.87), with $B_{\text{attr}} = 0$. The results obtained with the HFL model are systematically larger for K and smaller for α (with 2–4 Å²) than those obtained (but not shown here) with the new model. However, both of these follow the same qualitative trends as expected on physical grounds (see Section 2.2.3): decrease of K and increase of α with the decrease of $-u_{i0}/k_B T$. It is impossible to decide without detailed numerical analysis (planned for the future), which one of the two models leads to more reliable results for the W|O interface because, when applying the HFL isotherm, one forces the system to have $\beta = 0$, which might not always be true.

An interesting and surprising effect, related to the parameters α and β , is exhibited by the $\Gamma_s(C^{2/3})$ plots for C₁₂H₂₅NMe₃Br at W|G and W|O interfaces in Figure 2.20: the adsorption Γ_s at W|G at small concentrations of C is smaller than that at the W|O interface. However, as C increases Γ_s at W|G increases faster than Γ_s at the W|O interface and the two adsorption curves intersect (the same type of behavior was found for C₁₂H₂₅NMe₃Cl and C₁₂H₂₅SO₄Na, as well as with other surfactants studied; for lack of space, we do not reproduce the respective plots here). Because the K values do not change with C , the reason must be sought in the role of the other parameters, α and β , more precisely, in the second virial coefficient, which encompasses both factors: $B_2 = 2\alpha(1 - 2\beta)$, cf. Equation 2.106. According to the data in Table 2.3, $\beta \approx 0.5$ at the W|G interface so that $B_2 \ll 2\alpha$ for the three surfactants. For the W|O interface, $B_2 = 2\alpha$ is larger because $\beta = 0$. This means that the repulsive forces between the adsorbed surfactant ions will be larger in the latter case, thus hindering the increase of the adsorption. The effect of B_2 on the adsorption isotherm is also visible from the plots of $\pi^S(C^{2/3})$ in Figure 2.3: whereas the plots for the W|G systems are linear almost up to cmc, those for the W|O interface exhibit noticeable curvature.

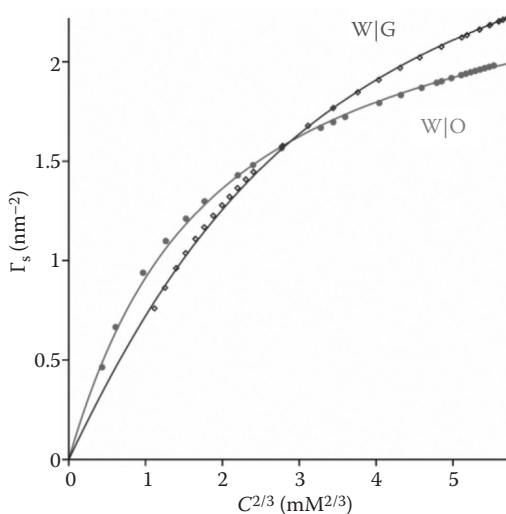


FIGURE 2.20 Illustration of the difference in the adsorptions Γ_s versus mean surfactant activity $C^{2/3}$ for C₁₂H₂₅NMe₃Br at W|G and W|O interface. “Experimental” values of Γ_s were obtained using Rehfeld’s procedure (Equation 2.136). The lines are theoretical predictions based on the HFL model (W|O), (Equations 2.128), and the new model (W|G; Equations 2.129), with parameters as in Table 2.3.

2.3.2.3 Electrostatic and Ion-Specific Effects on the Adsorption Parameters K , α , and β

The data in Table 2.3 exhibit a marked dependence of the area per molecule α on the ion-specific adsorption energy $-u_{i0}$, in agreement with Equation 2.124. We applied Equation 2.124 to calculate the values of α_0 for $C_{12}H_{25}SO_4Na$, $C_{12}H_{25}NMe_3Cl$, and $C_{12}H_{25}NMe_3Br$ at the W|G surface by using the values of $-u_{i0}/k_B T$ for the counterions Na^+ , Cl^- , and Br^- (cf. Table 2.3). If the theory and the calculations are correct, the values of α_0 , obtained from Equation 2.124, must coincide for different counterions, if the surfactant ion and everything else is the same. Indeed, the values of α for $C_{12}H_{25}NMe_3Cl$ and $C_{12}H_{25}NMe_3Br$ differ significantly (31.2 vs. 23.3 \AA^2 , respectively), whereas the α_0 's are closer (63.8 vs. 74.3 \AA^2) as required by the theory. The small difference of approximately 10 \AA^2 is probably due to experimental errors. Despite the close values of the α 's, the α_0 is much smaller for $C_{12}H_{25}SO_4Na$ than for $C_{12}H_{25}NMe_3Cl$ and Br (because $-u_{i0}/k_B T$ is also smaller). Unfortunately, for the time being, we cannot perform similar calculations for adsorption at the W|O interface because a complete theory of the ion-specific adsorption energy u_{i0}^{WO} at such interface is lacking. Still, the same qualitative trend of α for $C_{12}H_{25}NMe_3Cl$ and Br at W|O interface is obeyed: $\alpha_{Cl} > \alpha_{Br}$.

There should be no direct influence of the ion-specific effect on the attraction constant β because it depends only on the van der Waals interaction energy. However, it can be affected indirectly by the ion-specific effect through its dependence on α (e.g., see Equation 33 in ref. [33]). It is conceptually easy to account for this dependence but such effort is hardly worthwhile, first, because it involves trivial but lengthy calculations, and second, because of the large errors in the β values.

The observed strong ion-specific effect on the area per molecule α is an indication of electrostatic repulsion between the surfactant ions, which is dampened by the counterions. This suggests that there is also probably some electrostatic effect on the values of the experimentally determined area α . Indeed, the hard core cross-sectional areas of $C_{12}H_{25}NMe_3Cl$ and Br must be almost equal but the values obtained for the respective α 's differ significantly. To check this hypothesis, we analyzed the available data for adsorption of the same surfactant, $C_{12}H_{25}SO_4Na$, at similar W|O interfaces but at different concentrations of added NaCl. Because the surfactant and all ions are the same, there should be no ion-specific effect. In Figure 2.21, $\ln\alpha$ is plotted versus the square of the Debye length, $1/\kappa^2 \equiv \epsilon k_B T / 2e_0^2 C_i$, because we hypothesized that at these relatively low salt concentrations, the area α must be related to the square of the Debye length, $1/\kappa$. The good linearity and the reasonable value of $\alpha = 19.3 \text{\AA}^2$ at $1/\kappa = 0$ (i.e., in the absence of electrostatic effect) seem to confirm our hypothesis.

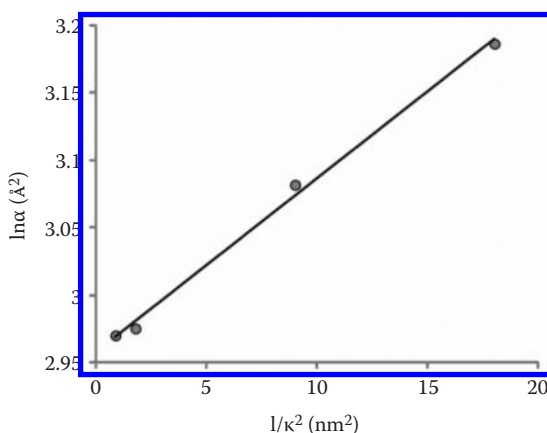


FIGURE 2.21 Dependence of the area per molecule α on the Debye length $1/\kappa$. Plot of $\ln\alpha$ versus $1/\kappa^2$ for $C_{12}H_{25}SO_4Na$ adsorption at W|O interface at various electrolyte concentrations: $C_{el} = 0$ for heptadecane [51], 0.05 M and 0.1 M for petroleum ether [53], and 0.01 M for hexadecane [34]. For the system, without added electrolyte, the value of C_s at $\pi^S = 20$ mN/m was used for the calculation of κ . Line, linear regression of the data. The intercept $\ln\alpha_0 = 2.96$ corresponds to $\alpha_0 = 19.3 \text{\AA}^2$.

Unfortunately, in the absence of theory and of more experimental data, it is impossible to interpret the obtained value for the slope. Levine et al. [100] and Warszynski et al. [7] have proposed theoretical models of this effect but, because of their complexity and lack of experimental confirmation, we will not discuss them.

The relation between the adsorption constants K and K_0 for the three surfactants under consideration at the W|G surface confirms the findings in Section 2.4.1 (Table 2.3). The difference in K between $C_{12}H_{25}NMe_3Cl$ and $C_{12}H_{25}NMe_3Br$ is significant (60.6 vs. 113, respectively), but the values of K_0 , calculated from Equation 2.56, are much closer (29.6 vs. 35.4). They are also close to the value $K_0 = 26.6$ from the intercept of the respective line in Figure 2.11—according to the theory, this should be so for identical surfactant ions. The nonspecific adsorption constant K_0 for $C_{12}H_{25}SO_4Na$ at the W|G surface was found to be $K_0 = 131$ (cf. Table 2.4), in fair agreement with the value 122 from Figure 2.11. This value is larger than the constants K_0 for the two $C_{12}H_{25}NMe_3^+$ salts, certainly because of the larger value of the adsorption constant K_s for dodecylsulfate surfactants (Equation 2.40; Figure 2.11). At the same time, the ratio $K/K_0 = 1.18$ is smaller for $C_{12}H_{25}SO_4Na$ than it is for the two $C_{12}H_{25}NMe_3^+$ surfactants (2.04 for $C_{12}H_{25}NMe_3Cl$ and 3.19 for $C_{12}H_{25}NMe_3Br$) because of the much smaller absolute value of the ion-specific adsorption energy u_{i0} of $C_{12}H_{25}SO_4Na$.

We believe that the results in this section confirm the self-consistency of our theory and calculation procedures.

2.4 HOFMEISTER EFFECT ON cmc OF IONIC SURFACTANTS AND DISJOINING PRESSURE IN FOAM FILMS

It was shown in Section 2.2.3 that the ion-specific energy u_{i0} depends only on the ion and its interaction with the bulk phases and not on the type of the surfactant. This makes it possible to use the same value of u_{i0} for a given counterion for the interpretation of data obtained with various surfactants in different phenomena. To check the latter hypothesis, we attempted in ref. [30] to interpret two phenomena that were rather different from the adsorption of surfactant: the cmc of the ionic surfactant and the disjoining pressure in thin liquid films. In this section, we give a brief account of the obtained results.

2.4.1 EFFECT OF COUNTERION ON THE CMC OF IONIC SURFACTANTS

A number of properties of micellar solutions of ionic surfactants show correlation to Hofmeister series. For example, the degree of binding [101], micelle aggregation number and shape [102], clouding point [103], enthalpy of micellization [104], and viscosity of micellar solutions [105]. The “classic” example is, of course, the cmc; the counterion effect on cmc was extensively investigated experimentally [25,106]. Correlation to ion size and polarizability was observed [24].

In this section, the cmc of surfactant solutions will be explicitly related to the counterion adsorption energy u_{i0} . Only the case of ionic surfactants that are 1:1 electrolytes will be considered. The ion-specific effects will be investigated by extending the semiempirical approach of Shinoda et al. [25], which predicts the cmc of ionic surfactants in the absence of a Hofmeister effect. Shinoda’s approach is based on Gouy theory, and successfully explains the experimentally observed dependence of cmc on the electrolyte concentration C_{ei} , known as Corrin–Harkins equation [107]:

$$\ln cmc = \text{const} - K_g \ln(cm c + C_{ei}) \quad (2.137)$$

Following Shinoda et al. [25], we assume that the micellar solution can be regarded as consisting of bulk solution of monomers (indexed with superscript “B”) and of micellar pseudo-phase (superscript “M”). The monomer bulk solution of concentration C_s is assumed to be ideal, and the ionic surfactant to be totally dissociated. In such case, the chemical potential of the surfactant monomers will be $\mu^B = \mu_0^B + k_B T \ln C_s$ (Equation 2.3). Next, we assume, as Shinoda did, that the electrostatic

contribution to the chemical potential μ^M of the surfactant ion in the micelle is equal to the electrostatic work $E_{el} = K_g e_s \Phi^S$ for transferring the surfactant (monovalent) ion into the micelle, that is,

$$\mu^M = \mu_0^M + K_g e_s \Phi^S \quad (2.138)$$

Here, K_g is an empirical correction coefficient, whose physical meaning was discussed by Shinoda, who conjectured that $0 < K_g < 1$ with the argument that “it is logical to assume that every monomer introduces charge smaller than 1 into the micelle, due to the counterions that accompany it” [25]. Similar approaches were used by other authors, such as Nagarajan [108] and Rao and Ruckenstein [109]. The experimental values of K_g typically lay in the range between 0.4 and 0.6, usually close to 1/2 [25].

The condition for chemical equilibrium is the equality of the potentials defined by Equations 2.3 and 2.138. If this equality is solved for the surfactant concentration C_s in the monomer solution, the following relation is obtained:

$$\ln C_s = \frac{\mu_0^M - \mu_0^S}{k_B T} + K_g \Phi^S \quad (2.139)$$

where the dimensionless potential Φ^S is given by Equation 2.24. To determine C_s and Φ^S , we also need the electroneutrality condition, that is, the Gouy equation. The curvature effect can be readily taken into account [110]; however, following Shinoda and for the sake of simplicity, we will neglect this effect. Therefore, we will use the Gouy equation for flat surfaces with ion-specific effects included (Equation 2.50).

Let Γ_s be the number of surfactant molecules per unit area of the micelle, that is, it is the micellar aggregation number divided by the area of the micelle. Once again following Shinoda, we assume that Γ_s is a constant, independent of the salt concentration. This assumption, in which it was assumed that the ion-specific effect modifies both the adsorption and the surface potential while the surfactant and the electrolyte concentrations remain constant, makes the iterative procedure used in Section 2.2.3.1 inapplicable. On the contrary, in the case of micelles, the adsorption Γ_s is constant whereas the ion-specific effect changes only Φ^S and thereby, through the equilibrium condition (Equation 2.139), the surfactant concentration C_s , that is, the cmc. This modifies the calculation as follows. The Gouy equation (Equation 2.50) written for one surfactant ion and one counterion reads:

$$e_0^2 \Gamma_s^2 / 2\epsilon = e_0 C_t e^{-u_{i0}/k_B T} \int_0^{\Phi^S} e^{e_0 \phi / k_B T} e^{-(u(z) - u_{i0}) / k_B T} d\phi \quad (2.140)$$

When analyzing Equation 2.50 to obtain Equation 2.53, it was shown that the result was proportional to $\exp(\Phi_0^S)$. We will make a similar approximation about Equation 2.140. However, in this case, no iteration is possible because Γ_s is assumed constant. Therefore, to obtain meaningful results, one must keep, as the upper limit of the integral in Equation 2.140, the true surface potential Φ^S corresponding to a given counterion concentration. Then, the integral must be replaced by $-k_B T \exp(\Phi^S) / e_0$, rather than by $-k_B T \exp(\Phi_0^S) / e_0$, as in Equation 2.51 (where F_u is negligible). Then, Equation 2.140 yields:

$$\Gamma_s^2 = \frac{4}{\kappa_0^2} C_t e^{-u_{i0}/k_B T} e^{\Phi^S} \quad (2.141)$$

which is the counterpart of Equation 2.53. Thus, Equation 2.141 yields the following expression for Φ^S :

$$\Phi^S = \ln \frac{\kappa_0^2 \Gamma_s^2}{4C_t} + \frac{u_{i0}}{k_B T} \quad (2.142)$$

Eliminating Φ^S from the chemical equilibrium condition (Equation 2.139) and the generalized Gouy equation (Equation 2.142), one obtains an equation for C_s :

$$\ln C_s + K_g \ln C_t = (1 + K_g) \ln C_0 + K_g \frac{u_{i0}}{k_B T} \quad (2.143)$$

where C_0 stands for the standard cmc:

$$\ln C_0 = \frac{\mu_0^M - \mu_0^S}{(1 + K_g)k_B T} + \frac{K_g}{1 + K_g} \ln \frac{\kappa_0^2 \Gamma_s^2}{4} \quad (2.144)$$

C_0 is the hypothetical cmc of the ionic surfactant in the absence of ion-specific effects. An expression similar to (Equation 2.144) was derived by Shinoda et al. [25]. If the ion-specific adsorption energy u_{i0} is set equal to zero, Equation 2.143 is reduced to the Corrin–Harkins equation (Equation 2.137), with explicit expression for the constant there.

In the absence of added electrolyte, the total electrolyte concentration C_t is equal to the surfactant concentration C_s , and Equation 2.143 can be solved for C_s (i.e., for cmc)

$$\ln C_s = \ln C_0 + \frac{K_g}{1 + K_g} \frac{u_{i0}}{k_B T} \quad (2.145)$$

This simple equation explicitly accounts for the Hofmeister effect on the cmc of ionic surfactants in the absence of added salt (the cmc in the presence of added salt with the same counterion is described in Equation 2.143). For the typical case where $K_g = 1/2$, one finds the dependence of cmc on the counterion $C_s = C_0 \exp(u_{i0}/3k_B T)$, where the values of u_{i0} are those listed in Table 2.2.

Equation 2.143 was generalized for the important case of different counterions of the surfactant and the added electrolyte [30]. We will consider once again only the case of 1:1 electrolytes. We must use the more general form of the Gouy equation for a mixture of counterions (Equation 2.53) where Φ_0^S must be replaced by Φ^S . For a micellar solution with only two monovalent counterions, the result reads:

$$\left(C_1 e^{-u_{i0}/k_B T} + C_2 e^{-u_{20}/k_B T} \right) e^{\Phi^S} = \frac{\kappa_0^2}{4} \Gamma_s^2 \quad (2.146)$$

which is the analogue of Equation 2.142 for the case of two counterions. Usually, one of the counterions is introduced into the solution with the ionic surfactant (so that $C_1 \equiv C_s$) and the other one is introduced with the added electrolyte ($C_2 \equiv C_{el}$). Eliminating Φ^S from Equation 2.146 and the condition for chemical equilibrium from Equation 2.139, one obtains

$$\ln C_s = (1 + K_g) \ln C_0 - K_g \ln \left(C_s e^{-u_{s0}/k_B T} + C_{el} e^{-u_{c10}/k_B T} \right) \quad (2.147)$$

where C_0 is defined by Equation 2.144; u_{s0} and u_{e10} are, respectively, the adsorption energies at the micellar interface of the counterions stemming from the surfactant (“s”) and the added electrolyte (“el”). Equation 2.147 is a generalization of Equation 2.143 and the Corrin–Harkins equation (Equation 2.137) for the case of two different monovalent counterions.

Experimental results for the ion-specific effect on cmc are summarized in ref. [30]. Only data for 1:1 electrolytes were used. The theory was checked with experimental data for alkyltrimethylammonium salts (Figure 2.22 through Figure 2.25) and dodecylsulfate salts. The data for cmc of the homologous series of alkyltrimethyl ammonium salts ($C_{10}H_{21} - C_{18}H_{37}$) NMe_3^+ in the absence of added salts [17,25,106,111–126] are presented in Figure 2.22. They were obtained with data from 62 measurements with 17 different surfactants. The data are plotted as $\ln C_s$ versus $-u_{i0}/k_B T$ according to Equation 2.145. Because a complete theory of u_{i0} at the W|O interface is still absent, we assumed that for micelles one can use the data for u_{i0} at the W|G interface from Table 2.2. One of the reasons for doing so was the fact that the average density of the hydrophobic chains inside the micelle is probably lower than it is in a typical oil phase. This assumption is supported by the fact that the calculated free energy per unit area due to the W|O interface of micelles is less than half of the typical value for σ_0 of the water–alkane interface [39]. The other reason was that our preliminary

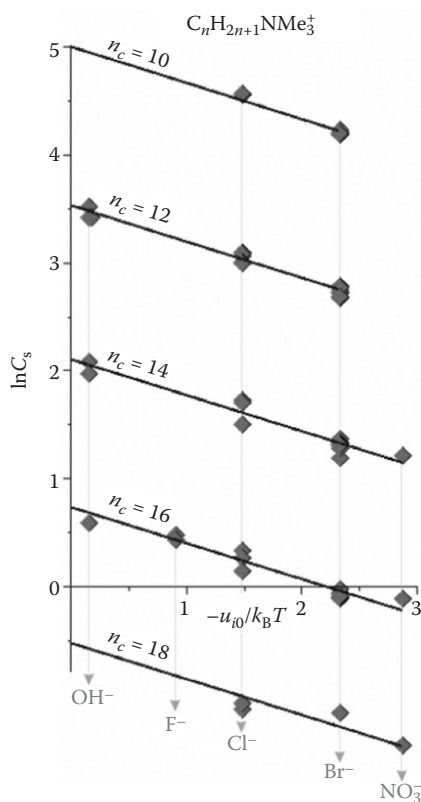


FIGURE 2.22 Dependence of $\ln C_s$ (mM) on the counterion adsorption energy $-u_{i0}/k_B T$ for different hydrocarbon chain lengths n_c of the surface active ion $C_n H_{2n+1} NMe_3^+$ [17,25,106,111–126]; $T = 25^\circ C$ to $30^\circ C$. The black parallel lines are the theoretical dependences according to Equation 2.145 with $K_g = 1/2$. The slope is consequently $K_g/(1 + K_g) = 1/3$ for all lines. The values of $\ln C_0$, obtained from the intercepts, are used in Figure 2.23. (Reprinted from *Adv. Colloid Interface Sci.*, 168, Ivanov, I.B., R.I. Slavchov, E.S. Basheva, D. Sidzhakova, and S.I. Karakashev, Hofmeister effect on micellization, thin films and emulsion stability, 93–104. Copyright 2011, with permission from Elsevier.)

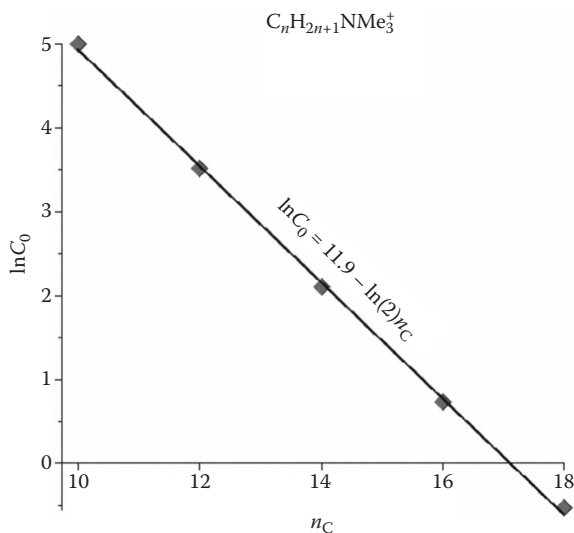


FIGURE 2.23 Dependence of $\ln C_0$ (mM) on the carbon chain length n_C of the surface active ion $C_n H_{2n+1} NMe_3^+$. The values of C_0 were obtained from the intercept of the cmc dependence on the adsorption energy, $\ln C_s(u_{i0})$, shown in Figure 2.22. The value of the slope of the linear dependence $\ln C_0 = A + B n_C$ is $B = -\ln 2$ [25,127]. (Reprinted from *Adv. Colloid Interface Sci.*, 168, Ivanov, I.B., R.I. Slavchov, E.S. Basheva, D. Sidzhakova, and S.I. Karakashev, Hofmeister effect on micellization, thin films and emulsion stability, 93–104. Copyright 2011, with permission from Elsevier.)

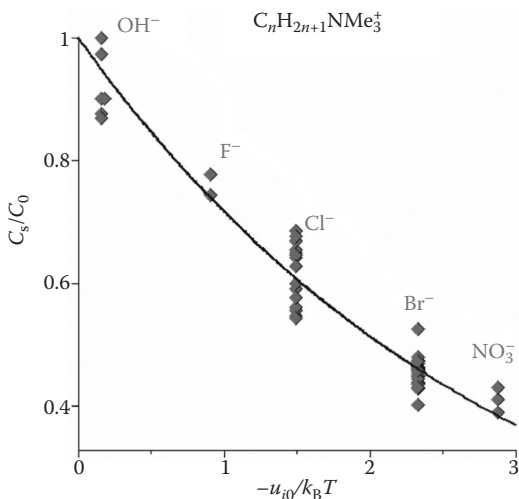


FIGURE 2.24 Normalized cmc, C_s/C_0 , versus the counterion adsorption energy $-u_{i0}/k_B T$ for $C_n H_{2n+1} NMe_3^+$ ion ($n_C = 10 - 18$) with different anions. In agreement with Equation 2.145, the normalized cmc does not depend on the carbon chain length n_C —that is why all experimental points in Figure 2.24 now fall on a single curve. (Reprinted from *Adv. Colloid Interface Sci.*, 168, Ivanov, I.B., R.I. Slavchov, E.S. Basheva, D. Sidzhakova, and S.I. Karakashev, Hofmeister effect on micellization, thin films and emulsion stability, 93–104. Copyright 2011, with permission from Elsevier.)

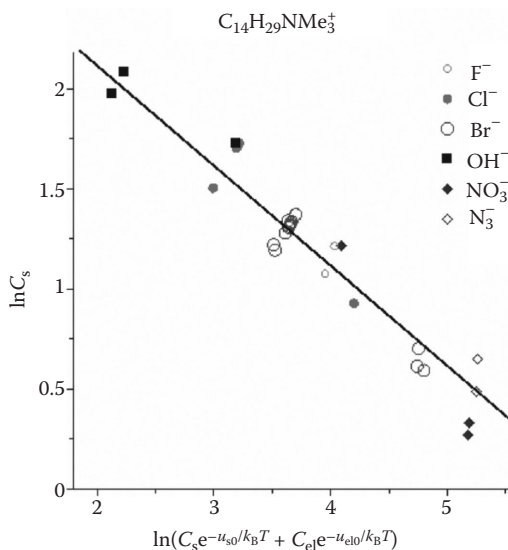


FIGURE 2.25 Dependence of $\ln C_s$ on the added salt concentration and the ion adsorption energy u_{i0} , according to Equation 2.145. The points are experimental data for $C_{14}H_{29}NMe_3^+$ ions with different anions and anion mixtures, with and without added salt. The symbol “F⁻” refers to $C_{14}H_{29}NMe_3Br$ with the addition of NaF [128]; “Cl⁻” to $C_{14}H_{29}NMe_3Cl$ alone [106,113–115,23], or $C_{14}H_{29}NMe_3Br$ with the addition of NaCl [128]; “Br⁻” to $C_{14}H_{29}NMe_3Br$ alone [112,114,117,121], or $C_{14}H_{29}NMe_3Br$ with the addition of bromides [128,112]; “OH⁻” to $C_{14}H_{29}NMe_3OH$ alone [120,121]; “NO₃⁻” to $C_{14}H_{29}NMe_3NO_3$ alone [119], or $C_{14}H_{29}NMe_3Br$ with NaNO₃ [128]; “N₃⁻” to $C_{14}H_{29}NMe_3Br$ with the addition of NaN₃ [128]. The line is the theoretical dependence (Equation 2.145), with slope $K_g = 1/2$. $T = 25^\circ C$ to $30^\circ C$. (Reprinted from *Adv. Colloid Interface Sci.*, 168, Ivanov, I.B., R.I. Slavchov, E.S. Basheva, D. Sidzhakova, and S.I. Karakashev, Hofmeister effect on micellization, thin films and emulsion stability, 93–104. Copyright 2011, with permission from Elsevier.)

estimates of u_{i0} for W|O showed that it was only approximately 10% higher than it was at the W|G interface. Finally, the good agreement obtained below between the experimental data and the theoretical equations (Equations 2.143, 2.145, and 2.147) suggests that such an assumption is probably legitimate.

The cmc data in Figure 2.22 follows the Hofmeister series (Equation 2.2). The linear dependence from Equation 2.145 is obeyed, within experimental accuracy. The slope is fixed to $1/3$, corresponding to $K_g = 1/2$. The intercept is the only fitting parameter, and gives the standard cmc, C_0 . The value of C_0 depends on the structure of the surface active ion, but not on the counterion (Equation 2.144). The C_0 values, determined from Figure 2.22, are presented in Figure 2.23 as a function of the carbon chain length, n_C . The known linear dependence $\ln C_0 = A + Bn_C$ is obeyed. Our value of the slope B coincides with the known value $B = -\ln 2$, valid for all monovalent nonbranched ionic surfactants [25,27]. The value of the intercept, obtained as fitting parameter, namely, $A = 11.9$, refers to the whole alkyltrimethylammonium salts homologous series. The above values of A and B , along with knowledge of the counterion adsorption energy u_{i0} (Table 2.2 for a list of u_{i0} values), allow the prediction of the cmc of any alkyltrimethylammonium salt.

The data from Figure 2.22 are plotted in Figure 2.24 as C_s/C_0 versus $-u_{i0}/k_B T$. All data fall on the same curve; indeed, according to Equation 2.145, the ratio C_s/C_0 for a given surfactant head depends only on $u_{i0}/k_B T$. The effect of the counterion is quite large—its change can shift cmc by approximately $\pm 50\%$.

The data for cmc of $C_{14}H_{29}NMe_3^+$ in the presence of a mixture of counterions are presented in Figure 2.25. Typically, the Br⁻ counterion comes with the surfactant, and the second counterion is

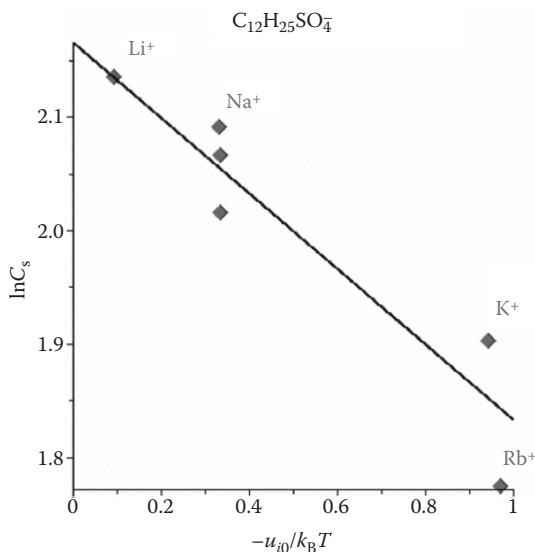


FIGURE 2.26 Dependence of cmc of $C_{12}H_{25}SO_4^-$ salts on the counterion used: $\ln C_s$ (mM) versus the ion adsorption energy $-u_{i0}/k_B T$ according to Equation 2.145. Data from refs. [69,128]; $T = 30^\circ\text{C}$ to 33°C . (Reprinted from *Adv. Colloid Interface Sci.*, 168, Ivanov, I.B., R.I. Slavchov, E.S. Basheva, D. Sidzhakova, and S.I. Karakashev, Hofmeister effect on micellization, thin films and emulsion stability, 93–104. Copyright 2011, with permission from Elsevier.)

added with the salt. The concentration of both ions was commensurable. The data compared well with our Equation 2.147 with a slope of $K_g = 1/2$.

Other ionic surfactants exhibit similar behavior [30]. This is illustrated in Figure 2.26, where data for the cmc of the anionic $C_{12}H_{25}SO_4^-$ with different cations are shown. The model (Equation 2.145) describes the data well within experimental error. Convincing results were also obtained for cmc of $C_{12}H_{25}SO_4^-$ in the presence of a mixture of cations [30]. Our model with dodecylammonium $C_{12}H_{25}NH_3^+$ and dodecanoate $C_{12}H_{25}COO^-$ salts with various counterions [25,106] was less successful, probably due to hydrolysis: the data followed the linear dependence of $\ln C_s$ on $u_{i0}/k_B T$, as required by Equation 2.147, but the value of K_g was significantly smaller than $K_g = 1/2$.

The order of decrease of cmc of the surfactants shown in Figures 2.24 and 2.26 is:



The above sequences correspond to the order of increase of the adsorption constant K_{12} (Equations 2.76 and 2.77).

2.4.2 ION-SPECIFIC EFFECT ON THE DISJOINING PRESSURE OF FOAM FILMS STABILIZED WITH IONIC SURFACTANTS

Although the adsorption energies of the counterions, u_{i0} , are not very large, they may significantly change the electrostatic component Π_{el} of the disjoining pressure Π of a thin film. The theory of the electrostatic disjoining pressure has been developed by many authors, above all by Churaev and

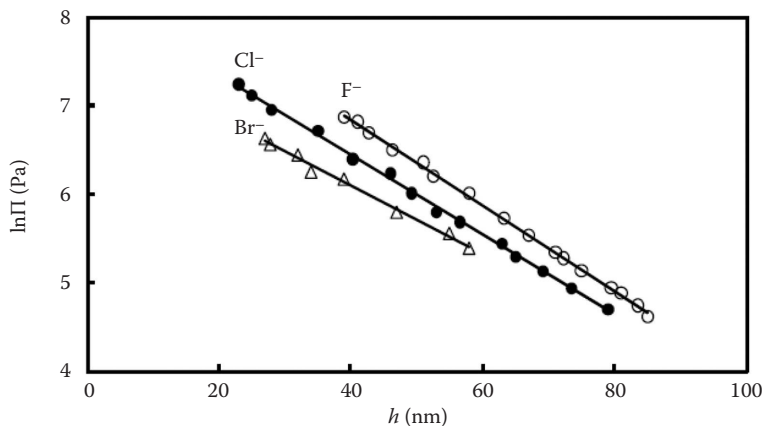


FIGURE 2.27 Plot of $\ln\Pi$ (Pa) versus h (nm) for foam films stabilized with $C_{16}H_{33}NMe_3Br$ and NaX ($X = F^-$, Cl^- , Br^-). (Reprinted from *Adv. Colloid Interface Sci.*, 168, Ivanov, I.B., R.I. Slavchov, E.S. Basheva, D. Sidzhakova, and S.I. Karakashev, Hofmeister effect on micellization, thin films and emulsion stability, 93–104. Copyright 2011, with permission from Elsevier.)

associates [129]. According to their theory, which neglects the ion-specific effects, if the electrostatic potential in the middle of the film is low (this is equivalent to either $\kappa h \gg 1$ or $\Phi_0^S \ll 1$), the electrostatic disjoining pressure, Π_{el} is given by the following expression:

$$\Pi_{el} = 64k_BTC_1 \tanh^2\left(\Phi_0^S/4\right) \exp(-\kappa h) \equiv \Pi_0 \exp(-\kappa h) \quad (2.150)$$

where C_1 is the total ion concentration. Because during the derivation of Equation 2.150 in ref. [129] no assumptions about the surface potential were made, we decided that to account for the ion-specific effects, it should be sufficient to merely replace Φ_0^S in Equation 2.150 with Φ^S from Equation 2.57.

The equation obtained was tested in ref. [30] by measuring the disjoining pressure Π in foam films stabilized with* 0.01 mM $C_{16}H_{33}NMe_3Br$ with the addition of 0.09 mM of one of the salts NaX ($X = F^-$, Cl^- , Br^-). The films were formed in a thin film pressure balance by using the Mysels–Jones porous plate technique [130,131], and the thickness h was measured interferometrically. Because the films are rather thick, one can disregard the contribution of the van der Waals disjoining pressure. This permits identifying Π with Π_{el} , and therefore, Equation 2.150 can be used for the calculation of Π , if Φ_0^S is replaced with Φ^S . The lines in Figure 2.27 obey Equation 2.150, which in logarithmic form reads:

$$\ln\Pi_{el} = \ln\Pi_0 - \kappa h \quad (2.151)$$

These lines are shifted, but close to parallel, which means that the ion-specific effect affects mainly Π_0 , which can be calculated from the intercepts. Thus, from Equation 2.150 (with Φ^S instead of Φ_0^S) one can calculate Φ^S for the three systems. Equation 2.57 and the second equation (Equation 2.58) suggest to plot the experimental Φ^S versus the dimensionless ion adsorption potential $-u_{i0}/k_B T$. This is done in Figure 2.28. The relatively good linearity and the value of the experimental slope

* A mistake was made in Section 4 of ref. [30], where the cited values of the surfactant and salt concentrations are a hundred times larger than the true values given here.

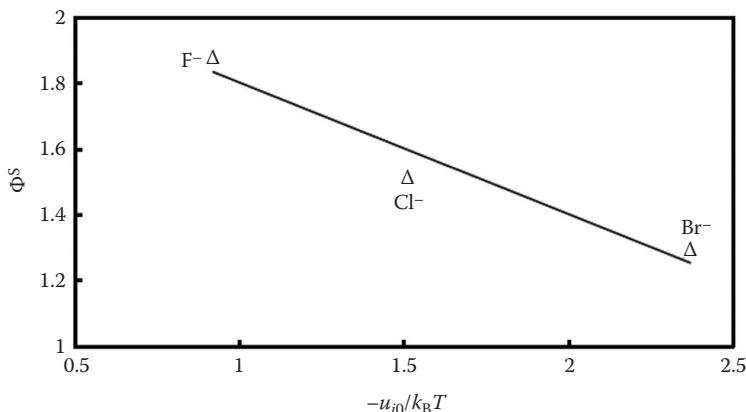


FIGURE 2.28 Combined surface potential Φ^S versus $-u_{i0}/k_B T$ for foam films stabilized with $C_{16}H_{33}NMe_3Br$ and NaX (where $X = F^-, Cl^-, Br^-$). The potential Φ^S was determined from the line intercepts in [Figure 2.27](#) and Equations 2.150 and 2.151. The intercept yields the purely electrostatic potential, $\Phi_0^S = 2.2$ (Equation 2.58). The absolute value of the slope is 0.4, which is close to the theoretical value 1/2 in Equation 2.58. (Reprinted from *Adv. Colloid Interface Sci.*, 168, Ivanov, I.B., R.I. Slavchov, E.S. Basheva, D. Sidzhakova, and S.I. Karakashev, Hofmeister effect on micellization, thin films and emulsion stability, 93–104. Copyright 2011, with permission from Elsevier.)

(0.4), which is close to the theoretical slope (1/2; cf. Equation 2.58), seem to confirm the role of the ion-specific effect on the disjoining pressure. It was also confirmed qualitatively by experimental studies on the effect of counterions on the stability of emulsion drops stabilized by ionic surfactants [30]. The efficiency of the counterions in decreasing the surface potential Φ^S follows the order

$$F^- < Cl^- < Br^- \quad (2.152)$$

This sequence is similar to the respective series (Equations 2.76 and 2.148) based on the adsorption constant K and the values of the cmc.

2.5 SUMMARY AND CONCLUSIONS

Our analysis of Davies' adsorption isotherm (Equations 2.39) revealed that (i) when neutral electrolyte has been added, it remains valid but instead of surfactant concentration, C_s , one must use mean ion activity C (Equation 2.34); and (ii) the nonspecific adsorption constant K_0 of ionic surfactants must be independent of C and is closely related to a constant K_s accounting for the field-independent contribution to K_0 . The theoretical expression (Equation 2.7) for Henry's adsorption constant was corrected in two respects. First, a statistical derivation showed that the "thickness of the adsorbed layer" δ_a is determined by the transfer energy u_{CH_2} of a $-CH_2-$ group from water to the interface, rather than being equal to the extended length ($\sim 20 \text{ \AA}$) of the surfactant tail as suggested by Davies and Rideal [26,27]. Second, the expression for the adsorption energy E_a was corrected by introducing a new term, $\sigma_0 \alpha_L$, accounting for the disappearance of area α_L , equal to the cross-sectional area of the surfactant chain, when the latter penetrates the pure interface of interfacial tension σ_0 . The last effect was checked by plotting $\ln K_0$ of $C_{12}H_{25}SO_4Na$ versus the interfacial tensions σ_0 of the pure $W|O$ interfaces for several oils—the plot in [Figure 2.7](#) was linear with a slope equal to the theoretical one.

The other theoretical conclusions and the surface tension isotherms (Equations 2.41 and 2.44) were confirmed in Section 2.2.4 by using numerous data for the adsorption of ionic surfactants. It was found that at the $W|G$ surface, the dependence of the surface pressure π^S on $C^{2/3}$ has a kink at

intermediate concentrations, followed by a linear region with a negative intercept π_0 (Figure 2.3). This intercept is due to the hydrophobic tails forming an oil-like LE film on the water phase. There is no intercept at the W|O interface, which is due to the absence of such an LE film. The dependence of $\ln K_0$ on the number of carbon atoms n_C in the hydrophobic chain revealed that the free energies u_{CH_2} for transfer of one $-\text{CH}_2-$ group to both interfaces are equal, that is, the oil-like LE adsorbed layer behaves as an oil phase.

Section 2.2.3 is devoted to the counterion-specific effects on the adsorption of ionic surfactants. The generalized Poisson–Boltzmann equation (involving the London potential; Equation 2.49) was integrated analytically. This led to simple relations between the ion-specific adsorption energy, u_{i0} , the ion-specific quantities (surface potential Φ^S and adsorption constant K) and the respective non-specific ones (Φ_0^S and K_0 ; cf. Equations 2.56 and 2.57). Equations 2.65 and 2.66 for u_{i0} encompass the most important effects, determining the occurrence of the ion-specific phenomena: radii of the bare and hydrated ions, R_b and R_h , possible deformation of the hydration shells at the interface for large ions, polarizabilities α_p and ionization potentials I of the counterions and of the pure bulk phase. Table 2.2 summarizes the values of $u_{i0}/k_B T$ for a number of ions, calculated without using any adjustable parameter. They were tested in Figure 2.11 against the values of K from the plots of π^S versus $C^{2/3}$ for several surfactants and counterions. All data fall well within the lines $\ln K$ versus $-u_{i0}/k_B T$ drawn with the theoretical slope $1/2$.

The analysis of the popular models for adsorption of surfactants at fluid interfaces (those of Frumkin [77] and van der Waals [79]) revealed that they are flawed in the definitions of all constants involved: the adsorption constant K , the area per molecule α , and the attraction constant β [31–33]. Hence, in ref. [32], new EOS and adsorption isotherms for nonionic surfactants were derived (Equations 2.118 and 2.119). Their hard core part is based on the practically exact HFL model for hard discs [80] (Equation 2.87). The attraction interaction is accounted for by the sticky potential (Equation 2.103) of Baxter [88]. In the present article, these results were used to derive new analytical EOS and adsorption isotherms for ionic surfactants, accounting also for ion-specific effects (Equations 2.129, 2.118, and 2.132). They were tested by adsorption data for three surfactants ($\text{C}_{12}\text{H}_{25}\text{SO}_4\text{Na}$, $\text{C}_{12}\text{H}_{25}\text{NMe}_3\text{Cl}$, and Br) on two interfaces: W|G and water–hexane. The results obtained by this new model were encouraging (cf. Table 2.4 and the comments thereafter). Moreover, some interesting new electrostatic and ion-specific effects were found. It turned out that similar to the adsorption constant K , the area per molecule α exhibits strong ion-specific effects (cf. Equation 2.124): its nonspecific values α_0 at W|G for $\text{C}_{12}\text{H}_{25}\text{NMe}_3^+\text{Cl}^-$ and Br^- are about two to three times larger than the respective α 's determined by the fit of the adsorption data with the adsorption isotherm (Table 2.4). However, because the repulsion is dampened by the ion-specific effect, the experimental values of the α 's are smaller than the α_0 's and those of the K 's are larger than the K_0 's. More importantly, the α_0 's and K_0 's are almost equal for the two counterions, Cl^- and Br^- , as they should be according to the theory. We consider these results as strong confirmation of our theory. The electrostatic nature of α was confirmed by plotting $\ln \alpha$ versus the square of the Debye length $1/\kappa^2$ for different electrolyte concentrations (cf. Figure 2.21 and the related discussion). Another surprising effect is exhibited by the comparison of the adsorption Γ_s of the same surfactant at W|O and W|G interfaces (Figure 2.20). At small concentrations C , the adsorption Γ_s at W|G is smaller than that at W|O, but as C increases, the adsorption at W|G becomes larger. This leads to an intersection of the two curves $\Gamma_s(C)$. We attributed this effect to the second virial coefficient B_2 (leading to repulsion), which is smaller at the W|G interface than at the W|O interface.

When deriving the expressions (Equations 2.65 and 2.66) for u_{i0} , no assumptions were made about the phenomenon studied or the nature of the ionic surfactants. Hence, we decided to use the present theory of the ion-specific effects and the calculated values of u_{i0} from Table 2.2 to interpret two other phenomena involving ionic surfactants: the cmc and the disjoining pressure of thin films. In Section 2.4, Shinoda's theory of the cmc of ionic surfactants was generalized to account for the

specific effect of the counterion (Equation 2.143). The new theory was confirmed by experimental data for cmc of several surfactants with different counterions (Figures 2.22 and 2.26)—in agreement with Equation 2.145, the plots of $\ln \text{cmc}$ versus $-u_{i0}/k_B T$ were linear with theoretical slope $-1/3$. A model for a mixture of several counterions is proposed (Equation 2.147), and confirmed with experimental data (Figure 2.25). Finally, the Derjaguin-Landau-Verwey-Overbeek (DLVO) theory of the electrostatic disjoining pressure Π_{el} of thin liquid films was also extended to account for ion-specific effects. From the experimental curves $\Pi_{el}(h)$ (where h is the film thickness) for films stabilized with $C_{16}H_{33}NMe_3Br$ and with the addition of excess amounts of the salts NaX ($X = F^-$, Cl^- , Br^-), the values of the surface potential Φ^S were calculated and plotted versus $-u_{i0}/k_B T$ of the respective counterions (Figure 2.28). Although we deal with three points only, the interpolation gave a line with slope -0.4 , slightly different from the theoretical value $-1/2$ (Equation 2.57).

Based on all these results, we may conclude that the simple theory of the counterion-specific effects, presented above, is surprisingly efficient and universal—it has thus far been successfully applied to several different phenomena and led not only to correct interpretations (in all cases, quantitative) of the considered effects but also helped us predict and explain several new effects that have not been observed previously. An important general result was that (with one exception—the NH_4^+ ion) in all studied phenomena, the sequence of the ions was ordered by efficiency following Hofmeister's series (Equations 2.1 and 2.2) but the ordering of the anions was in reverse (compare Equations 2.76 and 2.1). A similar reversal of the Hofmeister series was attributed in refs. [3,4] to the sign of the interfacial charge. It is worthwhile to remind the readers that the theory is based on a single quantity, the ion-specific adsorption energy u_{i0} , which was calculated from Equations 2.65 and 2.66 without using any adjustable parameters. That is why we hope that u_{i0} is (at least for ionic surfactants and, possibly, for proteins) the main quantity involved in Hofmeister effects.

2.6 PROSPECTS

As mentioned above, the theory of the ion-specific adsorption energy u_{i0} in Section 2.2.3 and its experimental verification suggest that it depends solely on the nature of the counterion and, possibly, of the hydrophobic phase. Our preliminary unpublished calculations show that, at least for $W|O$ interfaces, the latter effect is quite small. This makes us believe that this study is a good basis for further investigations of ion-specific effects. Part of these investigations should lead to a better understanding of several new effects, described above. These are (i) the dependence of the intercept π_0 of $\pi^S(C^{2/3})$ on the ion adsorption energy u_{i0} and its relation to the structure of the oil-like layer formed by the hydrocarbon tails of the surfactant (Figure 2.12); (ii) the role of the surfactant head on the value of the nonspecific constant K_0 of the surfactant ion; and (iii) the electrostatic effect, mentioned above, on the area per molecule α . We are planning to clarify these issues in the near future.

There are several other phenomena, which seem closely related to the ion-specific adsorption energy u_{i0} . We hope that they could be tackled without need for significant modifications of the present theory. These tasks are (i) the application of the present theory to a study of the ion-specific effect on the electrostatic interaction of proteins; this can be done in at least three ways: by interpreting data for the second virial coefficient, by investigating spread protein layers, or by studying thin liquid films stabilized by proteins at low ionic strength. In every case, one must vary at least the counterion, pH, and salt concentrations; (ii) Application of the theory to interpret the ion-specific effects on the micellar aggregation number and the transition from spherical to cylindrical micelles [102]; and (iii) More detailed analysis of the ion-specific effects on the DLVO theory and use of the results to modify the coalescence theory of drops and bubbles.

As the van der Waals forces are ever present, so are the ion-specific effects. This is confirmed by a short list of phenomena in which ion-specific effects have been revealed and in which our theory could possibly be applied: surface tension of electrolyte solutions [2,6–8,54], microemulsions [14] and vesicles [132], and properties of lipid monolayers [96,97]. Our approach might be applicable even for systems not involving surfactants or lipids. Indeed, Parsons et al. [133] recently

successfully calculated the interaction energy between silica and alumina particles using a theory whose main features are similar to our theory of the ion-selective adsorption energy u_{i0} , developed in ref. [29] and used in the present article.

LIST OF SYMBOLS AND ABBREVIATIONS

B_2	second virial coefficient ($B_2 = B_{\text{hc}} + B_{\text{attr}}$)
B_{attr}	attractive part of the second virial coefficient
B_{hc}	hard core (repulsive) part of the second virial coefficient
C_{el}	concentration of added electrolyte in the bulk
C_s	surfactant concentration in the bulk
C_t	total electrolyte concentration, $C_t \equiv C_s + C_{\text{el}}$
C	mean ion activity ($C = \gamma C_t^{1/2} C_s^{1/2}$)
d	rod length (one-dimensional adsorption of solid rods)
E_a	adsorption energy
E_{head}	energy of transfer of the surfactant's head from the bulk to the interface
e_0	elementary charge
e_i	charge of the i th component
I	ionization potential
k_B	Boltzmann constant
K	adsorption constant of an ionic surfactant ($\Gamma_s = KC^{2/3}$; $K = K_0 e^{-u_{i0}/2k_B T}$)
K_0	adsorption constant in the absence of ion-specific effect, $K_0^3 \equiv 4K_s/\kappa_0^2$
K_s	Henry's constant ($\Gamma_s = K_s C_s^S$)
L_{ij}	London constant
N_w	number of water molecules displaced by an ion upon adsorption
n_w	number of water molecules in the hydration shell of an ion
u_{i0}	specific adsorption energy of the counterion
u_{CH_2}	free energy for transfer of $-\text{CH}_2-$ from water to the hydrophobic phase
x_i	composition of salt mixture, $x_i \equiv C_i/C_t$
x_i^S	surface composition of salt mixture, $x_i^S \equiv \Gamma_i/\Gamma_s$
z	Cartesian coordinate
α	area of a molecule
α_L	area of a molecule in isotherms, based on Langmuir's model
α_p	static polarizability
α_V	area of a molecule in isotherms, based on Volmer's model
β	attraction parameter
γ	activity coefficient
Γ_s	surfactant adsorption
Γ_i^{DL}	adsorption of an ion in the diffuse double layer
δ_a	adsorption thickness
ϵ	absolute dielectric constant
κ	reciprocal Debye radius
κ_0	concentration-independent part of the Debye parameter, $\kappa_0^2 = 2e_0^2/\epsilon k_B T$
μ	chemical potential
μ^S	chemical potential at the interface (function of Γ_s)
σ	interfacial tension
σ_0	tension of a pure interface (in the absence of surfactant and salt)
π_0	spreading (or negative cohesive) pressure
π^S	surface pressure, $\sigma_0 - \sigma$
Π	disjoining pressure

ϕ	electrostatic potential
ϕ^S	surface potential
Φ^S	the absolute value of the dimensionless surface potential, $\Phi^S \equiv e_0 \phi^S / k_B T$
Ac ⁻	acetate ion, CH ₃ COO ⁻
cmc	critical micelle concentration
EOS	equation of state
HFL	Helfand–Frisch–Lebowitz model
LE	liquid-expanded adsorption layer
Me	methyl group, –CH ₃
W G	water–gas interface
W O	water–oil interface

ACKNOWLEDGMENTS

This work was supported by the Bulgarian National Science Fund Grants DDVU 02/12 and DDVU 02/54. We are indebted to Prof. Makoto Aratono and Prof. Piotr Warszynski for providing some of their experimental data used in this chapter, and to Dora Dimitrova for obtaining and processing some experimental data.

REFERENCES

1. F. Hofmeister. About regularities in the protein precipitating effects of salts and the relation of these effects with the physiological behaviour of salts. *Arch. Exp. Pathol. Pharmacol.*, **24**, 247–260 (1887).
2. W. Kunz (Ed.). *Specific Ion Effects*. World Scientific Publishing Co., New York (2011).
3. M. Boström, F.W. Tavares, S. Finet, F. Skouri-Panet, A. Tardieu and B.W. Ninham. Why forces between proteins follow different Hofmeister series for pH above and below pI. *Biophys. Chem.*, **117**, 217–224 (2005).
4. N. Schwierz, D. Horinek and R.R. Netz. Reversed anionic Hofmeister series: The interplay of surface charge and surface polarity. *Langmuir*, **26**, 7370–7379 (2010).
5. Issues 1 and 2 of *Curr. Opin. Colloid Interface Sci.*, **9**(1–2), 1–198 (2004).
6. B.W. Ninham and V. Yaminsky. Ion binding and ionspecificity: The Hofmeister effect and Onsager and Lifshitz theories. *Langmuir*, **13**, 2097–2108 (1997).
7. M. Boström, D.R.M. Williams and B.W. Ninham. Surface tension of electrolytes: Specific ion effects explained by dispersion forces. *Langmuir*, **17**, 4475–4478 (2001).
8. M. Boström, W. Kunz and B.W. Ninham. Hofmeister effects in surface tension of aqueous electrolyte solution. *Langmuir*, **21**, 2619–2623 (2005).
9. L.A. Moreira, M. Boström, B.W. Ninham, E.C. Biscaia and F.W. Tavares. Hofmeister effects: Why protein charge, pH titration and protein precipitation depend on the choice of background salt solution. *Colloids Surf. A*, **282–283**, 457–463 (2006).
10. M. Boström and B.W. Ninham. Contributions from dispersion and Born self free energies to the solvation energies of salt solutions. *J. Phys. Chem. B*, **108**, 12593–12595 (2004).
11. M. Boström and B.W. Ninham. Dispersion self-free energies and interaction free energies of finite-sized ions in salt solutions. *Langmuir*, **20**, 7569–7574 (2004).
12. M. Boström, D.R.M. Williams and B.W. Ninham. Specific ion effects: Why DLVO theory fails for biology and colloid systems. *Phys. Rev. Lett.*, **87**, 168103/1–4 (2001).
13. W. Kunz, L. Belloni, O. Bernard and B.W. Ninham. Osmotic coefficients and surface tensions of aqueous electrolyte solutions: Role of dispersion forces. *J. Phys. Chem. B*, **108**, 2398 (2004).
14. S. Murgia, M. Monduzzi and B.W. Ninham. Hofmeister effects in cationic microemulsions. *Curr. Opin. Colloid Interface Sci.*, **9**, 102–106 (2004).
15. W. Kunz, P. Lo Nostro and B.W. Ninham. The present state of affairs with Hofmeister effects. *Curr. Opin. Colloid Interface Sci.*, **9**, 1–18 (2004).
16. F.W. Tavares, D. Bratko, H.W. Blanch and J.M. Prausnitz. Ion-specific effects in the colloid–colloid or protein–protein potential of mean force: Role of salt–macroion van der Waals interactions. *J. Phys. Chem. B*, **108**, 9228–9235 (2004).

17. P. Warszynski, K. Lunkenheimer and G. Czichocki. Effect of counterions on the adsorption of ionic surfactants at fluid–fluid interfaces. *Langmuir*, **18**, 2506–2514 (2002).
18. G. Para, E. Jarek and P. Warszynski. The Hofmeister series effect in adsorption of cationic surfactants—Theoretical description and experimental results. *Adv. Colloid Interface Sci.*, **122**, 39–55 (2006).
19. G. Para, E. Jarek and P. Warszynski. The surface tension of aqueous solutions of cetyltrimethylammonium cationic surfactants in presence of bromide and chloride counterions. *Colloids Surf. A*, **261**, 65–73 (2005).
20. H.H. Li, Y. Imai, M. Yamanaka, Y. Hayami, T. Takiue, H. Matsubara and M. Aratono. Specific counterion effect on the adsorbed film of cationic surfactant mixtures at the air/water interface. *J. Colloid Interface Sci.*, **359**, 189–193 (2011).
21. M. Aratono, S. Uryu, Y. Hayami, K. Motomura and R. Matuura. Phase transition in the adsorbed films at water/air interface. *J. Colloid Interface Sci.*, **98**, 33–38 (1984).
22. K. Shimamoto, A. Onohara, H. Takumi, I. Watanabe, H. Tanida, H. Matsubara, T. Takiue and M. Aratono. Miscibility and distribution of counterions of imidazolium ionic liquid mixtures at the air/water surface. *Langmuir*, **25**, 9954–9959 (2009).
23. Y. Hayami, H. Ichikawa, A. Someya, M. Aratono and K. Motomura. Thermodynamic study on the adsorption and micelle formation of long chain alkyltrimethylammonium chlorides. *Colloid Polym. Sci.*, **276**, 595–600 (1998).
24. E.D. Goddard, O. Harva and T.G. Jones. The effect of univalent cations on the critical micelle concentration of sodium dodecyl sulfate. *Trans. Faraday Soc.*, **49**, 980–984 (1953).
25. K. Shinoda, T. Nakagawa, B.-I. Tamamushi and T. Isemuta. *Colloidal Surfactants, Some Physicochemical Properties*. Academic Press, New York (1963).
26. J.T. Davies and E. Rideal. *Interfacial Phenomena*. Academic Press, New York (1963).
27. J.T. Davies. Adsorption of long-chain ions I. *Proc. R. Soc. London, Ser. A*, **245**, 417–428 (1958).
28. R.P. Borwankar and D.T. Wasan. Equilibrium and dynamics of adsorption of surfactants at fluid–fluid interfaces. *Chem. Eng. Sci.*, **43**, 1323–1337 (1988).
29. I.B. Ivanov, K.G. Marinova, K.D. Danov, D. Dimitrova, K.P. Ananthapadmanabhan and A. Lips. Role of the counterions on the adsorption of ionic surfactants. *Adv. Colloid Interface Sci.*, **134–135**, 105–124 (2007).
30. I.B. Ivanov, R.I. Slavchov, E.S. Basheva, D. Sidzhakova and S.I. Karakashev. Hofmeister effect on micellization, thin films and emulsion stability. *Adv. Colloid Interface Sci.*, **168**, 93–104 (2011).
31. I.B. Ivanov, K.P. Ananthapadmanabhan and A. Lips. Adsorption and structure of the adsorbed layer of ionic surfactants. *Adv. Colloid Interface Sci.*, **123–126**, 189–212 (2006).
32. T.D. Gurkov and I.B. Ivanov. Layers of nonionic surfactants on fluid interfaces; Adsorption and interactions in the frames of a statistical model. In Proceedings of the 4th World Congress on Emulsions, Lyon, France; Paper No. 2.1, p. 509 (2006).
33. I.B. Ivanov, K.D. Danov, D. Dimitrova, M. Boyanov, K.P. Ananthapadmanabhan and A. Lips. Equations of state and adsorption isotherms of low molecular non-ionic surfactants. *Colloids Surf. A*, **354**, 118–133 (2010).
34. T.D. Gurkov, D.T. Dimitrova, K.G. Marinova, C. Bilke-Crause, C. Gerber and I.B. Ivanov. Ionic surfactants on fluid interfaces: Determination of the adsorption; role of the salt and the type of the hydrophobic phase. *Colloids Surf. A*, **261**, 29–38 (2005).
35. E.D. Shchukin, A.V. Pertsov and E.A. Amelina. *Colloid Chemistry*. Univ. Press, Moscow (1982) [in Russian]. Elsevier, Amsterdam (2001) [in English].
36. P.A. Kralchevsky, K.D. Danov, G. Broze and A. Mehreteab. Thermodynamics of ionic surfactant adsorption with account for the counterion binding: Effect of salts of various valency. *Langmuir*, **15**, 2351–2365 (1999).
37. K.D. Danov, P.A. Kralchevsky, K.P. Ananthapadmanabhan and A. Lips. Interpretation of surface-tension isotherms of n-alkanoic (fatty) acids by means of the van der Waals model. *J. Colloid Interface Sci.*, **300**, 809–813 (2006).
38. C. Tanford. *The Hydrophobic Effect*. Wiley, New York (1980).
39. J.N. Israelachvili. *Intermolecular and Surface Forces*. Academic Press, New York (2011).
40. A.J. Kumpulainen, C.M. Persson, J.C. Eriksson, E.C. Tyrode and C.M. Johnson. Soluble monolayers of n-decyl glucopyranoside and n-decyl maltopyranoside. Phase changes in the gaseous to the liquid-expanded range. *Langmuir*, **21**, 305–315 (2005).
41. J.W. Gibbs. *The Collected Works of J. W. Gibbs*, Vol. I. Longmans, Green, New York (1931).
42. L.G. Gouy. Sur la constitution de la charge électrique à la surface d'un électrolyte. *J. Phys. Radium*, **9**, 457–468 (1910).

43. R.A. Robinson and R.H. Stokes. *Electrolyte Solutions*. Butterworth Scientific Publications, London (1959).
44. E.H. Lucassen-Reynders. Surface equation of state for ionized surfactants. *J. Phys. Chem.*, **70**, 1777–1785 (1966).
45. E.H. Lucassen-Reynders. Adsorption at fluid interfaces. In *Anionic Surfactants: Physical Chemistry of Surfactant Action*, E.H. Lucassen-Reynders (Ed.), Chap. 1, Surfactant Science Series, Vol. 11. Marcel Dekker, New York (1981).
46. I. Langmuir. Oil lenses on water and the nature of monomolecular expanded films. *J. Chem. Phys.*, **1**, 756–776 (1933).
47. N.K. Adam. *The Physics and Chemistry of Surfaces*. Clarendon Press, Oxford (1941).
48. A. Goebel and K. Lunkenheimer. Interfacial tension of the water/n-alkane interface. *Langmuir*, **13**, 369–372 (1997).
49. E.A. Guggenheim. Specific thermodynamic properties of aqueous solutions of strong electrolytes. *Philos. Mag.*, **19**, 588–643 (1935).
50. K. Wojciechowski, A. Bitner, P. Warszynski and M. Zubrowska. The Hofmeister effect in zeta potentials of CTAB-stabilised toluene-in-water emulsions. *Colloids Surf. A*, **376**, 122–126 (2011).
51. S.J. Rehfeld. Adsorption of sodium dodecyl sulfate at various hydrocarbon-water interfaces. *J. Phys. Chem.*, **71**, 738–745 (1967).
52. J.D. Hines. The preparation of surface chemically pure sodium n-dodecyl sulfate by foam fractionation. *J. Colloid Interface Sci.*, **180**, 488–492 (1996).
53. D.A. Haydon and F.H. Taylor. On adsorption at the oil/water interface and the calculation of electrical potentials in the aqueous surface phase I. *Phil. Trans. R. Soc. Lond. A*, **252**, 225–248 (1960).
54. R.I. Slavchov, J.K. Novev, T.V. Peshkova and N.A. Grozev. Surface tension and surface $\Delta\chi$ -potential of concentrated Z⁺:Z⁻ electrolyte solutions. *J. Colloid Interface Sci.* **403**, 113–126 (2013).
55. K.D. Collins. Charge density-dependent strength of hydration and biological structure. *Biophysical*, **72**, 65–76 (1997).
56. N.A. Izmailov. *Electrochemistry of Solutions*, 3rd ed. Khimia, Moscow (1976) [in Russian].
57. Y. Marcus. *Ion Properties*. Marcel Dekker, New York (1997).
58. Y. Marcus. Thermodynamics of ion hydration and its interpretation in terms of a common model. *Pure. Appl. Chem.*, **59**, 1093–1101 (1987).
59. B.P. Nikolskij. *Handbook of Chemistry*. Khimija, Leningrad (1963) [in Russian].
60. B. Dietrich, J.-P. Kintzinger, J.-M. Lehn, B. Metz and A. Zahidi. Stability, molecular dynamics in solution, and x-ray structure of the ammonium cryptate [NH₄⁺.cntnd.2.2.2]hexafluorophosphate. *J. Phys. Chem.*, **91**, 6600–6606 (1987).
61. D.R. Lide (Ed.). *CRC Handbook of Chemistry and Physics*, 83rd ed. CRC Press, Boca Raton, FL (2002).
62. W.R. Gillap, N.D. Weiner and M. Gibaldi. Effect of hydrocarbon chain length on adsorption of sodium alkyl sulfates at oil/water interfaces. *J. Colloid Interface Sci.*, **26**, 232–236 (1968).
63. R. Aveyard and B.J. Briscoe. Adsorption of n-alkanols at alkane/water interfaces. *J. Chem. Soc., Faraday Trans.*, **168**, 478–491 (1972).
64. D.A. Haydon and F.H. Taylor. Adsorption of sodium octyl and decyl sulphates and octyl and decyl trimethylammonium bromides at the decane-water interface. *Trans. Faraday Soc.*, **58**, 1233–1250 (1962).
65. M. Aratono. Personal communication (2010).
66. V. Bergeron. Disjoining pressures and film stability of alkyltrimethylammonium bromide foam films. *Langmuir*, **13**, 3474–3482 (1997).
67. C. Das and B. Das. Effect of tetraalkylammonium salts on the micellar behavior of lithium dodecyl sulfate: A conductometric and tensiometric study. *J. Mol. Liq.*, **137**, 152–158 (2008).
68. D. Dimitrova. Personal communication (2011).
69. J.R. Lu, A. Marrocco, T. Su, R.K. Thomas and J. Penfold. Adsorption of dodecyl sulfate surfactants with monovalent metal counterions at the air-water interface studied by neutron reflection and surface tension. *J. Colloid Interface Sci.*, **158**, 303–316 (1993).
70. P. Koelsch and H. Motschmann. Varying the counterions at a charged interface. *Langmuir*, **21**, 3436–3442 (2005).
71. J. Rogers and J.H. Schulman. A Mechanism of the Selective Flotation of Soluble Salts. In: *Proceedings of the Second International Congress of Surface Activity*, vol. III: Electrical phenomena, solid-liquid interface, ed. Schulman J.H. London: Butterworth, 243, 1957.
72. D.F. Sears and J.H. Schulman. Influence of water structures on the surface pressure, surface potential, and area of soap monolayers of lithium, sodium, potassium, and calcium. *J. Phys. Chem.*, **68**, 3529–3534 (1964).

73. I. Weil. Surface concentration and the Gibbs adsorption law. The effect of the alkali metal cations on surface behavior. *J. Phys. Chem.*, **70**, 133–140 (1969).
74. L. Onsager and N.N.T. Samaras. The surface tension of Debye-Hückel electrolytes. *J. Chem. Phys.*, **2**, 528–536 (1934).
75. V.V. Kalinin and C.J. Radke. An ion-binding model for ionic surfactant adsorption at aqueous-fluid interfaces. *Colloids Surf. A*, **114**, 337–350 (1996).
76. I. Langmuir. The adsorption of gases on plane surfaces of glass, mica and platinum. *J. Am. Chem. Soc.*, **40**, 1361–1403 (1918).
77. A. Frumkin. Electrocapillary curve of higher aliphatic acids and the state equation of the surface layer. *Z. Phys. Chem.*, **116**, 466 (1925).
78. M. Volmer. Thermodynamische Folgerungen aus der Zustandsgleichung für adsorbierte Stoffe. *Z. Phys. Chem.*, **115**, 253–260 (1925).
79. J.H. De Boer. *The Dynamical Character of Adsorption*. Clarendon Press, Oxford (1953).
80. E. Helfand, H.L. Frisch and J.L. Lebowitz. Theory of the two- and one-dimensional rigid sphere fluids. *J. Chem. Phys.*, **34**, 1037–1042 (1961).
81. T.L. Hill. *An Introduction to Statistical Thermodynamics*. Addison-Wesley, Reading, MA (1962).
82. A.W. Adamson and A.P. Gast. *Physical Chemistry of Surfaces*, 6th ed. Wiley, New York (1997).
83. L. Tonks. The complete equation of state of one, two and three-dimensional gases of hard elastic spheres. *Phys. Rev.*, **50**, 955–963 (1936).
84. H. Reiss, H.L. Frisch and J.L. Lebowitz. Statistical mechanics of rigid spheres. *J. Chem. Phys.*, **31**, 369–380 (1959).
85. F. Lado. Equation of state of the hard disk fluid from approximate integral equations. *J. Chem. Phys.*, **49**, 3092–3096 (1968).
86. A.I. Rusanov. The essence of the new approach to the equation of the monolayer state. *Colloid J.*, **69**, 131–143 (2007).
87. A.I. Rusanov. Equation of state and phase transitions in surface monolayer. *Colloids Surf. A*, **239**, 105–111 (2004).
88. R.J. Baxter. Percus-Yevick equation for hard spheres with surface adhesion. *J. Chem. Phys.*, **49**, 2770–2774 (1968).
89. M. Yamanaka, M. Aratono, K. Motomura and R. Matuura. Effect of pressure on the adsorption and micelle formation of aqueous dodecyltrimethylammonium chloride solution-hexane system. *Colloid Polym. Sci.*, **262**, 338–341 (1984).
90. P.C. Hemmer and G. Stell. Strong short-range attractions in a fluid. *J. Chem. Phys.*, **93**, 8220 (1990).
91. C. Tutschka and J.A. Cuesta. Overcomplete free energy functional for D=1 particle systems with next neighbor interactions. *J. Stat. Phys.*, **111**, 1125–1148 (2003).
92. A.V. Makievski and D.O. Grigoriev. Adsorption of alkyl dimethyl phosphine oxides at the solution/air interface. *Colloids Surf. A*, **143**, 233–242 (1998).
93. P. Warszynski and K. Lunkenheimer. Influence of conformational free energy of hydrocarbon chains on adsorption of nonionic surfactants at the air/solution interface. *J. Phys. Chem. B*, **103**, 4404–4411 (1999).
94. L. Malysa, R. Miller and K. Lunkenheimer. Relationship between foam stability and surface elasticity forces: Fatty acid solutions. *Colloids Surf.*, **53**, 47–62 (1991).
95. K. Lunkenheimer and R. Hirte. Another approach to a surface equation of state. *J. Phys. Chem.*, **96**, 8683–8686 (1992).
96. E.D. Goddard and H.C. Kung. Counterion effects in long-chain sulfonate monolayers. *J. Colloid Interface Sci.*, **37**, 585–594 (1971).
97. E.D. Goddard, O. Kao and H.C. Kung. Counterion effects in charged monolayers. *J. Colloid Interface Sci.*, **27**, 616–624 (1968).
98. G. Loglio, P. Pandolfini, L. Liggieri, A.V. Makievski and F. Ravera. Determination of interfacial properties by the pendant drop tensiometry: Optimisation of experimental and calculation procedures. In *Bubble and Drop Interfaces*, R. Miller and L. Liggieri (Eds.), Chap. 2, Book Series: Progress in Colloid and Interface Science, Vol. 2. Brill, Leiden (2011).
99. K. Motomura, M. Aratono, N. Matubayasi and R. Matuura. Thermodynamic studies on adsorption at interfaces III. Sodium dodecyl sulfate at water | hexane interface. *J. Colloid Interface Sci.*, **67**, 247–254 (1978).
100. S. Levine, K. Robinson, G.M. Bell and J. Mingins. The discreteness-of-charge effect at charged aqueous interfaces I. *J. Electroanal. Chem.*, **38**, 253–269 (1972).
101. L. Gaillon, J. Lelievre and R. Gaboriaud. Counterion effects in aqueous solutions of cationic surfactants: Electromotive force measurements and thermodynamic model. *J. Colloid Interface Sci.*, **213**, 287–297 (1999).

102. J.V. Joshi, V.K. Aswal, P. Bahadur and P.S. Goyal. Role of counterion of the surfactant molecule on the micellar structure in aqueous solution. *Curr. Sci.*, **83**, 47–49 (2002).
103. M. Benraou, B.L. Bales and R. Zana. Effect of the nature of the counterion on the properties of anionic surfactants I. *J. Phys. Chem. B*, **107**, 13432–13440 (2003).
104. M.H. Ropers, G. Czichocki and G. Brezesinski. Counterion effect on the thermodynamics of micellization of alkyl sulfates. *J. Phys. Chem. B*, **107**, 5281–5288 (2003).
105. S. Kumar, D. Sharmav and Kabir-ud-Din. Effect of additives on the clouding behavior of sodium dodecyl sulfate plus tetra-n-butylammonium bromide system. *J. Surfactants Deterg.*, **7**, 271–275 (2004).
106. M.J. Rosen. *Surfactants and Interfacial Phenomena*, 3rd ed. Wiley, New York (2004).
107. M.L. Corrin and W.D. Harkins. The effect of salts on the critical concentration for the formation of micelles in colloidal electrolytes. *J. Am. Chem. Soc.*, **69**, 683–688 (1947).
108. R. Nagarajan. Micellization, mixed micellization and solubilization—The role of interfacial interactions. *Adv. Colloid Interface Sci.*, **26**, 205–264 (1986).
109. I.V. Rao and E. Ruckenstein. Micellization behavior in the presence of alcohols. *J. Colloid Interface Sci.*, **113**, 375–387 (1986).
110. V. Srinivasan and D. Blankshtein. Effect of counterion binding on micellar solution behavior I. *Langmuir*, **19**, 9932–9945 (2003).
111. A. Jakubowska. Interactions of different counterions with cationic and anionic surfactants. *J. Colloid Interface Sci.*, **346**, 398–404 (2010).
112. R. Zielinski. Micelle formation in aqueous NaBr solutions of alkyltrimethylammonium bromides. *Pol. J. Chem.*, **72**, 127–136 (1998).
113. A. Malliaris, J. Lang and R. Zana. Micellar aggregation numbers at high surfactant concentration. *J. Colloid Interface Sci.*, **110**, 237–242 (1986).
114. T.M. Perger and M. Bester-Rogac. Thermodynamics of micelle formation of alkyltrimethylammonium chlorides from high performance electric conductivity measurements. *J. Colloid Interface Sci.*, **313**, 288–295 (2007).
115. S. Durand-Vidal, M. Jardat, V. Dahirel, O. Bernard, K. Perrigaud and P. Turq. Determining the radius and the apparent charge of a micelle from electrical conductivity measurements by using a transport theory: Explicit equations for practical use. *J. Phys. Chem. B*, **110**, 15542–15547 (2006).
116. B.L. Bales and R. Zana. Characterization of micelles of quaternary ammonium surfactants, as reaction media I. *J. Phys. Chem. B*, **106**, 1926–1939 (2002).
117. D.F. Evans and P.J. Wightman. Micelle formation above 100-degrees-C. *J. Colloid Interface Sci.*, **86**, 515–524 (1982).
118. P.F. Grieger and C.A. Kraus. Properties of electrolytic solutions. 35. Conductance of some long chain salts in methanol-water mixtures. *J. Am. Chem. Soc.*, **70**, 3803–3811 (1948).
119. A. Gonzalez-Perez, J. Czapkiewicz, J.L. Del Castillo and J.R. Rodriguez. Micellar properties of tetradecyltrimethylammonium nitrate in aqueous solutions at various temperatures and in water–benzyl alcohol mixtures at 25 degrees C. *Colloid Polym. Sci.*, **282**, 1359–1364 (2004).
120. S. Hashimoto, J.K. Thomas, D.F. Evans, S. Mukherjee and B.W. Ninham. Unusual behavior of hydroxide surfactants. *J. Colloid Interface Sci.*, **95**, 594–596 (1983).
121. P. Lianos and R. Zana. Use of pyrene excimer formation to study the effect of NaCl on the structure of sodium dodecyl-sulfate micelles. *J. Phys. Chem.*, **84**, 3339–3341 (1980).
122. S.K. Mehta, K.K. Bhasin, R. Chauhan and S. Dham. Effect of temperature on critical micelle concentration and thermodynamic behavior of dodecyltrimethylammonium bromide and dodecyltrimethylammonium chloride in aqueous media. *Colloids Surf. A*, **255**, 153–157 (2005).
123. H.B. Klevens. Critical micelle concentrations as determined by refraction. *J. Phys. Colloid Chem.*, **52**, 130–148 (1948).
124. J. Osugi, M. Sato and N. Ifuku. Micelle formation of cationic detergent solution at high pressures. *Rev. Phys. Chem. Jpn.*, **35**, 32 (1965).
125. H. Okuda, T. Imae and S. Ikeda. The adsorption of cetyltrimethylammonium bromide on aqueous surfaces of sodium-bromide solutions. *Colloids Surf.*, **27**, 187–200 (1987).
126. A.P. Brady and S. Ross. The measurement of foam stability. *J. Am. Chem. Soc.*, **66**, 1348–1356 (1944).
127. A.B. Scott, H.V. Tartar and E.C. Lingafelter. Electrolytic properties of aqueous solutions of octyltrimethylammonium octanesulfonate and decyltrimethylammonium decanesulfonate. *J. Am. Chem. Soc.*, **65**, 698–701 (1943).
128. K. Maiti, D. Mitra, S. Guha and S.P. Moulik. Salt effect on self-aggregation of sodium dodecylsulfate (SDS) and tetradecyltrimethylammonium bromide (TTAB): Physicochemical correlation and assessment in the light of Hofmeister (lyotropic) effect. *J. Mol. Liq.*, **146**, 44–51 (2009).

129. N.V. Churaev, B.V. Derjagiun and V.M. Muller. *Surface Forces*. Springer, New York (1987).
130. K.J. Mysels and M.N. Jones. Direct measurement of variation of double-layer repulsion with distance. *Discuss. Faraday Soc.*, **42**, 42–50 (1966).
131. V. Bergeron and C.J. Radke. Equilibrium measurements of oscillatory disjoining pressures in aqueous foam films. *Langmuir*, **8**, 3020–3026 (1992).
132. M. Gradzielski. Vesicle gel—Phase behavior and processes of formation. *Curr. Opin. Colloid. Interface Sci.*, **9**, 149–153 (2004).
133. D.F. Parsons, M. Boström, T.J. Maceina, A. Salis and B.W. Ninham. Why direct or reversed hofmeister series? Interplay of hydration, non-electrostatic potentials, and ion size. *Langmuir*, **26**, 3323–3328 (2010).

